

22 also contain abundant mantle-derived mafic microgranular enclaves, whereas such enclaves are rare
23 in the W granites. A model is proposed in which the protolith to the W granites released W to the
24 melt as a result of the breakdown of muscovite. The temperature of melting, however, was too low
25 for biotite to melt. Upwelling of mantle material, particularly along the Chenzhou-Linwu fault,
26 however, led to higher temperatures in the west (the location of the Sn and Sn-W deposits), thereby
27 enabling the breakdown of both muscovite and biotite and the consequent release of both W and Sn
28 to form Sn and Sn-W granites. This model, which is based on differences in the protolith melting
29 temperature and thus mobilization temperatures for Sn and W, is potentially applicable to any Sn-
30 W metallogenic province in which the Sn and Sn-W deposits occur separately from the W deposits.

31

32 Keywords: tin; tungsten; decoupling; anhydrous melting; metallogenic province

33

34 **Introduction**

35 Magmatic tin-tungsten mineralization is commonly associated with highly evolved reduced granites
36 that have undergone extensive magmatic fractionation, followed by the partitioning of tin and
37 tungsten into late-magmatic hydrothermal fluids (Ishihara, 1977; Lehmann, 1990). The spatial
38 distribution of magmatic Sn and W mineralization in discontinuous belts along the margins of
39 cratons reflects the distribution of (i) sedimentary protoliths, which have experienced intense
40 chemical alteration (loss of Na, Ca) on the continent before they were redistributed to the continent
41 margin, and (ii) heat sources leading to the partial melting of these protoliths (Romer and Kroner,
42 2015, 2016). The nature of the sedimentary protoliths determines both the melting behavior of the
43 source rocks and the nature of the metal-sequestering phases in the protolith, which in turn control

44 the partitioning of Sn and W between melt and restite phases (e.g., Simons et al., 2017; Wolf et al.,
45 2018).

46 Tin and tungsten are concentrated in the same type of granite, and develop deposits that occur
47 within the same metallogenic province and have similar tectonic settings. Nonetheless, the two
48 metals typically form separate deposits or one metal predominates strongly over the other metal. At
49 the scale of individual intrusions, possible explanations for this separation of tin and tungsten
50 include differences in fractionation and oxidation state (Blevin and Chappell, 1992), contrasting
51 magmatic histories (Cheng et al., 2018), or different paths of metal redistribution during late stage
52 magmatic and hydrothermal processes (Schmidt, 2018). At the scale of metallogenic provinces,
53 however, such a regional predominance of Sn over W mineralization and *vice versa* has to be linked
54 to features that operate over the entire province.

55 In South China, there are two age groups of Sn-W mineralization that define separate belts,
56 which formed above subduction zones during periods of back-arc extension and extension
57 associated with the changing relative movement direction of the Paleo-Pacific plate, which change
58 from subduction oblique to the continental margin to subduction parallelism with the continental
59 margin (Mao et al., 2013). The more important of these belts developed mainly between 160 and
60 150 Ma (Yuan et al., 2008, 2011; Hu et al., 2012, 2017; Hu and Zhou, 2012), and is located in the
61 Nanling region (Fig. 1A). This belt constitutes the largest W-Sn metallogenic province in the world,
62 accounting for more than 54% of global tungsten resources and appreciable resources of tin and rare
63 metals (Yuan et al., 2018). The spatial distribution of these Sn-W deposits is heterogeneous with W
64 deposits occurring throughout the region (although mainly in the east) and Sn deposits being largely
65 restricted to the western part, especially along the deep, NE-trending Chenzhou-Linwu fault (Fig.

66 1B). Although many of the deposits contain economic concentrations of both Sn and W, they are
67 typically dominated by one of the metals. Among the deposits in which Sn and W were decoupled,
68 the giant Yaogangxian W deposit and the giant Furong Sn deposit are the most prominent examples
69 (Fig. 1B). The Nanling Sn-W metallogenic province, therefore, provides an ideal setting in which
70 to investigate the reasons for the separation or decoupling between Sn-W, Sn and W deposits at a
71 regional scale.

72 The partitioning of W and Sn during partial melting of sedimentary rocks is thought to be
73 controlled largely by the restite mineralogy and melting temperature (e.g., Wolf et al., 2018). Thus,
74 the contrasting distribution of Sn and W mineralization within Sn-W metallogenic provinces may
75 reflect variations in protolith composition and/or the conditions at which it melted. Using available
76 whole-rock geochemical and zircon Hf isotopic data for Sn-, Sn-W-, and W-related granites in the
77 Nanling W-Sn metallogenic province, we demonstrate that the protoliths of the granites related to
78 Sn and Sn-W mineralization melted at higher temperatures than those with related W-Sn and W
79 mineralization. In so doing, we are able to make the case that the difference in the source temperature
80 was the key control on the spatial decoupling of Sn and W mineralization in the Nanling
81 metallogenic province.

82

83 **Geological setting**

84 The Nanling region is located in the northwestern part of the Cathaysia block of South China (Fig.
85 1A, B). After assembly of the Yangtze Craton and Cathaysia Block along the Qinhang tectonic belt,
86 at ~1.1- 0.83 Ga to form the South China Block (Chen and Jahn, 1998; Zhao et al., 2011), South
87 China was extensively reworked by Early Paleozoic and Early Mesozoic orogenies as well as the

88 Late Mesozoic subduction of the Paleo-Pacific plate. This produced large volumes of granitic rocks.
89 Only the Late Mesozoic granites, however, are enriched in Sn and W (Fig. 1A, Mao et al., 2013).
90 These granites formed during two separate tectono-magmatic events, the first of which occurred in
91 the Late Jurassic (160-150 Ma) and is mainly represented in the Nanling region. This event took
92 place in response to the opening of a large slab window or the development of an intra-arc rift during
93 the subduction of the Palaeo-Pacific plate (Jiang et al., 2009; Mao et al., 2013), and is the focus of
94 this paper (Fig. 1B). The second event occurred in the Early-Mid Cretaceous (120-80 Ma) and was
95 a response to the development of pull-apart basins along the South China continental margin (Fig.
96 1A, Mao et al., 2013).

97 Multiple tectono-thermal events in Nanling region created a regional basement consisting of
98 Sinian-Silurian metamorphic rocks, which are unconformably overlain by a cover sequence of
99 Devonian to Triassic marine and continental strata, including clastic and carbonate facies (Li and
100 Zhong, 1991). These strata, especially the Upper Devonian and Carboniferous carbonate facies, are
101 widely exposed in the western part of the region, where they were intruded by Late Jurassic Sn-W-
102 bearing granites. In the east, the exposed strata are mainly Sinian to Cambrian clastic rocks and
103 were intruded by Late Jurassic W-bearing granites (Fig. 1B).

104

105 **The W-Sn Mineralization**

106 The type of tungsten and tin mineralization in the Nanling region varies considerably due in large
107 part to the variable nature of the rocks that host the intrusions. Tungsten mineralization occurs
108 throughout the region. In the east, it occurs dominantly as quartz-vein-type wolframite deposits
109 hosted by siliciclastic rocks, whereas in the west, it mainly takes the form of skarn-type scheelite

110 deposits hosted by carbonate rocks. In contrast to W, the Sn and Sn-W mineralization is restricted
111 to the western part of the region (especially along the deep, NE-trending Chenzhou-Linwu fault),
112 where it occurs mainly in skarns hosted by carbonate rocks and to a much lesser extent in cassiterite-
113 sulfide veins hosted by siliciclastic rocks (Fig. 1B).

114 The quartz-vein-type wolframite deposits mainly occur along the contacts between the Late
115 Jurassic granite plutons and their siliciclastic sedimentary host rocks, especially near the intersection
116 of NNE and EW trending faults. In addition to wolframite, the veins contain minor proportions of
117 bismuthinite, molybdenite, arsenopyrite, cassiterite, pyrite, scheelite, galena, chalcopyrite and
118 sphalerite (Hu et al., 2012). The quartz gangue is accompanied by minor K-feldspar, mica, topaz,
119 tourmaline, chlorite and calcite (Hu et al., 2012; Ni et al., 2015). On the basis of mineral textures
120 and crosscutting vein relationships, an early oxide-sulfide stage is interpreted to have been followed
121 by a silicate stage and finally by a carbonate stage (Hu et al., 2012). Vein emplacement was
122 associated with silicification of the wall rocks and, locally, minor greisenization and sericitization
123 (Wu et al., 1987).

124 The skarn type deposits (W, Sn and Sn-W) are found invariably at the interface between Late
125 Jurassic granitic plutons and Late Paleozoic carbonate rocks and appear to have been controlled
126 structurally by NE-trending faults. They mainly belong to the oxidized calcic skarn class, which is
127 characterized by prograde stage characterized by a high garnet/pyroxene ratio, andradite-rich garnet
128 and diopside-rich pyroxene and a retrograde stage comprising epidote, actinolite, and chlorite. In
129 some cases, e.g., the giant Shizhuyuan W-Sn-Mo-Bi deposit in southern Hunan Province, both the
130 adjacent granite and the skarn was subjected to greisenization and overprinted by a quartz stockwork
131 (Lu et al., 2003). The mineralization of the skarn-type deposits takes the form of scheelite and/or

132 cassiterite and is mainly restricted to the retrograde skarns (Lu et al., 2003; Yuan et al., 2011). In
133 addition to the main ore minerals there are minor proportions of molybdenite, bismuthinite,
134 arsenopyrite, pyrrhotite, galena and sphalerite.

135

136 **The geochemistry of the Sn and W granites**

137 Late Jurassic granites of the Nanling belt with associated Sn and W mineralization are interpreted
138 to have originated from highly fractionated crustal melts (high SiO₂ and Rb/Sr ratios, Fig. 2 A and
139 B, Supplementary Table 1). Only the granite related to the giant Furong Sn deposit provides
140 evidence of being less evolved (lower SiO₂ concentration and a low Rb/Sr ratio; Figure 2). Although
141 some of the W-specialized granites have Fe₂O₃/FeO ratios indicative of a slightly higher oxygen
142 fugacity (Fig. 2), most of the Sn- and W-mineralized granites are ilmenite series, peraluminous
143 granites (Fe₂O₃/FeO<0.5, Fig. 2) (Ishihara, 1981). Furthermore, there is no correlation between the
144 Fe₂O₃/FeO and Rb/Sr ratios (Fig. 2), indicating that the oxygen fugacity reflects the magma source
145 and not the fractionation (Burnham and Ohmoto, 1980; Blevin and Chappell, 1992; Sato, 2012).
146 Even though some of the W and Sn granites are geochemically distinct, most of the Late Jurassic
147 granites with associated Sn and W deposits have broadly overlapping chemical compositions (Fig.
148 2), indicating that they experienced a similar degree of fractionation and have the same reduced
149 redox state (Ishihara, 1981). Thus, magma evolution and redox state alone cannot account for the
150 regional W-Sn decoupling of Late Jurassic W-Sn mineralization in the Nanling belt. Instead, the
151 decoupling reflects contrasting sources and/or conditions of metal mobilization from the source
152 rocks.

153

154 **The temperature of melting and sources of heat and protolith**

155 Two key factors controlling the regional distribution of Sn mineralization are (i) the distribution of
156 intensely altered sedimentary protoliths in the melting volume and (ii) the availability of a heat
157 source to facilitate biotite-controlled anhydrous melting (Romer and Kroner, 2015, 2016). The
158 exogenic chemical alteration of the protolith results in a residual enrichment of Sn and W, but more
159 importantly the loss of Na and Ca results in a protolith that during prograde metamorphism stabilizes
160 large amounts of muscovite and biotite. This, in turn, allows for the generation of large amounts of
161 melt and multiple stages of melt extraction (Wolf et al., 2018). Tin and tungsten may behave
162 differently during partial melting, depending largely on the restite mineralogy. During muscovite-
163 controlled anhydrous melting, Sn partitions preferentially into the restite, whereas W may remain
164 in the melt. Thus, the loss of these low-temperature melts (c. 720-740 °C, Viruete et al., 2000) results
165 in the enrichment of Sn in the restite and may deplete W in the restite. Biotite-controlled anhydrous
166 melting of the restite at higher temperature (c. >800 °C, Barbero, 1995) results in melts that may be
167 strongly enriched in Sn (Wolf et al., 2018).

168 We estimated the temperature of melting of Sn-, Sn-W-, and W-related granites using the
169 temperature of zircon-saturation (Watson and Harrison, 1983). The various granites in the region
170 show systematically lower zircon-saturation temperatures for more evolved samples that have
171 experienced fractional crystallization (Supplementary Fig. 1). Thus, the least evolved samples of
172 individual granite suites provide the best estimates of the melting temperature. The Sn and Sn-W
173 granites along the Chenzhou-Linwu fault in the western part of the Nanling region yield significant
174 higher melting temperatures (>800 °C) than the W-related granites in the eastern part (<750 °C; Fig.
175 3; Supplementary Fig. 1), which implies that the region along the Chenzhou-Linwu fault reached

176 higher temperature. This suggests that the spatial separation of Sn and W mineralization may be
177 related to the source rock mineralogy and temperature of melting. Some Sn (W)-bearing granites in
178 the western part of the Nanling region have higher Nb/Ta ratios than those of the W-bearing granites
179 (Fig. 2), which may also reflect differences in the extent of melting or different mineral assemblages
180 in the restite (Ballouard et al., 2016).

181 Internal heating of orogenically thickened crust may possibly generate minimum-temperature
182 melts by muscovite decomposition. Higher temperatures, however, are needed for biotite-controlled
183 anhydrous melting and this requires input of heat from the mantle (e.g., Clark et al., 2011), which
184 may be accomplished by the input of mantle melts in subduction and extensional zones or the
185 tectonic emplacement of UHT metamorphic rocks in collisional orogens (e.g., Romer and Kroner,
186 2015, 2016). In the Nanling region, Late Jurassic granitic magmatism took place in response to the
187 opening of a large slab window or the development of an intra-arc rift during the subduction of the
188 Palaeo-Pacific plate.

189 The Late Jurassic granites with associated Sn and W mineralization show a broad range of
190 whole-rock Nd and zircon Hf isotopic compositions. Consistent with the spatial separation of the
191 Sn and W mineralization, granites with associated Sn (W) mineralization along the Chenzhou-
192 Linwu fault in the western part of the Nanling region have significantly higher whole-rock ϵNd and
193 zircon ϵHf values than those associated with W mineralization in the eastern part (Fig. 4;
194 Supplementary Tables 1 and 2). The strongly negative ϵNd (-15.5~-9.8, Fig. 4; Supplementary Table
195 1) values of granites with associated W deposits reflect the melting of old continental crust. The
196 regionally contrasting Nd and Hf isotopic composition of granites could indicate differences in the
197 “average” age of the crustal blocks on both sides of the Chenzhou-Linwu fault or variable input of

198 mantle-derived melts in the source region of the granites with associated Sn mineralization.

199 Based on previous studies, the Mesozoic W-Sn-related granites in the Nanling region were
200 mainly derived from the regional metamorphic basement that was previously considered to have
201 formed in the Paleo-Mesoproterozoic (Xu et al., 2005). Recent detrital zircon dating and
202 geochemical studies of the basement metamorphic rocks from the western, central and eastern parts
203 of the Nanling region have shown that the protoliths to the granites are mainly late Neoproterozoic
204 metasedimentary rocks with major contributions from Grenvillian (1000 – 900 Ma) and
205 Mesoproterozoic sources and a minor contribution from an Archaean source. The geochemical
206 studies have also shown that these metasedimentary rocks do not vary significantly in composition
207 across the Nanling region, and are characterized by high La/Yb, a negative Eu anomaly, high
208 K_2O/Na_2O , La/Co and Th/Sc ratios and low Cr/Zr ratios. This suggests a high degree of maturity of
209 the supracrustal source, which was probably located along the northern margin of East
210 Gondwanaland (Yu et al., 2005, 2006a, b; Wei et al., 2009).

211 From the above observations, the metamorphic basement in the Nanling region is interpreted
212 to have formed after the assembly of the Yangtze Craton and Cathaysia Block and, thus, its
213 composition and distribution were not controlled by the Chenzhou-Linwu fault. This is also
214 supported by the observation that most of the Sn (W) deposits are located relatively the Chenzhou-
215 Linwu fault. Therefore, the contrasting Nd and Hf isotopic compositions of the ore-related granites
216 in the western and eastern parts of the Nanling region likely reflect variable inputs of mantle-derived
217 melts in the source region of the granites with associated Sn mineralization rather than differences
218 in the “average” age of the crustal blocks on opposite sides of the Chenzhou-Linwu fault.

219 It is notable that mantle-derived mafic microgranular enclaves (MMEs) are ubiquitous in the

220 western part of the Nanling region, most prominently in the Furong Sn granite and Lisong granite
221 whereas they are absent in granitic rocks in the eastern part of the Nanling region (Li et al., 2009;
222 Zhao et al., 2012). It is also of note that zircon collected from MMEs in the Lisong granite have
223 high $\epsilon_{\text{Hf}}(t)$ (3.1~8.0) and low $\delta^{18}\text{O}$ (5.1‰~6.5‰) values, suggesting that they crystallized in
224 equilibrium with mantle-derived melts (Li et al., 2009). Moreover, He-Ar isotopic studies of pyrite
225 from Sn- and Sn-W deposits in the western part of the Nanling region provide evidence for a
226 significant mantle input, whereas corresponding studies of W deposits in the eastern part of the
227 regions indicate that the mantle input was insignificant (Li Z.L., et al., 2007; Li G.L., et al., 2011).
228 Because of the low Sn content of the mantle (0.6 ppm; Lehmann, 1990), the role of the mantle was
229 not to provide a source for Sn, but rather to supply the heat needed to generate high-temperature
230 granitic melts.

231

232 **A Model for the spatial decoupling of W and Sn deposits**

233 Anhydrous melting is controlled by the breakdown of hydrous minerals such as muscovite, biotite
234 and amphibole (Clemens and Viezeuf, 1987). The amount of melt formed by muscovite breakdown
235 in pelitic rocks depends on the proportion of muscovite (Clemens and Viezeuf, 1987; Breton and
236 Thompson, 1988), which may be high in intensely altered metamorphosed sedimentary rocks that
237 have low contents of Ca and Na (cf. Wolf et al., 2018). Melting by biotite-breakdown requires higher
238 temperature (Clemens and Viezeuf, 1987; Schmidt et al. 2004) and is only possible with heat input
239 from the mantle (Clark et al. 2011).

240 The behavior of Sn and W during partial melting is controlled by the stability of their host and
241 whether the released Sn and W remain in the melt or partition back into restite minerals, which

242 depends on the P-T conditions of melting and the mineral assemblage of the restite. The available
243 evidence suggests that biotite incorporates Sn more easily than does muscovite and consequently
244 low-temperature melts lose Sn as long as biotite is stable in the restite (Chappell et al., 1987; Simons
245 et al., 2017). Thus, during low-temperature melting Sn remains preferentially in the restite (Wolf et
246 al., 2018) and may be repartitioned from the melt into restite biotite to a much higher extent than W.
247 Tin is released mostly during biotite melting. These observations suggest that the regional separation
248 of Sn and W deposits may result from differences in the temperature at which the protoliths for the
249 corresponding granites melt.

250 The separation of the mineralization in the Nanling region into a western Sn, Sn-W domain
251 and an eastern W domain is consistent with the higher melting temperature of the protoliths forming
252 the Sn and Sn-W granites compared to that of the protoliths for the W granites in the east (Fig. 1,
253 3). It is also consistent with the higher whole rock ϵ_{Nd} and zircon ϵ_{Hf} values of the Sn granites
254 relative to the W granites (Figs. 4), and the abundance of mantle-derived MMEs in the Sn and Sn-
255 W granites but not in the W granites. We therefore propose that the spatial decoupling of Sn and W
256 mineralization in the Nanling Region was a direct response to the difference in the temperature of
257 melting of the protoliths for the corresponding granites. This also satisfactorily explains why the
258 Sn-W deposits are associated with the Sn(W) deposits in the west but not the W-only deposits in the
259 east (Fig. 1); melting temperatures in the west were high enough to melt both muscovite (the source
260 of W) and biotite (the main source of Sn).

261 The Late Jurassic granitic rocks and associated W-Sn mineralization in the region are
262 interpreted to have resulted from extension above the subducting Palaeo-Pacific plate that led to the
263 creation of a large slab window or intra-arc rift (Jiang et al., 2009; Mao et al., 2013). The deep

264 Chenzhou-Linwu fault in the western part of the belt, which represents a major tectonic boundary
265 separating the Yangtze and Cathaysia blocks (Wang et al., 2003), may have localized the upwelling
266 of mantle material, thereby accounting for both the higher melting temperature and the addition of
267 mantle melts to the Late Jurassic granites that are associated with Sn and Sn-W mineralization in
268 the western part of the Nanling belt.

269 The model proposed above, which involves differences in the protolith melting temperature
270 and thus mobilization temperature for Sn and W, is potentially applicable to any Sn-W metallogenic
271 province in which the Sn deposits occur separately from the W deposits. Simply put, granites with
272 associated W mineralization reflect muscovite-dehydration melting, whereas granites with
273 associated Sn mineralization reflect biotite-dehydration melting, possibly with an earlier loss of
274 low-temperature melts. At a low temperature of melting (muscovite-dehydration melting), W is
275 partitioned preferentially into the melt, whereas Sn remains in the restite.

276

277 **Acknowledgements**

278 This research was supported financially by the National Natural Science Foundation of China
279 (Nos. 41822304, 41672095, 41373047) and the National Nonprofit Institute Research Grant of
280 CAGS (YYWF201711).

281

282

283 **References:**

284 Ballouard, C., Poujol, M., Boulvais, P., Branquet, Y., Tartèse, R., and Vigneresse, J.L., 2016, Nb-Ta
285 fractionation in peraluminous granites: A marker of the magmatic-hydrothermal transition:

- 286 Geology, v. 44, p. 231-234.
- 287 Barbero, L., 1995, Granulite-facies metamorphism in the Anatectic Complex of Toledo, Spain: late
288 Hercynian tectonic evolution by crustal extension: *Journal of the Geological Society*, v. 152, p.
289 365-382.
- 290 Blevin, P.L., and Chappell, B.W., 1992, The role magma sources, oxidation states and fractionation
291 in determining the granite metallogeny of eastern Australia: *Earth and Environmental Science*
292 *Transactions of the Royal Society of Edinburgh*, v. 83, p. 305-316.
- 293 Breton, N.L., and Thompson, A.B., 1988, Fluid-absent (dehydration) melting of biotite in
294 metapelites in the early stages of crustal anataxis: *Contrib. Mineral Petrol*, v. 99, p. 226-237.
- 295 Burnham, C.W., and Ohmoto, H., 1980, Late-stage processes of felsic magmatism, *in* Ishihara, S.,
296 and Takenouchi, S. eds., *Granitic Magmatism and Related Mineralization: Mining Geology*
297 *Special Issue*, v. 8, p. 1-11.
- 298 Chappell, B.W., White, A.J.R., and Wyborn, D., 1987, The importance of residual source material
299 (restite) in granite petrogenesis: *Journal of Petrology*, v. 28, p. 1111-1138.
- 300 Chen, J.F., and Jahn, B.M., 1998, Crustal evolution of southeastern China: Nd and Sr isotopic
301 evidence: *Tectonophysics*, v. 284, p. 101-133.
- 302 Cheng, Y., Spandler, C., Chang, Z., and Clarke, G., 2018, Volcanic-plutonic connections and metal
303 fertility of highly evolved magma systems. A case study from the Herberton Sn-W-Mo
304 Mineral Field, Queensland, Australia: *Earth and Planetary Science Letters*, v. 486, p. 84-93.
- 305 Clark, C., Fitzsimmons, I.C.W., and Healy, D., 2011, How does the continental crust get really hot?:
306 *Elements*, v. 7, p. 235-240.
- 307 Clemens, J.D., and Vielzeuf, D., 1987, Constraints on melting and magma production in the crust:

- 308 Earth and Planetary Science Letters, v. 86, p. 287-306.
- 309 Hu, R.Z., and Zhou, M.F., 2012, Multiple Mesozoic mineralization events in South China—an
310 introduction to the thematic issue: *Mineralium Deposita*, v. 47, P. 579-588.
- 311 Hu, R.Z., Chen, W.T., Xu, D.R., and Zhou, M.F., 2017, Reviews and new metallogenic models of
312 mineral deposits in South China: An introduction: *Journal of Asian Earth Sciences*, v.137, p. 1-
313 8.
- 314 Hu, R.Z., Wei, W.F., Bi, X.W., Peng, J.T., Qi, Y.Q., Wu, L.Y., and Chen, Y.W., 2012, Molybdenite
315 Re-Os and muscovite $^{40}\text{Ar}/^{39}\text{Ar}$ dating of the Xihuashan tungsten deposit, central Nanling
316 district, South China: *Lithos*, v. 150, p. 111-118.
- 317 Ishihara, S., 1977, The magmetite-series and ilmenite-series granitic rocks: *Mining Geology*, v.27,
318 p. 293-305.
- 319 _____ 1981, The granitoid series and mineralization: *Economic Geology*, v. 75, p. 458-484.
- 320 Jiang, Y.H., Jiang, S.Y., Dai, B.Z., Liao, S.Y., Zhao, K.D., and Ling, H.F., 2009, Middle to late
321 Jurassic felsic and mafic magmatism in southern Hunan Province, southeast China:
322 Implications for a continental arc to rifting: *Lithos*, v. 107, p. 185-204.
- 323 Lehmann, B., 1990, *Metallogeny of tin*: Berlin, Springer, 211 p.
- 324 Li, G.L., Hua, R.M., Zhang, W.L., Hu, D.Q., Wei, X.L., Huang, X.E., Xie, L., Yao, J.M., and Wang,
325 X.D., 2011, He-Ar isotope composition of pyrite and wolframite in the Tieshanlong tungsten
326 deposit, Jiangxi, China: Implications for fluid evolution: *Resource Geology*, v. 61, p. 356-366.
- 327 Li, X.H., Li, W.X., Wang, X.C., Li, Q.L., Liu, Y., and Tang, G.Q., 2009, Role of mantle-derived
328 magma in genesis of early Yanshanian granites in the Nanling Range, South China: in situ
329 zircon Hf-O isotopic constraints: *Science in China series D: Earth Sciences*, v. 52, p. 1262-1278.

- 330 Li, Y.Q., and Zhong, X.Y., 1991, Mineralogy of tungsten deposits in Nanling and neighboring area,
331 China: China University of Geosciences Press, Wuhan, p, 1-455(in Chinese with English
332 abstract.
- 333 Li, Z.L., Hu, R.Z., Yang, J.S., Peng, J.T., Li, X.M., Bi, and X.W., 2007, He, Pb and S isotopic
334 constraints on the relationship between the A-type Qitianling granite and the Furong tin deposit,
335 Hunan Province, China: *Lithos*, v. 97, p. 161-173.
- 336 Liu, X.C., Xing, H.L., and Zhang, D.H., 2014, Fluid focusing and its link to vertical morphological
337 zonation at the Dajishan vein-type tungsten deposit, South China: *Ore Geology Reviews*, v. 62,
338 p. 245-258.
- 339 Lu, H.Z., Liu, Y.M., Wang, C.L., Xu, Y.Z., and Li, H.Q., 2003, Mineralization and fluid inclusion
340 study of the Shizhuyuan W-Sn-Bi-Mo-F skarn deposit, Hunan Province, China: *Economic
341 Geology*, v. 98, p. 955-974.
- 342 Mao, J.W., Cheng, Y.B., Chen, M.H., and Pirajno, F., 2013, Major types and time-space distribution
343 of Mesozoic ore deposits in South China and their geodynamic setting: *Mineralium Deposita*,
344 v. 48, p. 267-294.
- 345 Mao, J.W., Xie, G.Q., Guo, C.L., and Chen, Y.C., 2007, Large-scale tungsten-tin mineralization in
346 the Nanling region, South China: Metallogenic ages and corresponding geodynamic processes:
347 *Acta Petrologica Sinica*, v. 23, p. 2329-2338 (in Chinese with English Abstract).
- 348 Meinert, L.D., Dipple, G.M., and Nicolescu S., 2005, World skarn deposits: *Economic Geology*, v.
349 100th Anniversary, p. 299-336.
- 350 Ni, P., Wang, X.D., Wang, G.G., Huang, J.B., Pan, J.Y., and Wang, T.G., 2015, An infrared
351 microthermometric study of fluid inclusions in coexisting quartz and molframite from Late

- 352 Mesozoic tungsten deposits in the Gannan metallogenic belt, South China: *Ore Geology*
353 *Reviews*, v. 65, p. 1062-1077.
- 354 No. 932 Team, Guangdong Metallurgical Geological Exploration Corp., 1966, How to apply the
355 “five-floor mineral model” to assessment, prospecting and exploration for the wolframite-
356 quartz vein type of tungsten deposits: *Geol. Explor.*, v.5, p. 15-19 (in Chinese).
- 357 Romer, R.L., and Kroner, U., 2015, Sediment and weathering control on the distribution of
358 Paleozoic magmatic tin-tungsten mineralization: *Mineralium Deposita*, v. 50, p. 327-338.
- 359 _____ 2016, Phanerozoic tin and tungsten mineralization—tectonic controls on the distribution of
360 enriched protoliths and heat sources for crustal melting: *Gondwana Research*, v. 31, p.60-95.
- 361 Sato, K., 2012, Sedimentary crust and metallogeny of granitoid affinity: implications from the
362 geotectonic histories of the Circum-Japan Sea Region, Central Andes and southeastern
363 Australia: *Resource Geology*, v. 62, p. 329–351.
- 364 Schmidt, C., 2018, Formation of hydrothermal tin deposits: Raman spectroscopic evidence for an
365 important role of aqueous Sn(IV) species: *Geochimica et Cosmochimica Acta*, v. 220, p. 499–
366 511.
- 367 Schmidt, M.W., Vielzeuf, D., and Auzanneau, E., 2004. Melting and dissolution of subducting crust
368 at high pressures: the key role of white mica: *Earth and Planetary Science Letters*, v. 228, p.
369 65-84.
- 370 Simons, B., Andersen, J.C., Shail, R.K., and Jenner, F.E., 2017, Fractionation of Li, Be, Ga, Nb, Ta,
371 In, Sn, Sb, W and Bi in the peraluminous Early Permian Variscan granites of the Cornubian
372 Batholith: precursor processes to magmatic-hydrothermal mineralization: *Lithos*, v. 278, p.
373 491-512.

- 374 Viruete, J.E., Indares, A., and Arenas, R., 2000, P-T paths derived from garnet growth zoning in an
375 extensional setting: an example from the Tormes gneiss dome (Iberian massif, Spain): *Journal*
376 *of Petrology*, v. 41, p. 1489-1515.
- 377 Wang, Y.J., Fan, W.M., Guo, F., Peng, T.P., and Li, C.W., 2003, Geochemistry of Mesozoic mafic
378 rocks adjacent to the Chenzhou-Linwu fault, South China: implications for the lithospheric
379 boundary between the Yangtze and Cathaysia blocks: *International Geology Review*, v. 45, p.
380 263-286.
- 381 Watson, E.B., and Harrison, T. M., 1983, Zircon saturation revisited: temperature and composition
382 effects in a variety of crustal magma types: *Earth and Planetary Science Letters*, v. 64, p. 295-
383 304.
- 384 Wei, Z.Y., Yu, J.H., Wang, L.J., and Shu, L.S., 2009, Geochemical features and tectonic
385 significances of Neoproterozoic metasedimentary rocks from Nanling Range: *Geochimica*, v.
386 38, p. 1-19. (in Chinese with English abstract)
- 387 Wolf, M., Romer, R.L., Franz, L., and López-Moro, F.J., 2018, Tin in granitic melts: The role of
388 melting temperature and protholith composition: *Lithos*, v. 310-311, p. 20-30.
- 389 Wu, Y.L., Mei, Y.W., Liu, P.C., Cai, C.L., and Lu, T.Y., 1987, *Geology of Xihuashan tungsten deposit*:
390 Geol. Publ. House, Beijing, China, p. 320 (in Chinese).
- 391 Xu, X.S., O'Reilly, S.Y., Griffin, W.L., Deng, P., and Pearson, N.J., 2005, Relict Proterozoic
392 basement in the Nanling Mountains (SE China) and its tectonothermal overprinting. *Tectonic*,
393 v. 24, TC2003.
- 394 Yao, Y., Chen, J., Lu, J.J., Wang, R.C., and Zhang, R.Q., 2014, Geology and genesis of the
395 Hehuaping magnesian skarn-type cassiterite-sulfide deposit, Hunan Province, southern China:

- 396 Ore Geology Reviews, v. 58, p. 163-184.
- 397 Yu, J.H., Wang, L.J., Zhou, X.M., Jiang, S.Y., Wang, R.C., Xu, X.S., and Qiu, J.S., 2006a,
398 Compositions and formation history of the basement metamorphic rocks in Northeastern
399 Guangdong Province: *Earth Sci.* v. 31, p. 38-48. (in Chinese with English abstract)
- 400 Yu J.H., Wei Z.Y., Wang L.J., Wang R.C., Jiang S.Y., Shu L.S., and Sun T., 2006b, Cathaysia Block:
401 A young continent composed of ancient materials: *Geol. J. China Univ.* v. 12, p. 440-447. (in
402 Chinese with English abstract)
- 403 Yu J.H., Zhou X.M., O'Reilly S.Y., Zhao L., Griffin W.L., Wang R.C., Wang L.J., and Chen X.M.,
404 2005, Formation history and protolith characteristics of granulites facies metamorphic rock in
405 Central Cathaysia deduced from U-Pb and Lu-Hf isotopic studies of single zircon grains:
406 *Chinese Sci. Bull.*, v. 50, p. 2080-2089.
- 407 Yuan, S.D., Peng, J.T., Hao, S., Li, H.M., Geng, J.Z., and Zhang, D.L., 2011, In situ LA-MC-ICP-
408 MS and ID-TIMS U-Pb geochronology of cassiterite in the giant Furong tin deposit, Hunan
409 Province, South China: New constraints on the timing of tin-polymetallic mineralization: *Ore
410 Geology Reviews*, v. 43, p. 235-242.
- 411 Yuan, S.D., Peng, J.T., Hu, R.Z., Li, H.M., Shen, N.P., and Zhang, D.L., 2008, A precise U-Pb age
412 on cassiterite from the Xianghualing tin-polymetallic deposit (Hunan, South China):
413 *Mineralium Deposita*, v. 43, p. 375-382.
- 414 Yuan, S.D., Williams-Jones, A.E., Mao, J.W., Zhao, P.L., Yan, C., and Zhang, D.L., 2018, The origin
415 of the Zhangjialong tungsten deposit, South China: implications for W-Sn mineralization in
416 large granite batholiths: *Economic Geology*, v.113, p. 1193-1208.
- 417 Zhao, J.H., Zhou, M.F., Yan, D.P., Zheng, J.P., and Li, J.W., 2011, Reappraisal of the ages of

418 Neoproterozoic strata in South China: No connection with the Grenvillian orogeny: *Geology*,
419 v. 39, p. 299-302.

420 Zhao, K.D., Jiang, S.Y., Yang, S.Y., Dai, B.Z., and Lu, J.J., 2012, Mineral chemistry, trace elements
421 and Sr-Nd-Hf isotope geochemistry and petrogenesis of Cailing and Furong granites and mafic
422 enclaves from the Qitianling batholith in the Shi-Hang zone, South China: *Gondwana Research*,
423 v. 22, p. 310-324.

424 Zhao, P.L., Yuan, S.D., Mao, J.W., Yuan, Y.B., Zhao, H.J., Zhang, D.L., and Shuang, Y., 2018,
425 Constraints on the timing and genetic link of the large-scale accumulation of proximal W-Sn-
426 Mo-Bi and distal Pb-Zn-Ag mineralization of the world-class Dongpo orefield, Nanling Range,
427 South China: *Ore Geology Reviews*, v. 95, p. 1140-1160.

428

429

430 **Figure captions**

431

432 Figure 1. A: The location of Jurassic to Cretaceous W/Sn deposits and associated granites in South
433 China (adapted from Mao et al., 2013). B: The distribution of Late Jurassic (160-150 Ma) W, Sn,
434 and Sn-W deposits and associated granites in the Nanling region, South China (modified from Zhao
435 et al., 2018).

436

437 Figure 2. Plot of $\text{Fe}_2\text{O}_3/\text{FeO}$ versus (A) SiO_2 , (B) Rb/Sr , (C) Nb/Ta , and (D) Zr/Hf , (C) A/NK versus
438 A/CNK , and (D) A/CNK versus $\epsilon_{\text{Nd}}(t)$ values for Late Jurassic (160-150 Ma) W-, Sn-, and Sn-W-
439 related granites in the Nanling region. Symbols as in Fig. 1B. Data are from Supplementary Table

440 1.

441

442 Figure 3. A plot of average zircon saturation temperature (T_{Zr}) versus vertical distance to the
443 Chenzhou-Linwu (CL) Fault. The maximum temperature for individual intrusions was used to
444 represent the initial magmatic temperature (see Supplementary Figure 1). Symbols as in Fig. 1B.

445

446 Figure 4. Probability distributions of (A) $\epsilon_{Nd}(t)$ values and (B) zircon $\epsilon_{Hf}(t)$ values for Late Jurassic
447 (160-150 Ma) W-, Sn-, and Sn-W-related granites in the Nanling region. The color of the lines is as
448 in Fig. 1B.

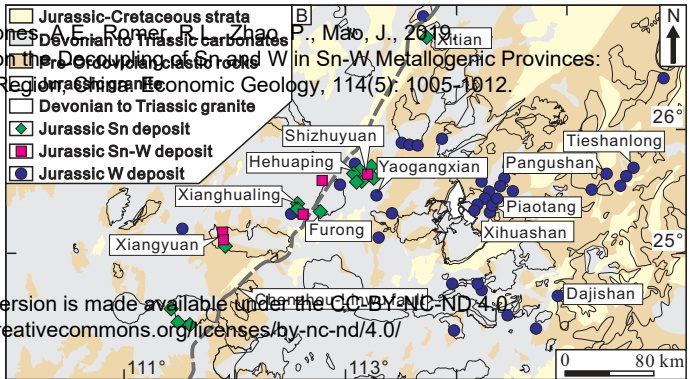
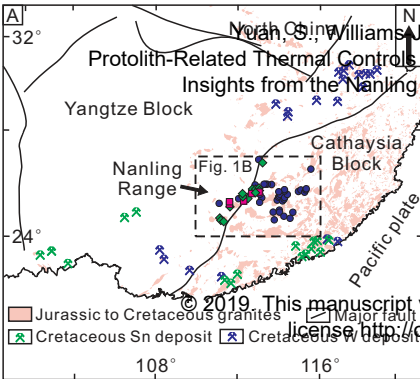
449

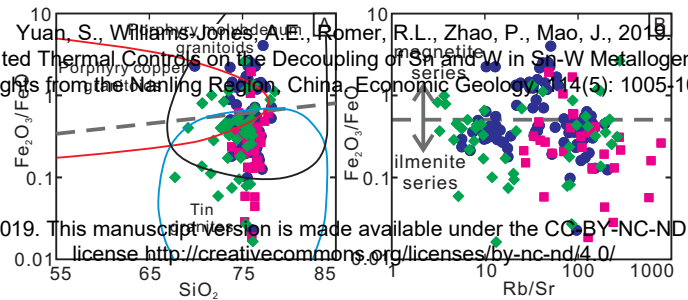
450 Supplementary Figure 1. Plots of zircon saturation temperature (T_{Zr} °C) versus Nb/Ta and Zr/Hf
451 ratios for the W-, Sn- and Sn-W-related granites in the Nanling region. The maximum zircon
452 saturation temperature was taken to approximate the initial magma temperature (see Watson and
453 Harrison, 1983). The Nb/Ta and Zr/Hf ratios are assumed to represent the degree of fractional
454 crystallization, except in the case of deposits hosting Nb-Ta mineralization (e.g., Xianghualing), for
455 which the Nb/Ta ratio may be an unreliable index of fractional crystallization. Symbols as in Fig.

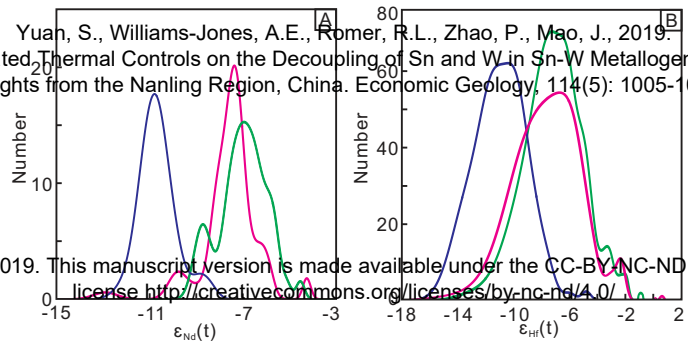
456 1B.

457

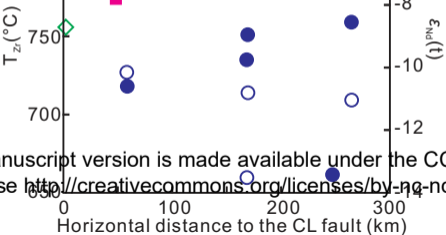
458







Williams-Jones, A.E., Romer, R.L., Zhao, P., Ma
Controls on the Decoupling of Sn and W in Sn-W
the Nanling Region, China. *Economic Geology*, 11



manuscript version is made available under the CC
se <http://creativecommons.org/licenses/by-nc-nd/4.0/>

Table DR1 Whole-rock geochemical and Sm-Nd isotopic data of the representative Late Jurassic (160-150 Ma) W-Sn-related granite in the Nanling region, South China

Deposit	Sample Number	Rock type	SiO ₂	TiO ₂	Al ₂ O ₃	TFe ₂ O ₃	FeO	Fe ₂ O ₃	MnO	MgO	CaO	Na ₂ O	K ₂ O	P ₂ O ₅	La	Ce	Pr	Nd	Sm	Eu
Xihuashan W deposit	XHS-3		75.95	0.13	12.82	1.4	0.8	0.51	0.07	0.22	0.64	3.03	4.95	0.05	33.4	63.7	8.02	29.5	7.75	0.39
	XHS-4		75.39	0.12	12.95	1.57	0.94	0.52	0.07	0.2	0.47	2.85	5.27	0.04	21.6	41.5	5.86	23.4	8.72	0.29
	XHS-7		75.84	0.08	12.83	1.23	0.87	0.26	0.07	0.16	1	3.39	4.56	0.02	15.9	35.7	4.48	18	6.52	0.29
	XHS-8		76.47	0.07	12.73	1.17	0.78	0.3	0.07	0.16	0.9	3.35	4.66	0.03	14.8	31.7	4.22	16.9	6.22	0.23
	XHS-9		74.53	0.09	13.25	1.28	0.88	0.31	0.07	0.17	0.96	3.42	4.86	0.04	16.7	35.5	4.71	19.1	7	0.35
	XHS-10	The first	74.71	0.1	13.31	1.24	0.94	0.2	0.07	0.19	1.09	3.36	4.95	0.03	16.9	36.4	4.83	19.7	6.84	0.41
	XHS-11	medium-grained	77.01	0.1	12.1	1.45	1.02	0.32	0.08	0.2	0.98	3.18	4.5	0.03	19	44.7	5.67	23.3	8.29	0.28
	XHS-25	porphyritic	74.61	0.14	13.42	1.59	1.13	0.33	0.06	0.29	1.35	2.86	5.15	0.04	17.9	37.3	4.92	19.8	6.37	0.5
	XHS-30	biotite granite	75.51	0.09	12.69	1.35	0.88	0.37	0.07	0.15	1.03	3.23	4.81	0.03	26.5	55	6.61	24.4	6.54	0.3
	XHS-31		76.05	0.08	12.62	1.18	0.77	0.33	0.07	0.13	0.92	3.22	4.88	0.02	27.3	55.9	6.51	23.8	6.47	0.28
	XHS-32		76.45	0.09	12.41	1.38	0.91	0.36	0.08	0.16	0.95	3.12	4.84	0.03	23.4	50.7	6.24	23.9	7.29	0.3
	XHS-33		75.15	0.09	13.06	1.31	0.89	0.32	0.07	0.15	1.01	3.19	5.19	0.03	26.9	57.6	6.89	25.9	6.89	0.32
	XHS-34		76.78	0.09	11.99	1.38	0.94	0.34	0.08	0.15	0.88	3.09	4.69	0.03	18.6	39.3	4.95	19.2	5.66	0.26
	XHS-35		74.77	0.09	13.26	1.17	0.78	0.3	0.07	0.14	1.04	3.43	5.07	0.03	22	47.1	5.8	22.2	6.86	0.41
	X09-3		75.79	0.02	13.07	0.86	0.54	0.26	0.12	0.05	0.46	3.99	4.4	0.01	5.9	15.2	2.49	11.8	7.06	0.071
	X09-4		76.31	0.01	13.02	0.75	0.56	0.13	0.12	0.06	0.51	4.14	4.48	0.01	4.98	12.6	2.06	9.84	6.25	0.054
	X09-5	The second	76.01	0.02	12.94	0.78	0.56	0.15	0.11	0.07	0.54	3.92	4.63	0.01	6.99	16.7	2.52	11.1	6.05	0.095
	XHS-1	garnet-bearing	76.8	0.01	12.66	0.79	0.62	0.1	0.11	0.04	0.6	3.8	4.69	0.01	4.49	12.9	2.41	12.7	8.73	0.06
	XHS-2	fine-grained	76.03	0.01	13.06	0.86	0.61	0.18	0.11	0.04	0.55	4.02	4.66	0.01	4.68	11.3	1.85	8.89	5.64	0.061
XHS-12	biotite granite	75.67	0.01	13.26	0.65	0.42	0.19	0.06	0.04	0.54	3.99	4.71	0.01	6.33	16.2	2.68	12.9	7.84	0.067	
XHS-13		75.52	0.02	13.01	0.77	0.51	0.21	0.08	0.05	0.6	4.11	4.58	0.01	8.1	21.5	3.4	15.6	9.5	0.069	

XHS-14		75.69	0.02	12.93	0.75	0.55	0.14	0.1	0.05	0.64	4.13	4.36	0.01	5.38	13.7	2.27	11	6.96	0.063
XHS-21		76.09	0.02	12.95	0.85	0.56	0.23	0.09	0.06	0.65	4.14	4.35	0.01	7.24	19.3	3.3	16	10.7	0.057
XHS-22		76.2	0.02	12.91	0.82	0.54	0.22	0.08	0.06	0.71	4.04	4.35	0.01	6.67	16.4	2.62	12.1	6.98	0.1
XHS-23		75.81	0.01	13.02	0.83	0.56	0.21	0.08	0.04	0.59	4.02	4.66	0.01	5.02	12.9	2.1	10.3	6.45	0.065
XHS-24		76.19	0.02	13.11	0.82	0.49	0.28	0.07	0.04	0.58	4.13	4.41	0.01	6.26	16.5	2.86	14.2	9.22	0.066
XHS-15		75.33	0.08	12.96	1.61	1.09	0.4	0.1	0.12	0.7	3.49	4.51	0.03	27.7	63.5	7.84	30.5	10.6	0.26
XHS-16		75.59	0.07	12.74	1.34	0.5	0.78	0.1	0.13	0.59	3.45	4.52	0.03	27.1	60.4	7.37	28.9	10	0.23
XHS-17		74.97	0.09	13.43	1.58	1.5	-	0.1	0.13	0.75	3.58	4.64	0.03	37.6	84.7	10.5	41.3	13.8	0.29
XHS-18	The third garnet-bearing	75.82	0.08	13.06	1.2	0.81	0.3	0.1	0.13	0.57	3.51	4.78	0.03	28.7	64	7.71	29.8	10.2	0.24
XHS-19	fine-grained	75.88	0.06	13.09	1	0.65	0.28	0.1	0.11	0.7	3.73	4.54	0.02	25.5	59.5	7.34	29.4	10.7	0.18
XHS-20	porphyritic	75.1	0.08	12.94	1.34	0.93	0.3	0.09	0.15	0.69	3.6	4.55	0.03	31	67.6	8.45	33.2	11.5	0.25
XHS-26	biotite granite	78.07	0.04	12.08	0.78	0.48	0.25	0.09	0.08	0.44	3.71	4.23	0.02	13.5	32.9	4.19	17	7.16	0.093
XHS-27		76.03	0.07	13	1.09	0.71	0.3	0.07	0.13	0.6	3.54	4.87	0.03	25.8	57.9	7.24	28.7	10	0.22
XHS-28		76.26	0.03	12.66	0.79	0.54	0.19	0.09	0.06	0.52	3.88	4.7	0.01	11.3	25.8	3.44	13.4	5.74	0.077
XHS-29		76.29	0.03	12.84	0.82	0.6	0.15	0.09	0.05	0.55	4.03	4.48	0.01	10.9	24.4	3.42	13.6	6.25	0.064
X-1		73.85	0.06	12.66		0.84	0.15	0.06	0.46	1.29	3.63	4.46	0.02	12.9	27.9	3.62	16.1	6.64	0.23
X-2		74.51	0.09	13.73		1.04	0.3	0.07	0.15	0.96	3.68	4.76	0.03	16.3	34.5	4.36	18.3	7.03	0.28
X-4	Medium-grained	75.6	0.08	13.33		1.1	0.25	0.07	0.14	0.93	4.55	4.27	0.03	10.4	22	2.88	12.5	5.6	0.25
X-5	porphyritic	75.55	0.09	13.45		1.15	0.31	0.07	0.16	0.98	4.07	4.43	0.03	13.2	27.9	3.63	15.6	6.65	0.28
X-6	biotite granite	75.1	0.1	12.82		1.19	0.32	0.08	0.18	0.89	5.23	4.21	0.03	18.4	39.3	4.97	20.6	7.72	0.29
X-18		74.38	0.09	13.09		0.88	0.37	0.07	0.13	0.99	3.8	4.74	0.02	15.4	32.7	4.12	17.3	6.24	0.3
X-19		74.77	0.09	12.67		0.85	0.34	0.07	0.12	1.03	4.11	4.33	0.02	17	36.3	4.58	19.4	7.27	0.29
X-21		75.39	0.07	13.01		0.75	0.24	0.06	0.08	0.89	3.79	4.65	0.01	11.3	26.6	3.53	16.1	7.21	0.23
X-8	Medium-grained	76.26	0.02	13.05		0.45	0.16	0.11	0.03	0.49	4.69	4.41	0.003	5.8	15.6	2.34	11.8	7.81	0.05
X-9	biotite granite	75.58	0.02	12.99		0.62	0.23	0.09	0.03	0.59	4.24	4.24	0.003	4.8	11.4	1.73	8.1	4.9	0.06

	X-11		75.7	0.02	12.93	0.71	0.25	0.1	0.02	0.61	4.26	4.42	0.002	4.08	10.4	1.49	7.25	4.56	0.06
	X-12		76.1	0.02	13.49	0.48	0.22	0.1	0.04	0.57	4.93	4.23	0.003	4.51	11.5	1.62	7.68	4.53	0.06
	X-13		75.7	0.03	12.96	0.52	0.23	0.09	0.03	0.64	4.61	4.23	0.005	8.71	20.6	2.79	12.6	6.21	0.1
	X-14		75.85	0.02	12.87	0.5	0.19	0.08	0	0.55	4	4.64	0.002	4.58	11.6	1.67	7.84	4.4	0.06
	X-16		75.4	0.02	12.96	0.59	0.24	0.07	0.01	0.57	4.19	4.47	0.001	4.59	13.1	1.96	9.22	5.5	0.06
	X-17		75.71	0.02	12.95	0.56	0.17	0.1	0	0.56	4.18	4.36	0.001	4.52	13.1	2.16	11.2	8.17	0.05
	X-20		76.1	0.02	12.87	0.44	0.28	0.08	0.03	0.62	4.65	4.16	0.003	5.53	14.2	2.04	9.54	5.65	0.06
	X-22		76.49	0.02	12.51	0.53	0.29	0.09	0.06	0.66	4.18	4.36	0.003	5.12	13.1	1.96	9.33	6.04	0.08
	X-23		75.43	0.02	12.93	0.48	0.27	0.11	0.01	0.59	4.28	4.14	0.001	4.8	14	2.36	12.7	8.96	0.06
	X-10	Fine-grained	76.42	0.02	13.08	0.6	0.27	0.15	0.03	0.51	4.6	4.23	0.001	3.97	11.3	2.05	11.3	8.7	0.05
	X-7	two-mica granite	75.7	0.02	13.06	0.75	0.24	0.07	0.02	0.6	4.59	4.25	0.004	10.5	25.6	3.8	16.8	8.99	0.06
	PT03	K-feldspar granite	73.97	0.08	13.87		1.09	0.14	0.01	0.72	4.19	4.9	0.02	7.72	21	3.41	17.6	11.6	0.14
	PT06		72.78	0.09	14.49		2.67	0.56	0.04	1.13	2.05	4.1	0.03	14.8	35.8	4.7	19.9	7.58	0.14
	PT11		74.57	0.08	13.4		1.24	0.16	0.06	0.87	3.29	4.9	0.03	10.4	25.6	3.61	15.6	8.1	0.16
Piaotang W deposit	PT-01	Biotite monzogranite	76.61	0.11	12.36	0.8	1.05	0.17	0	0.65	3.15	4.88	0.02	8.35	22.5	3.14	13.8	7.19	0.08
	PT-03		76.63	0.12	12.38	0.93	1.28	0.08	0.07	0.72	3.43	4.26	0.02	13.1	31.6	3.99	15.7	6.22	0.13
	PT-04		76.96	0.12	12.37	0.77	1.09	0.07	0.05	0.75	3.33	4.64	0.02	12.9	30.9	4.37	19.4	9.46	0.15
	PT-06		76.55	0.1	12.6	0.79	0.93	0.1	0.02	0.63	3.57	4.59	0.02	10.3	25.8	3.42	14.4	6.53	0.09
	PT-07		75.38	0.09	12.87	0.44	0.74	0.1	0.07	0.61	3.81	4.46	0.02	6.79	17.4	2.54	12.5	7.55	0.04
	TS-5	The main-phase coarse-medium grained porphyritic biotite granite	75.3	0.03	13.7	0.47	0.09	0.12	0.47	1.42	0.13	5.17	0.04	12.1	28.3	3.57	13.8	5.65	0.1
	TS9-1		76	0.04	13.3	0.88	0.02	0.11	0.07	0.55	3.32	4.86	0.05	17.9	42.6	5.23	20	7.19	0.1
Tieshanlong W deposit	TS9-3		75.9	0.04	13.5	0.75	0.15	0.09	0.07	0.61	3.69	4.43	0.05	15.8	43.3	4.92	18.2	5.63	0.04
	TS9-4		76	0.04	13.5	0.75	0.27	0.12	0.12	0.5	3.14	4.48	0.08	11.4	25.4	3.32	12.5	4.62	0.1
	TS9-24		73.4	0.13	14.4	1.03	0.39	0.11	0.22	0.88	3.16	5.16	0.19	23.2	54.1	5.47	18.5	4.09	0.32
	TS9-5	76.1	0.06	13.8	1.23	0.16	0.17	0.17	0.43	0.13	5.82	0.05	26.8	64.2	7.54	29	9.38	0.11	

	TS-7	Two-mica granite and muscovite granite	75.5	0.04	13.7	0.61	0.06	0.09	0.33	0.6	3.08	4.6	0.05	10.9	26	3.21	12.1	4.73	0.07
	TS-26		77.1	0.03	13.7	1.21	0.15	0.18	0.09	0.29	3.11	3.73	0.07	3	8.4	0.83	2.9	0.96	0.02
	TSY-1		76.7	0.02	13.4	0.69	0.12	0.16	0.17	0.48	3.57	3.75	0.06	9.3	24.5	3.29	12.8	5.21	0.03
	TSY-7		76.5	0.01	13.5	0.63	0.14	0.17	0.16	0.57	2.81	3.99	0.06	7.1	18.2	2.47	9.1	4.25	0.03
Yaogangxian W deposit	YGX-21-7		75.62	0.03	12.75	0.86	0.14	0.01	0.56	3.62	4.57	0.01	5.99	16.4	2.48	11.3	6.65	0.06	
	YGX-23-8		75	0.04	12.85	1.13	0.11	0.02	0.63	3.39	4.76	0.02	13.6	32.6	4.43	18.7	8.35	0.13	
	YGX-23-12	Coarse-grained two-mica granite	74.68	0.05	12.98	1.08	0.1	0.04	0.77	3.58	4.64	0.01	10.8	24.7	3.26	13.4	5.62	0.16	
	YGX-23-14		74.34	0.07	13.15	1.23	0.07	0.1	0.9	3.56	4.57	0.02	18.2	38.6	4.95	19.3	6.39	0.32	
	YGX-23-15		74.4	0.05	12.94	1.11	0.1	0.03	0.73	3.57	4.61	0.02	12.9	29.1	3.84	16.1	6.77	0.16	
	YGX-23-17		74.99	0.04	12.88	1.06	0.09	0.04	0.66	3.76	4.53	0.02	7.6	18.5	2.68	12.4	6.37	0.11	
	YGX-23-24		75.31	0.04	12.83	0.87	0.11	0.01	0.6	3.85	4.42	0.01							
	YGX-19-2		75.66	0.03	12.53	1.09	0.14	0	0.52	3.6	4.39	0.01	4.67	12.9	1.83	8.91	5.58	0.05	
	YGX-19-3		74.49	0.02	12.92	0.88	0.13	0.03	0.52	3.67	4.88	0.01	2.6	9.78	1.13	5.16	3.05	0.02	
	YGX-19-12		75.77	0.03	12.92	0.86	0.14	0.02	0.61	4.09	4.36	0.01	3.95	13.4	1.52	6.83	4.02	0.04	
	YGX-19-18	Coarse- to	75.69	0.03	12.92	0.98	0.11	0.01	0.58	3.97	4.41	0.01	2.55	10.2	0.99	4.32	2.28	0.02	
	YGX-21-10	medium-grained	75.57	0.02	12.79	0.95	0.16	0.02	0.6	3.33	4.68	0.01							
	YGX-21-12	two-mica granite	75.86	0.03	12.58	1	0.15	0.01	0.53	3.72	4.34	0.01	2.65	10.3	1.04	4.89	2.75	0.03	
	YGX-23-13		74.75	0.03	13.24	0.89	0.11	0.04	0.63	3.93	4.55	0.01	5.07	14.7	1.66	7.51	3.39	0.06	
	YGX-23-21		74.74	0.03	13.01	0.98	0.13	0.04	0.53	4.13	4.43	0.01	4.41	15.1	1.56	6.8	3.44	0.03	
	YGX-23-29		76.65	0.03	12.65	0.91	0.13	0.03	0.6	3.93	4.39	0.01	5.3	14	1.63	6.95	3.54	0.05	
	YGX-16-7		76.67	0.03	13.09	0.96	0.16	0.01	0.53	3.38	5.07	0.01	8.57	21.4	3.13	13.7	8.33	0.07	
	YGX-16-13		75.11	0.03	13.05	0.87	0.08	0.02	0.51	4.35	4.73	0.01	2.6	10.9	1.11	4.85	2.95	0.02	
	YGX-23-4	Fine-grained	75.72	0.03	12.62	0.96	0.1	0	0.55	4.03	4.28	0.01	3.38	12.4	1.11	4.8	2.49	0.02	
	YGX-23-25	muscovite granite	75.32	0.03	12.72	0.92	0.12	0	0.56	4.1	4.3	0.01	5.94	15	2.04	9.24	5.15	0.06	
YGX-1-1		76.55	0.02	12.99	0.82	0.12	0.08	0.51	4.21	4.18	0.01	1.51	5.98	0.68	3.13	1.69	0.01		

	YGX-1-2		77.04	0.02	12.91		0.83	0.11	0	0.49	4.16	4.03	0.01	1.99	7.39	0.96	3.95	1.7	0.01	
	YGX-1-3		75.89	0.02	12.9		0.68	0.14	0	0.48	4	4.22	0.01	2.37	8.64	1.11	4.57	2.65	0.01	
	YGX-1-7		76.8	0.02	12.71		0.82	0.14	0	0.45	3.72	4.27	0.01	2.21	10.8	0.97	4.68	3.18	0.01	
	NLSD2-1348		76.57	0.11	12.31		1.06	0.25	0.08	0.1	0.83	3.21	5.04	0.02	11.1	22.1	2.85	11.1	2.87	0.48
Pangushan	NLSD2-1522	K-feldspar	73.72	0.16	12.85		1.35	0.67	0.09	0.22	1.14	3.31	4.77	0.03	25.2	55.6	7.37	28.8	8.34	0.5
W deposit	NLSD2-1880	granite	76.14	0.09	12.8		0.95	0.34	0.12	0.17	1.03	3.49	4.54	0.03	10.6	25.1	3.33	14.3	5.08	0.32
	NLSD2-1882		75.56	0.1	12.95		0.92	0.27	0.1	0.2	1.17	3.45	4.53	0.03	9.95	21.8	2.96	12.3	4.34	0.39
	DJS-01		73.67	0.08	14.77		0.24	0.52	0.07	0.13	0.44	4.59	4.09	0.03	2.345	7.0752	1.075	4.171	4.507	0.042
	DJS-05	Muscovite	69.88	0.08	16.66		0.25	0.56	0.17	0.04	0.53	4.28	6.28	0.03	2.896	10.646	1.62	6.944	7.846	0.046
	DJS-07	albite-rich garnite	75.34	0.07	14.3		0.15	0.38	0.03	0	0.24	5.06	3.72	0.03	2.007	6.688	1	3.922	4.616	0.037
	DJS-10		74.35	0.09	14.63		0.5	0.38	0.17	0.15	0.42	4.67	3.22	0.03	2.604	8.4536	1.322	5.22	5.117	0.037
	DJS-2	Muscovite	75.6	0.01	13.62		0.13	0.29	0.06	0.16	0.74	4.27	4.17	0.02	0.99	2.75	0.41	1.79	1.15	0.04
	DJS-20	albite-rich garnite	78.09	0.01	12.49		0.17	0.12	0.07	0.06	0.44	4.4	3.5	0.02	2.46	7.04	1.07	4.15	3.24	0.09
	DJS-7		73.62	0.02	14.8		0.17	0.15	0.05	0.09	0.59	4.42	5.2	0.02	4.26	13.1	2.03	8.23	7.79	0.1
Dajishan W deposit	DJS-14		75.83	0.01	14.58		0.08	0.2	0.13	0.13	0.33	5.05	3.64	0.02	2.74	7.82	1.45	5.62	6.75	0.09
	DJS-13		77.21	0.01	14.09		0.11	0.44	0.03	0.15	0.42	4.22	3.25	0.01	2.23	6.69	1.22	4.97	4.69	0.05
	DJS-12		76.87	0.01	13.83		0.18	0.24	0.11	0.14	0.66	4.11	3.8	0.02	3.05	7.98	1.34	4.95	3.4	0.07
	DJS-11	Muscovite	77.45	0.01	14.02		0.21	0.26	0.16	0.06	0.71	3.56	3.95	0.01	4.95	12.4	1.93	8.14	5.42	0.09
	DJS-8	K-feldspar	76.38	0	13.76		0.13	0.29	0.06	0.13	0.75	4.25	4.21	0.02	1.99	5.68	1.32	5.79	3.15	0.08
	DJS-6	granite	76.34	0.01	13.91		0.17	0.12	0.07	0.06	0.45	4.17	4.58	0.02	2.46	7.24	1.27	4.15	3.24	0.09
	DJS-5		75.31	0.01	13.99		0.42	0.59	0.24	0.08	0.32	4.66	4.43	0.02	2.13	0.7	1.14	5.1	4.19	0.12
	DJS-4		73.9	0.02	13.55		0.68	0.97	0.35	0.15	0.23	3.99	4.69	0.02	3.26	13.1	2.03	8.23	7.79	0.1
	DJS-3		74.42	0.01	14.18		0.78	0.96	0.55	0.18	0.32	4.47	4.29	0.02	3.66	13	2.12	9.6	7.21	0.04
	DJS-1		75.08	0.01	13.32		0.57	0.83	0.58	0.12	0.28	4.51	4.19	0.02	2.07	6.5	1.72	4.79	4.22	0.04
Shizhuyuan	SZY-23	The first-phase	74.28	0.2	12.85	0.51	0.4	0.07	0.02	0.27	2.43	2.66	4.98	0.06	39.2	75.4	9.09	33.9	7.97	0.49

Sn-W deposit	SZY-24	microfine-grained	73.65	0.22	13.09	1.29	0.76	0.45	0.03	0.35	1.77	2.59	5.5	0.07	44.8	84.3	10.4	38.8	8.73	0.59
	SZY-25	porphyritic	73.98	0.2	12.99	0.93	0.65	0.21	0.02	0.31	1.76	2.85	5.38	0.06	41.4	82.3	9.62	37	8.3	0.6
	SZY-26	biotite granite	73.7	0.23	13.17	1.33	0.87	0.36	0.02	0.36	1.6	2.81	5.5	0.07	40	77.2	9.43	35.4	7.91	0.57
	SZY-27		74.44	0.21	12.91	1.21	0.73	0.4	0.02	0.31	1.56	2.84	5.41	0.06	43.4	87	10.5	38.9	9.14	0.58
	SZY-28		74.24	0.24	12.99	1.33	0.91	0.32	0.02	0.33	1.5	2.87	5.29	0.07	42.8	84.8	9.98	37.7	8.2	0.72
	SZY-13	The second-phase fine-grained porphyritic biotite granite	73.31	0.27	13.47	0.39	0.34	0.01	0.03	0.39	1.74	2.54	6.79	0.11	37.8	66.6	10.5	40.8	8.64	0.69
	SZY-14		73.21	0.28	13.5	0.41	0.32	0.05	0.04	0.41	1.77	2.45	6.91	0.12	53.5	111	12.9	49	10.2	0.75
	SZY-29		74.07	0.22	12.88	1.91	1.29	0.48	0.07	0.29	1.16	3.45	4.58	0.06	52.3	112	12.9	49.8	12.1	0.55
	SZY-30		74.73	0.19	12.74	1.57	1.24	0.19	0.05	0.24	1.11	3.5	4.53	0.05	47.3	98.6	11.2	41.8	10	0.5
	SZY-31		74.67	0.22	12.71	1.84	1.21	0.5	0.06	0.27	1.13	3.45	4.52	0.06	52.5	113	12.8	47.8	11.6	0.48
	SZY-1		75.19	0.01	13.55	1.22	0.94	0.18	0.06	0.06	0.54	4.19	4.03	0.01	30.1	66.7	10.1	41.8	16.3	<0.05
	SZY-2	75.31	0.01	13.63	0.17	0.18	0	0.01	0.03	0.45	4.73	4.55	0.01	25.5	59.1	8.8	37.1	15.5	<0.05	
	SZY-3	76	0.01	13.33	0.61	0.54	0.01	0.03	0.03	0.5	3.91	4.53	0.01	18.5	57.9	6.75	27.4	10.9	<0.05	
	SZY-4	The third-phase medium-grained equigranular zinnwaldite granite	75.65	0.01	13.22	0.88	0.58	0.24	0.02	0.02	0.64	3.66	4.58	0.01	24.3	58.2	9.09	40.4	18	<0.05
	SZY-5		73.85	0.01	14.65	1.33	0.99	0.23	0.04	0.02	0.73	3.35	4.36	0.01	26.5	69.3	11	45.7	20.1	<0.05
	SZY-6		75.55	0.01	13.51	0.76	0.61	0.08	0.02	0.03	0.6	4.42	3.8	0.01	26	63.3	9.81	42.6	19.3	<0.05
	SZY-7		74.25	0.01	14.15	1.58	1.08	0.38	0.05	0.03	0.78	3.29	4.2	0.01	19.4	57.3	7.74	32.4	13.7	<0.05
	SZY-12		77.38	0.03	11.77	1.27	0.8	0.38	0.03	0.15	0.65	3.23	4.04	0.01	28.7	68.7	8.85	37.3	13.8	<0.05
	SZY-19		76.63	0.01	12.72	0.79	0.52	0.21	0.02	0.04	0.47	4.08	4.27	0.01	21.1	40.5	7.32	34.2	16.5	<0.05
	SZY-20	75.87	0.04	12.73	1.08	0.76	0.24	0.03	0.06	0.6	3.55	4.82	0.02	25.2	45.8	7.29	30.1	10.1	0.06	
	SZY-21	77.74	0.04	11.44	1.12	0.66	0.39	0.04	0.06	0.6	3.21	4.34	0.01	22.1	45.6	6.47	26.6	9.3	0.06	
	SZY-22	76.34	0.01	12.91	0.27	0.23	0.01	0.01	0.06	0.46	3.89	5.04	0.01	24.1	53	9.35	40.8	18.5	<0.05	
	JCT-29	Porphyritic	74.49	0.12	12.81		1.02	0.45	0.04	0.14	1.11	2.65	5.39	0.03	74	138	12.4	51.5	10.3	0.31
	SZY-19	biotite granite	74.87	0.11	12.6		1.03	0.5	0.04	0.17	1.16	2.82	5.23	0.03	122	261	23.5	74.8	11.4	0.27
	SZY-1	Equigranular	75.86	0.05	12.67		0.5	0.52	0.03	0.12	0.9	3.49	4.8	0.01	29	62	9.3	33.4	11.7	0.11

SZY-20	biotite granite	75.92	0.05	12.41		0.44	0.84	0.03	0.15	0.85	3.24	4.57	0.01	70	131	18.5	68.3	15.7	0.12
SZY-9		74.62	0.01	13.55		0.09	0.15	0.01	0.09	0.88	4.02	5.12	0.01	38	108	12.1	49	15.4	0.01
QLS-1		72.4	0.34	12.98	2.45			0.03	0.52	1.45	3.18	5.23	0.09	72.9	148	15.3	52.9	9.88	0.84
QLS-2		71.66	0.3	13.26	2.21			0.03	0.46	1.47	3.04	5.92	0.08	62.8	128	13.3	45.8	9	0.98
QLS-73		72.34	0.34	13.13	2.42			0.04	0.52	1.46	3.26	5.32	0.09	73.4	148	15.4	53.5	10.5	0.89
QLS-74	Porphyritic	71.87	0.32	13.42	2.25			0.03	0.48	1.46	3.24	5.67	0.09	71.6	145	15	51.1	9.76	1.01
QLS-76	biotite granite	72.48	0.32	13.12	2.31			0.03	0.51	1.44	3.25	5.26	0.09	62.2	126	13.3	46.4	9.34	0.77
QLS-156		72.53	0.33	12.81	2.33			0.03	0.51	1.4	3.13	5.24	0.09	73.3	150	15.7	54.3	10.9	0.93
QLS-157		71.71	0.33	13.34	2.34			0.04	0.51	1.41	3.25	5.4	0.09	66.6	134	13.9	47.2	9.25	0.9
QLS-158		72.59	0.32	12.96	2.43			0.03	0.51	1.46	3.27	5.18	0.09	74.1	149	15.4	51.7	9.32	0.85
QLS-115		74.43	0.02	14.01	0.62			0.03	0.42	0.62	5.24	4.37	0	21.4	58.6	8.07	32.2	13.5	0.03
QLS-116		76.04	0.01	13.34	0.68			0.03	0.14	0.5	4.4	4.32	0	24.1	59.7	9.17	38.8	16.9	0.03
QLS-117		74.78	0.02	13.52	0.72			0.03	0.17	0.61	3.53	5.19	0	22.5	60.2	8.73	36.4	17	0.03
QLS-119		75.07	0.02	13.46	0.69			0.03	0.16	1.07	3.72	4.58	0.01	15.4	41.7	5.87	24.4	10.2	0.03
QLS-152		76.35	0.02	12.75	0.52			0.03	0.13	0.46	4.68	3.89	0	20.8	50.8	7.59	31.3	13.6	0.03
QLS-154		75.11	0.02	13.53	0.81			0.05	0.15	0.45	4.21	4.53	0.01	20.5	50.7	7.57	30.8	14.1	0.03
QLS-155		75.82	0.02	13.06	0.78			0.04	0.19	0.54	3.99	4.43	0.02	24.1	66.2	9.01	37.3	17.1	0.03
QLS-46	Equigranular granite	75.47	0.04	12.59	0.72			0.03	0.18	0.66	3.98	4.76	0.03	21.2	54	6.44	26.2	9.85	0.05
QLS-48		76.33	0.05	12.26	1.13			0.04	0.18	0.73	3.47	4.82	0.01	33	82.7	10.3	42.4	14.9	0.08
QLS-81		74.62	0.02	14.06	1.22			0.08	0.17	0.4	4.73	3.53	0.04	21.4	79	8.29	33.6	13.3	0.02
QLS-83		74.53	0.02	14.06	0.81			0.04	0.45	0.57	5	3.83	0	30.6	82.9	11.5	47	20.2	0.02
QLS-147		74.22	0.02	14.01	0.78			0.05	0.14	0.46	4.74	4.04	0.01	24.1	73.7	9.34	39.3	16.4	0.02
QLS-150		74.61	0.02	13.93	0.81			0.05	0.15	0.56	4.61	3.88	0.01	26.5	70.7	10.6	44.4	19.7	0.02
QLS-151		74.95	0.02	13.79	0.54			0.04	0.13	0.5	5.05	3.57	0.01	26.8	70.5	10.3	42.9	18.1	0.02
QLS-29		75.05	0.03	13.36	0.79			0.03	0.14	1.02	3.88	4.74	0	17.8	45.1	6.29	26.3	11.3	0.02

Q1		75.2	0.14	12.61		1.5	0.05	0.14	0.08	2.29	4.87	0.03						
Q2		76.01	0.15	13.5		1.37	0.06	0.17	0.74	2.62	5.03	0.03						
Q3	Porphyritic	74.2	0.15	13		1.83	0.08	0.19	0.94	1.99	5.29	0.03	56.1	80.1	12.9	50.6	12.2	0.86
Q4	biotite granite	77.2	0.14	12.4		1.09	0.05	0.12	0.73	2.81	4.97	0.03	30.4	76.1	7.83	31.1	8	0.53
Q5		76.95	0.14	11.88		1.49	0.06	0.12	0.64	2.64	4.35	0.03	32.6	76.9	8.46	33.4	8.68	0.64
490-46		75.12	0.16	13.03		1.72	0.09	0.18	1.03	2.89	4.95	0.04	42.6	91.8	11.6	44.9	11.1	0.7
490-18		74.81	0.01	13.96		0.18	0.06	0.03	0.72	2.85	4.12	0.02	52.4	149	21.5	95.7	35.3	0.7
490-19		75.03	0.02	13.64		0.89	0.06	0.02	0.75	3.59	4.14	0.01	19.3	51.3	7.44	32.7	13.4	0.24
490-20		77.95	0.02	12.13		0.57	0.05	0.02	0.49	3.34	4.02	0	23.7	62.4	8.77	38.4	15	0.27
490-21		75.79	0.02	13.84		0.96	0.06	0.03	0.65	3.62	4.89	0	19.6	62.4	7.33	38.4	14.7	0.24
490-22	Equigranular	74.82	0.02	13.4		2.26	0.11	0.03	0.63	2.81	3.89	0.01	34.2	95.1	13.4	60.8	22.8	0.42
490-28	granite	75.71	0.04	13.44		0.73	0.05	0.02	0.79	3.15	4.94	0.02	29	75.8	9.92	43.1	15.4	0.33
490-29		74.84	0.02	13.84		0.86	0.05	0.02	0.72	3.54	4.09	0	25.8	67.5	9.41	40.4	14.3	0.32
490-31		77.84	0.04	11.95		0.48	0.05	0.05	1.67	2.13	5.07	0.02	26.7	69.3	8.84	37.2	13.5	0.3
490-32		78.68	0.03	10.92		0.49	0.05	0.02	1.79	2.11	4.43	0.01	15.9	32.7	3.89	14.2	4.03	0.24
490-33		77.85	0.04	11.62		0.64	0.06	0.05	1.36	2.29	4.75	0.01						
SZY-21-02		71.9	0.31	13.6	2.31		0.04	0.38	1.5	2.93	5.76	0.1	79.2	148	16.4	52.8	9.54	0.89
SZY-22		73.4	0.32	12.8	2.37		0.04	0.38	1.55	2.95	5.16	0.09	83.6	162	16.9	56.8	10.4	0.86
SZY-23-01	Phase-1	72.9	0.27	13	2.1		0.03	0.35	1.27	2.83	5.57	0.08	78.4	152	16	50.6	9.24	0.94
SZY-34-01	porphyritic	73	0.32	12.5	2.43		0.04	0.38	1.39	3.03	4.74	0.09	82.5	164	17.2	54.9	10.3	0.69
SZY-38	biotite granite	71.8	0.29	13.4	2.21		0.04	0.35	1.35	2.86	5.98	0.08	82.1	156	17.7	55.9	10.1	0.88
SZY-39		73.7	0.32	12.3	2.43		0.04	0.39	1.27	2.92	4.98	0.09	84.6	162	18.4	58.6	11.1	0.66
SZY-05	Phase-2	73.9	0.01	14.1	0.9		0.03	0.02	1.01	3.66	4.39	0.01	26.9	80.4	11.9	47.7	21.7	<0.03
SZY-06	equigranular	75.3	0.01	13.8	0.16		<0.01	0.14	0.66	3.94	4.59	0	31.1	91	12.9	50.2	21.3	<0.03
SZY-07	biotite granite	73.8	0.01	14.9	0.84		0.05	0.01	0.39	4.62	4.14	0	39.8	115.5	16.8	66.7	30.2	<0.03

	SZY-11-01		75.8	0.01	13.3	0.32		0.02	0.03	0.52	4.41	4.63	0.01	22.7	61.4	8.76	36.4	16.8	<0.03	
	SZY-11-02		75.3	0.01	13.4	0.39		0.02	0.02	0.52	4.11	4.83	0.01	25.2	70.1	9.98	41.6	19.8	<0.03	
	SZY-12		75.6	0.01	13.5	0.26		0.01	0.03	0.33	3.62	5.14	0.01	27.9	73.2	10.4	42.9	19.1	<0.03	
	SZY-13		75.7	0.01	13.6	0.22		0.01	0.02	0.47	4.59	4.56	0.01	25.9	68	9.64	39.2	17.4	<0.03	
	SZY-15		76.5	0.01	12.9	0.73		0.03	0.09	0.57	3.71	4.42	0.01	26.4	70.2	10.1	41	19.1	<0.03	
	SZY-16		73.5	0.01	14.4	1.27		0.08	0.12	0.88	3.71	3.79	0.01	47.1	150.5	22.4	88.2	40.3	<0.03	
	SZY-26-03		75.3	0.01	13.1	1.4		0.06	0.06	0.95	2.87	4.63	0.01	24.4	64.1	9.18	35.7	18.2	<0.03	
	SZY-36		75.1	0.01	13.2	0.9		0.04	0.02	0.59	3.46	4.96	0.01	24.7	63.5	8.95	37.2	15.9	0.03	
	SZY-37		76.3	0.01	13	1.25		0.05	0.02	0.53	3.73	4.54	0.01	22.1	55.6	7.69	29.8	11.7	0.03	
	JJL-01		76.18	0.11	12.68		1.02	0.21	0.03	0.09	0.69	3.55	4.92	0.03	40.14	91.92	11.92	46.72	12.71	0.15
	JJL-04	Biotite granite	75.49	0.11	12.5		1.02	0.29	0.02	0.09	0.79	3.55	4.44	0.02	33.86	78.19	10.3	40.16	10.78	0.17
	JJL-10		76.51	0.1	12.63		1.26	0.19	0.03	0.08	0.7	3.29	4.98	0.03	46.32	104.6	13.41	52.54	13.54	0.3
	JJL-18		75.88	0.1	12.12		1.19	0.32	0.03	0.08	0.65	3.03	5.1	0.02	16.69	34	4.77	20.11	5.28	0.15
	JJL-11		74.62	0.11	13.16		1.17	0.23	0.03	0.07	0.68	3.43	5.51	0.02	31.23	73.08	8.76	35.14	8.61	0.18
	JJL-12	Two-mica granite	74.73	0.13	13.33		1.13	0.36	0.03	0.07	0.77	3.49	5.15	0.03	46.19	112.68	13.51	52.57	13.21	0.29
	JJL-17		76.27	0.14	11.85		1.51	0.32	0.04	0.08	0.59	2.97	4.94	0.03	57.69	131.31	16.72	69.98	15.32	0.31
Xiangyuan Sn-W deposit	JJL-09		75.28	0.1	12.68		1.38	0.08	0.03	0.08	0.75	3.42	4.48	0.03	37.79	92.45	11.08	43	10.93	0.21
	PXM-01		76.94	0.05	12.5		0.81	0.25	0.03	0.02	0.21	3.41	4.86	0.01	19.1	48.1	5.9	23.29	6.17	0.07
	PXM-02		76.23	0.05	12.67		0.88	0.19	0.03	0.02	0.63	3.85	4.65	0.01	20.33	46.46	6.88	28.7	8.28	0.07
	PXM-03		76.1	0.05	12.68		0.95	0.12	0.03	0.06	0.7	3.41	4.7	0.01	23.68	56.2	7.64	31.95	9.45	0.08
	PXM-04	Two-mica granite	75.23	0.05	12.91		1.06	0.03	0.03	0.01	0.64	3.9	4.64	0.01	23.58	63.74	7.89	33.24	11.02	0.07
	PXM-05		76.88	0.03	12.2		0.84	0.11	0.06	0.22	0.67	2.53	4.57	0.01	32.36	66.81	11.02	49.43	15.42	0.09
	PXM-06		76.97	0.01	12.42		0.61	0.16	0.05	0	0.38	4.51	3.57	0.01	7.35	20.68	2.89	12.62	4.21	0.02
	PXM-07		76.33	0.01	12.93		0.88	0.05	0.06	0	0.49	3.92	3.9	0.01	10.67	30.89	4.45	19.75	7.53	0.03
	PXM-08		76.62	0.02	12.44		0.75	0.12	0.06	0	0.44	3.48	4.86	0.01	9.13	29.98	4.32	20.18	8.82	0.03

	JJL-07																			
	JJL-19																			
	JJL-20																			
	HGY-4		70.7	0.34	14.5	2.45	1.43	1.13	0.09	0.61	1.57	3.02	5.16	0.15	69.5	132	14.7	50	7.49	1.55
	HGY-7		72.7	0.32	13.4	2.88	2.12	0.84	0.06	0.4	1.13	3.08	4.86	0.15	62.5	123	14.1	50.7	10.4	1.17
	HGY-9		75.3	0.03	13.2	1.28	0.92	0.4	0.04	0.01	0.46	4.5	4.28	0.01	21.9	46.1	7.48	32.1	14.4	0.13
	D0017		71.7	0.3	15.2	2.23	1.18	1.17	0.09	0.54	0.54	3.79	4.03	0.12	45.3	80	8.58	29.3	4.41	0.9
	D0094	Phophyritic	76.1	0.1	12.6	1.86	1.83	0.03	0.05	0.17	0.37	3.25	4.55	0.04	30.3	54.8	7.27	27.3	6.62	0.39
	D5136	biotite monzonite	76.2	0.07	12.9	1.11	0.7	0.46	0.03	0.08	0.33	3.71	4.61	0.02	12.9	22.7	3.17	12.4	3.71	0.28
	D0041		75.5	0.04	13.2	1.38	1	0.42	0.09	0.04	0.35	4.33	4.37	0.02	11.8	41.3	3.64	14.4	5.56	0.13
	H13		73.58	0.2	13.36		1.75	0.78	0.04	0.16	0.95	2.87	5.63	0.05	89.2	172	19.5	67.6	12.3	1.06
	H4		70.67	0.34	14.46		1.43	1.13	0.09	0.61	1.57	3.02	5.16	0.15	69.5	132	14.7	50	7.5	1.55
Xitian Sn deposit	H7		72.67	0.32	13.43		2.12	0.84	0.06	0.4	1.13	3.08	4.86	0.15	62.5	123	14.1	50.7	10.4	1.17
	XT-60		74.64	0.12	12.72	1.41	1.17	0.11	0.05	0.34	1.33	1.92	4.28	0.03	50.33	112.12	13.1	45.7	11.81	0.3
	Xt0416	Medium- to fine-grained	73.07	0.26	13.44	2.5			0.08	0.31	0.87	3.29	4.79	0.13	37.44	81.61	9.79	36.52	7.6	0.044
	Dahu	two-mica monzonite	75.82	0.05	12.03	2.92	2.45	0.2	0.06	0.12	0.7	3.18	4.7	0.02	30.82	70.92	9.89	37.05	11.92	0.12
Shanyangkeng			75.52	0.07	12.06	3.07	2.28	0.54	0.08	0.2	0.62	3.23	4.45	0.01	20.63	45.86	6.16	25.64	8.57	0.13
	Bamuzhai		75.51	0.11	12.68	2.19	1.52	0.5	0.05	0.22	0.46	3.1	5.12	0.03	22.13	42.37	5.84	22.96	5.74	0.34
	Xt0413	Granite	73.92	0.03	15.28	1.19			0.04	0	0.4	3.97	4.67	0.01	19.66	50.96	6.79	26.34	9.78	0.05
	X0406	Medium- to fine-grained	69.36	0.39	13.4			3.01	0.07	0.93	1.71	3.32	4.39	0.13	58.89	121.1	13.65	47.65	7.603	0.935
	X0417		73.07	0.26	13.44			2.5	0.08	0.31	0.87	3.29	4.79	0.13	37.44	81.61	9.792	36.52	7.603	0.436
	X01	porphyritic	71.9	0.325	13.7		2.23	0.62	0.071	0.635	1.82	3.08	5	0.134	73.78	141.1	16.2	56.13	9.89	0.62
	X02	biotite monzonite	73.43	0.222	13.05		2.01	0.34	0.068	0.56	1.23	2.98	4.6	0.138	22.13	42.37	5.84	22.96	5.74	0.34

	X03	Medium-grained biotite monzonite	74.8	0.12	12.97	1.12	0.2	0.047	0.235	0.68	3.21	5	0.049	20.63	45.6	6.16	25.64	8.57	0.13
	ZK10C02-01	Fine-grained	74.39	0.03	13.72		0.69	0.04	0.42	1.93	0.27	3.54	0.01	14.1	42.9	7.1	32	14.2	0.02
	ZK10C02-17	granite	74.64	0.12	13.08		1.63	0.05	0.07	0.75	2.93	5.25	0.02	47.2	126	14.01	51.4	12.3	0.18
	ZK10C02-19	Porphyritic	75.31	0.12	12.78		1.58	0.05	0.09	0.8	2.85	4.84	0.02	44.8	122	13.61	50.8	12.6	0.16
	ZK10C02-20	quartz granite	75.22	0.13	12.52		1.81	0.06	0.14	0.86	2.42	4.92	0.02	51	134	14.84	54.1	12.4	0.18
	ZK10C02-36		76.68	0.09	12.35		1.44	0.04	0.06	0.82	2.04	4.95	0.02	12.5	35.3	5.64	25.6	11.2	0.07
	ZK10C02-30		73.54	0.06	12.84		1.39	0.08	0.2	2.22	0.1	5.85	0.01	18.8	52.5	7.87	33.2	12.1	0.08
	ZK10C02-22	Medium- to	75.76	0.15	13.09		1.48	0.05	0.28	0.86	0.16	5.04	0.02	57.2	148	16.11	58.3	12.6	0.24
	ZK10C02-25	fine-grained	76.95	0.19	13.57		1.23	0.03	0.14	0.25	0.07	3.88	0.02	61.2	154	16.38	58.9	12.1	0.28
	ZK10C02-12	porphyritic	74.9	0.13	12.7		1.87	0.08	0.13	0.81	2.34	5.12	0.02	49.2	128	14.09	51.5	11.7	0.17
	ZK10C02-03	granite	74.27	0.1	12.81		2.07	0.1	0.11	1.45	0.14	5.87	0.02	34.9	98.2	11.22	41.8	10.8	0.1
	ZK10C02-15		74.29	0.12	12.49		1.66	0.05	0.09	0.81	3.93	4.91	0.02	49.4	128	14.06	51.8	11.8	0.2
	ZK10C02-27		74.54	0.06	13.48		1.57	0.05	0.18	0.91	0.15	5.07	0.02	11.7	33.5	5.58	26.5	12.1	0.08
	ZK10C02-07	Fine-grained porphyritic biotite granite	75.84	0.1	12.88		1.52	0.07	0.17	0.94	0.1	5.55	0.02	36.4	98.4	11.02	40.5	9.7	0.14
	ZK10C02-33	Fine-grained porphyritic biotite monzonite	76.12	0.05	12.56		1.35	0.05	0.38	0.7	2.97	4.71	0.02	13.2	37.5	5.78	25.1	9.9	0.07
Hehuaping Sn deposit	WXL-15		75.95	0.04	12.73	1.46	1.07	0.06	0.05	0.63	3.29	4.75	0.01	29.7	60.7	8.5	32.6	10	0.07
	WXL-16	Biotite monzonite	77.24	0.04	12.26	1.03	7.18	0.02	0.11	0.72	3.24	4.5	0.01	34.3	71.7	10.6	43.3	14.9	0.12
	WXL-17		76.09	0.03	12.82	1.16	0.81	0.04	0.04	0.61	3.57	4.6	0.02	34.5	74.7	11.1	44.6	16	0.09

	WXL-18		77.98	0.03	11.76	0.97	0.49		0.04	0.08	0.47	3.07	4.64	0.01	32.7	71.4	9.65	38.2	13.2	0.07
	ZK16003-3		75.94	0.12	12.35	1.59	0.99	0.5	0.02	0.1	0.83	2.57	4.73	0.03	74.8	154	17.8	64.7	12.4	0.36
	ZK16003-4		74.91	0.12	13.11	1.54	1	0.44	0.02	0.1	0.91	2.7	5.01	0.03	72.3	149	17.1	62.3	12.5	0.45
	ZK12802-4		73.19	0.1	14.3	1.2	0.77	0.35	0.02	0.15	0.99	2.95	5.28	0.02	59.9	120	13.6	51.5	10.2	0.71
	ZK12802-8		73.28	0.28	12.94	2.49	1.68	0.62	0.03	0.24	1.69	2.78	4.22	0.09	94.7	201	23.2	87.6	17.2	0.66
	ZK14401-4		73	0.18	13.65	2.02	1.04	0.86	0.03	0.21	1.07	2.44	5.37	0.01	73.4	147	17	62.9	11.3	0.75
	ZK11202-27		73.57	0.22	13.31	2.04	1.43	0.46	0.03	0.16	1.47	3	4.63	0.06	70.6	147	16.8	63.7	12.4	0.66
	ZK11202-24		74.41	0.21	13.03	1.95	1.39	0.4	0.03	0.16	1.22	2.79	5.09	0.06	62.3	130	14.8	58.1	12.1	0.74
	ZK0004-6		76.34	0.06	12.39	1.17	0.65	0.45	0.03	0.05	0.78	3.18	4.57	0.04	26.7	60.4	7	28.6	6.9	0.1
	HHPD-42	Biotite granite	75.87	0.09	12.66	1.52	1.03	0.38	0.04	0.08	0.83	3.2	4.86	0.05	71.1	159.4	18.2	71	18	0.36
	HHPD-45		74.81	0.09	13.23	1.5	1.17	0.2	0.05	0.08	1.49	3.67	3.59	0.05	61.5	131.7	15.3	58.5	14.8	0.46
	HHPD38																			
	HHPD41																			
	HHPD43																			
	ZK45201-04																			
	ZK20001-03																			
	ZK20001-07																			
	ZK16002-2																			
	ZK11202-10																			
	ZK11202-20																			
	ZK11202-28																			
	ZK004-01																			
Furong Sn deposit	FR-63	Granite (Furong phase)	67.36	0.74	14.34		3.23	1.49	0.08	0.78	2.68	3.39	5.07	0.23	61.40	119.57	14.56	53.40	9.63	1.63
	FR-33		67.05	0.7	14.36		3.03	1.28	0.08	0.84	2.64	3.37	5.39	0.21	58.22	116.96	13.35	47.43	8.82	1.55
	FR-12		67.32	0.74	14.41		2.87	1.29	0.06	1.00	2.43	3.12	5.44	0.21	99.30	168.00	17.98	58.88	9.29	1.55

FR-19		70.28	0.28	13.77		2.04	0.88	0.09	0.46	1.8	3.36	6.21	0.09	83.97	154.11	17.59	62.01	13.19	0.60
GT-2-1		70.14	0.49	14.1		1.13	3.35	0.06	0.57	1.99	3.22	4.99	0.14	68.32	115.74	13.39	44.81	7.63	1.20
FR-43		68.90	0.53	14.29		2.36	0.88	0.06	0.65	2.15	3.21	5.42	0.16	59.63	117.51	12.46	42.56	7.65	1.33
GT-4-4		67.14	0.56	15.12		2.29	0.92	0.06	0.98	1.44	3.09	5.78	0.18	88.57	155.73	16.63	53.52	8.59	1.44
QTL-6		67.28	0.92	13.93		3.29	2.17	0.1	1.01	3.11	3.31	4.11	0.25	64.61	150.47	16.96	62.45	11.33	1.58
QTL-14		67.26	0.71	14.03		2.88	1.71	0.09	0.91	3.26	3.8	4.97	0.23	60.91	141.97	15.08	55.47	9.98	1.71
QT-27	Granite (Cailing phase)	67.64	0.86	12.6		4.32	1.8	0.15	1.1	2.5	2.92	4.46	0.3	78.29	184.10	16.16	73.64	14.39	0.90
QT-29		67.01	0.88	13.06		4.17	1.69	0.16	1.22	2.58	3.22	4.37	0.33	45.47	121.40	12.05	59.12	12.22	1.19
QT-30		66.5	0.72	14.01		3.41	1.45	0.11	1.1	2.2	3.07	4.94	0.3	100.30	177.90	18.80	69.17	12.29	1.81
QT-38		66.67	0.89	13.7		3.83	1.55	0.13	1.15	3.07	2.99	4.42	0.25	166.12	290.10	23.58	94.00	13.98	1.73
2ksc-10a		67.03	0.58	14.27	4.73		0.06	0.72	1.85	3.14	5.35	0.19		77.03	143.98	16.2	54.91	9.87	1.58
2ksc-10b		67.67	0.6	14.51	3.43		0.07	0.76	1.88	3	6.18	0.23		57.65	114.99	14.01	50.46	9.83	1.68
2ksc-10d		69.59	0.48	12.96	3.54		0.06	0.58	1.6	2.77	5.63	0.16		84.23	149.44	15.95	51.18	8.3	1.3
2ksc-10e		67.97	0.78	14.19	5.12		0.08	0.9	2.84	3.3	4.28	0.26		74.21	147.95	17.62	62.07	11.64	1.49
2ksc-12		66.48	0.72	14.33	4.95		0.07	0.85	2.5	3.42	4.77	0.24		80.66	153.55	17.55	59.91	10.88	1.49
2ksc-13		64.84	1.12	13.36	7.08		0.11	1.34	3.15	3	4.48	0.36		78.83	190.1	22.97	85.82	17.74	1.54
2ksc-14		74.57	0.24	12	2.06		0.03	0.25	1.31	2.84	5.37	0.09		50.92	90.23	9.48	30.08	4.47	0.88
2ksc-15	Granite	69.08	0.58	13.57	4.23		0.05	0.72	2.46	3.31	4.98	0.21		64.18	122.72	14.16	49.18	9.3	1.37
2ksc-16		69.19	0.64	13.85	4.32		0.07	0.75	2.35	3.12	5.52	0.21		89.77	178.85	18.08	60.02	10.12	1.47
2ksc-17		69.59	0.66	13.15	4.56		0.08	0.79	2.75	3.21	4.43	0.22		84.14	151.05	16.52	54.57	9.5	1.36
2ksc-18		67.63	0.58	13.47	4.41		0.07	0.56	2.26	2.99	5.56	0.21		53.86	108.92	13.77	52.45	10.61	1.87
2ksc-22a		70.55	0.45	13.88	3.39		0.05	0.52	2.02	3.15	5.08	0.12		70.47	128.68	14.21	47	8.16	1.23
2ksc-23		75.32	0.1	12.5	1.55		0.02	0.05	0.67	3.17	5.74	0		79.58	144.99	15.02	45.32	7.91	0.26
2ksc-24		76.59	0.13	11.78	1.4		0.02	0.09	0.66	2.82	5.7	0.01		88.54	148.47	14.38	40.42	5.16	0.59
2ksc-25		75.44	0.21	12.33	1.92		0.02	0.18	1.33	3.06	4.64	0.04		75.07	129.47	13.28	40.45	6.51	0.8

2ksc-26		72.41	0.15	13.36	3.39		0.05	0.43	1.83	3.22	4.99	0.11	79.04	141.73	15.64	50.67	8.94	1.01
2ksc-27a		66.14	0.29	14.81	4.39		0.07	0.86	2.34	3.21	5.83	0.21	35.43	79.42	10.76	43.31	9.39	1.72
2ksc-27b		65.95	0.94	13.77	6.03		0.09	1.21	2.81	3.07	4.84	0.28	52.95	112.04	14.61	55.89	11.38	1.65
2ksc-27c		67.25	0.81	14.03	5.06		0.08	0.95	2.81	2.99	4.17	0.26	40.79	92.93	12.47	48.69	10.15	1.51
D202_1		68.42	0.68	13.43	0.27	4.82	0	0.8	2	2.98	5.12	0.21	73.38	146.81	15.57	57.22	10.52	1.37
D202_2		65.84	0.88	14.36	0.32	5.14	0	1.29	2.57	3.46	4.22	0.25	63.93	127.54	13.66	50.9	10.08	1.28
D203_1		71.28	0.37	13.59	0.06	2.98	0	0.4	1.53	3.5	5	0.1	63.7	119.93	11.69	39.41	7.89	0.92
D208_1		68.88	0.56	13.88	0.16	4.02	0	0.68	2.02	3.31	5.24	0.17	69.13	136.34	15.24	54.49	11.02	1.27
D208_2		73.84	0.19	12.54	0.05	2.41	0	0.19	1.01	3.12	5.46	0.05	70.94	113.28	12.75	40.88	6.6	0.57
XN09-1		70.14	0.49	13.41	0.26	4.35	0	0.57	2	3.37	4.59	0.16	64.34	125.28	13.33	48.06	8.99	1.15
D210-1		70.94	0.42	13.19	0.14	3.86	0	0.45	1.67	3.09	4.9	0.13	75.93	123.59	14.73	49.33	8.74	1
D213-1	Granite	72.08	0.27	13.77	0.19	2.75	0	0.3	1.4	3.28	5.62	0.07	66.25	119.36	11.95	39.22	7.02	0.97
D219-1		67.28	0.72	14.17	0.6	4.36	0	1.02	2.55	3.09	4.95	0.23	96.59	159.86	16.5	54.66	8.97	1.57
D220-1		67.64	0.86	12.6	1.8	4.32	0.15	1.1	2.5	2.92	4.46	0.3	78.29	184.1	16.16	73.64	14.39	0.9
QT-27		66.67	0.89	13.7	1.55	3.83	0.13	1.15	3.07	2.99	4.42	0.25	166.1	290.1	23.58	94	13.98	1.73
QT-38		68.56	0.51	14.23	0.51	3.94	0	0.62	1.83	3.34	5.13	0.22	51.04	102.26	10.56	36.91	7.02	0.95
D215-1		75.72	0.1	12.27	0.11	2.17	0	0.08	0.55	3.4	5.09	0.02	67.03	124.45	12.1	38.43	7.19	0.24
D218-1		75.22	0.12	12.25	0	2.69	0	0.13	0.5	3.04	5.21	0.02	83.48	147.01	14.43	45.09	8.05	0.27
D218-2		72.37	0.24	13.11	0.21	2.9	0.05	0.35	1.46	3.25	4.8	0.15	64.54	117.33	11.31	36.12	6.12	0.54
XN04-1		72.71	0.19	13.14	0.35	2.61	0.05	0.29	1.51	2.55	5.18	0.17	48.95	96.7	9.67	32.03	5.6	0.54
C22		75.63	0.24	11.78	0.46	2.1	0.04	0.34	0.89	2.72	4.98	0.06	97.2	165.4	16.13	47.71	7.29	0.65
C41		75.38	0.15	11.8	0.55	2.6	0.04	0.15	0.61	3.07	4.99	0.02	87.24	161.8	17.43	55.11	9.48	0.29
C40	Granite	75.68	0.16	11.99	0.32	2.47	0.05	0.18	0.76	3.06	4.59	0.03	91.08	159	16.97	51.76	8.92	0.46
C43		73.75	0.21	12.36	0.32	2.97	0.05	0.24	1.13	2.97	5.27	0.04	71.54	126.8	13.32	43.98	7.76	0.6
C55		71.13	0.41	13.26	0.73	3.27	0.06	0.49	2.21	3.34	4.1	0.11	104.97	175.5	17.56	59.83	9.78	1.09

C24		71.57	0.48	12.9	0.58	3.02	0.06	0.6	1.77	2.82	2.29	0.13		91.74	158.6	16.51	53.6	8.72	1.08
C42		72.17	0.3	13.21	0.88	2.75	0.05	0.36	1.3	3.12	5.11	0.07		104.6	119.2	18.8	63.32	10.42	1.1
C21		67.89	0.61	13.74	1.49	3.65	0.08	0.66	2.45	3.14	5.09	0.21		89.4	161	17.8	58.08	11.24	1.73
C23		69.49	0.59	13.03	0.82	4.08	0.07	0.86	2.31	2.93	4.8	0.18		74.37	133.1	14.66	49.39	8.67	1.41
C48-1		67.96	0.75	13.47	1.24	3.9	0.08	0.95	2.52	2.87	4.84	0.24		79.04	143.2	16.86	59.45	10.99	1.59
C60		70.49	0.47	13.61	0.59	2.97	0.05	0.59	2.19	3	4.68	0.14		78.95	135.6	15.43	53.2	9.38	1.33
C47		68.38	0.73	13.17	0.78	4.5	0.09	1.07	2.81	2.86	4.26	0.23		57.37	119.8	15.22	61.26	12.8	1.39
C48-2		66.1	0.86	14.07	1.06	4.5	0.09	1.1	2.84	2.98	5.06	0.27		63.64	121.9	14.72	53.61	10.19	1.88
C54		65.92	0.82	14.32	1.23	3.98	0.09	1.08	3.01	3.02	4.97	0.25		67.83	126.9	14.63	55.1	9.9	2.01
FR-1		67.68	0.47	14.94			4.09	0.09	0.64	2.23	3.58	4.87	0.18	43.66	93.02	10.54	39.12	8.09	1.42
FR-10-1		57.35	0.61	18.25			4.698	0.15	0.71	2.77	7.5	0.99	0.28	26.17	57.94	7.11	29.9	8.04	0.64
FR-10-4		65.2	0.6	13.63			4.68	0.12	0.86	2.88	3.15	4.36	0.21	116.75	186.34	21.82	73.01	11.19	1.34
FR-19-12		71.62	0.41	12.83			3.47	0.11	0.57	1.78	2.86	4.99	0.13	82.2	134.92	14.4	45.81	7.49	0.91
FR-19-13		68.62	0.44	13.35			3.71	0.1	0.73	1.73	2.77	5.37	0.15	55	109.03	11.41	40.05	7.46	1.13
FR-19-31		66.48	0.64	14.07			4.7	0.11	0.787	2.61	3.52	4.81	0.22	52.41	106.85	11.9	43.66	8.14	1.55
FR-19-34		71.16	0.45	13.04			3.77	0.08	0.72	1.76	3.27	4.54	0.15	99.19	172.42	18.32	57.98	9.08	0.95
FR-19-41		65.17	0.83	14.47			5.33	0.13	1.12	3.05	3.26	4.85	0.3	58.94	127.49	14.84	56.07	11.07	1.66
FR-3	Granite	69.03	0.49	14.08			3.93	0.1	0.65	2.24	3.37	4.87	0.18	51.22	103.66	11.28	42.04	8.13	1.15
FR-32-1		68.5	0.52	13.76			4.32	0.12	0.7	2.3	3.26	4.91	0.19	52.65	106.92	11.5	41.68	7.84	1.28
FR-43-4		70.23	0.52	13.5			4.16	0.1	0.72	2.14	3.17	4.83	0.18	56.55	110.59	11.8	41.5	7.5	1.17
GTL-55-1		75.1	0.13	12.53			2.12	0.11	0.23	0.93	3.5	4.62	0.03	45.49	97.08	10.24	35.26	7.64	0.37
GTL-3-2		71.04	0.13	11.45			3.49	0.13	0.72	1.09	1.45	4.58	0.03	46.78	99.69	10.71	36.73	7.96	0.22
GTL-55-7		75.15	0.1	12.21			2.27	0.11	0.24	0.79	3.29	4.86	0.02	23.74	51.57	5.62	19.7	4.51	0.34
SMK-54-1		72.13	0.26	13.19			2.82	0.1	0.46	1.25	2.92	5.41	0.08	48.41	96.23	9.97	34.3	7.37	0.71
TXW-3-3		70.69	0.33	13.67			3.08	0.09	0.6	1.43	3.09	5.32	0.1	46.45	90.08	9.32	33.06	7.1	1

																				TXW-3-4	71.84	0.24	13.12											2.29	0.07	0.67	0.99	2.65	5.78	0.08	42.67	84.27	8.66	28.7	5.1	0.77
																				FR-32-3											33.99	85.72	10	33.46	9.49	0.18										
Gd	Tb	Dy	Ho	Er	Tm	Yb	Lu	Y	Rb	Sr	Zr	Nb	Hf	Ta	Rb/Sr	Nb/Ta	Zr/Hf	Fe ₂ O ₃ /FeO	T _{Zr} (°C)	εNd(t)	References																									
7.76	1.47	9.3	1.89	5.76	1.02	6.34	1.03	68.5	484	47.3	96.9	29.1	4.08	7.5	10.23	3.9	23.8	0.64	754																											
12.7	2.95	21.7	4.75	15	2.59	15.9	2.6	179	475	36.5	152	29.6	6.95	9.64	13.04	3.1	21.9	0.55	795	-10.8																										
9.29	2.08	15.1	3.18	10.2	1.68	11.6	1.83	106	487	47.2	99.8	23.5	4.8	7.99	10.32	2.9	20.8	0.30	750																											
9.05	2.2	16.3	3.55	11.4	1.99	12.6	2.06	124	515	37.4	86.8	22.5	4.54	7.91	13.77	2.8	19.1	0.38	740																											
8.33	1.85	13	2.83	8.58	1.48	9.49	1.54	95.6	588	55.6	85.3	21	4.13	8.8	10.58	2.4	20.7	0.35	737	-10.7																										
7.88	1.73	11.8	2.4	7.53	1.35	8.61	1.43	83.4	461	66.6	84.6	17.1	4.19	7.23	6.92	2.4	20.2	0.21	735																											
9.93	2.14	15.1	3.21	10.2	1.7	11.9	1.87	110	480	42	109	22.9	5.15	8.55	11.42	2.7	21.2	0.31	757																											
7.42	1.57	11.4	2.44	7.73	1.33	8.85	1.38	82.6	461	81.8	118	22.7	5.46	6.6	5.63	3.4	21.6	0.29	764	-11.2																										
6.91	1.35	9.13	1.84	5.97	0.98	6.87	1.06	66.3	467	41.3	91.7	28.8	4.11	7.08	11.32	4.1	22.3	0.42	742																											
6.33	1.26	8.33	1.68	5.47	0.92	6.4	1.01	60.2	470	35.8	96.5	28.1	4.29	6.9	13.14	4.1	22.5	0.43	747	-10.5																										
7.84	1.59	10.6	2.23	7.25	1.18	8.21	1.3	77.6	475	37.9	128	33.1	5.69	7.74	12.54	4.3	22.5	0.40	770		Guo et al., 2012																									
7.1	1.39	9.3	1.86	6.21	1.04	7.07	1.12	70	511	45.2	89.1	23.5	3.84	5.62	11.31	4.2	23.2	0.36	739																											
6.46	1.31	8.96	1.83	5.93	0.98	6.92	1.1	67.9	463	34.2	95.3	23.2	4.36	7.02	13.55	3.3	21.9	0.36	746	-10.4																										
7.49	1.49	9.79	1.95	6.6	1.1	7.56	1.2	74.3	492	54.8	98.5	23.5	4.69	6.43	8.97	3.7	21.0	0.38	746																											
11.8	2.89	21.7	4.77	15.3	2.61	19.5	2.92	163	725	7.85	68.5	28.6	5.23	12.4	92.44	2.3	13.1	0.48	723	-10.6																										
10.8	2.74	21.2	4.83	16.1	2.85	22	3.44	168	717	7.58	104	33.2	9.54	14.3	94.58	2.3	10.9	0.23	753																											
10.4	2.59	20	4.63	15.3	2.65	20	3.05	173	707	10	73.5	31.1	5.47	14	70.57	2.2	13.4	0.27	726																											
14.1	3.52	26	5.64	17.8	3.02	22.1	3.41	178	770	7.19	70.7	35.4	5.52	13.1	107.12	2.7	12.8	0.16	722	-10.9																										
9.77	2.42	19.2	4.29	14.4	2.5	18.6	2.93	149	772	6.69	68.7	39	5.49	14.6	115.45	2.7	12.5	0.30	720																											
12.1	2.97	22.4	4.91	16.4	2.85	20.3	3.24	173	826	7.3	59.6	29.3	4.9	15	113.14	2.0	12.2	0.45	710																											
13.7	3.27	23.5	4.93	15.1	2.66	17.1	2.73	170	764	8.85	67.5	29.4	5.24	16.9	86.35	1.7	12.9	0.41	717																											

11.4	2.83	21.5	4.72	15.7	2.78	19.7	3.19	169	742	7.62	62.2	29.6	4.96	13.7	97.33	2.2	12.5	0.25	711	-11.3	
16.9	4.03	29.4	6.05	19.2	3.22	22.2	3.45	208	783	6.71	84.3	33.4	6.86	17	116.69	2.0	12.3	0.41	735	-11	
10.8	2.59	19.2	4.09	13	2.24	15.5	2.41	142	748	13.2	76.2	28.7	5.3	12.5	56.73	2.3	14.4	0.41	727	-11.3	
10.1	2.54	19.4	4.27	13.6	2.43	16.7	2.63	160	803	7.67	70.4	25.5	5.46	12.5	104.76	2.0	12.9	0.38	721		
14.7	3.48	26.1	5.35	16.8	2.84	18.8	2.9	181	778	6.29	71.8	28.6	5.72	13.6	123.68	2.1	12.6	0.57	724		
12.4	2.6	17.7	3.6	11.3	1.99	14.2	2.28	129	888	25.4	109	36.5	5.78	14.1	34.99	2.6	18.9	0.37	762	-10.9	
11.7	2.42	16.8	3.44	10.5	1.92	13	2.13	127	781	21.4	105	30.9	5.46	14.7	36.53	2.1	19.2	1.56	759	-11	
14.6	2.95	19.2	3.72	11.4	2.13	14.7	2.48	146	929	29.4	109	25.5	5.73	11.7	31.6	2.2	19.0		761		
11.2	2.32	15.8	3.15	9.92	1.8	12.4	2.05	115	818	22.3	92.5	36.5	5.07	17.5	36.68	2.1	18.2	0.37	748	-11.2	
12.2	2.54	17.2	3.55	10.8	1.97	14.2	2.3	133	814	21.2	82.4	33.3	5.14	17.6	38.41	1.9	16.0	0.43	737	-10.4	
12.1	2.53	17.1	3.53	10.7	1.94	13.3	2.17	129	792	23.6	92.1	33.5	4.82	14.1	33.61	2.4	19.1	0.32	746		
9.99	2.35	18.4	4.03	13.9	2.64	19.7	3.31	140	703	9.96	76.7	46	5.4	15	70.62	3.1	14.2	0.52	733		
11	2.37	15.9	3.23	10.2	1.77	12.5	1.93	120	814	22.1	94.4	36.2	5.17	13.7	36.92	2.6	18.3	0.42	748		
7.86	1.89	14.1	3.15	10.7	1.89	13.4	2.13	119	727	9.11	87.7	39.3	5.82	18.1	79.81	2.2	15.1	0.35	738		
9.34	2.17	16.7	3.54	11.7	2.11	15.1	2.37	122	791	7.71	67.6	43.1	4.93	26.2	102.61	1.6	13.7	0.25	719		
9	1.97	16.3	3.75	10.5	1.76	12.5	1.75	115	625	35.5	87.8	22.6	5.04	10.8	17.7	2.09	17.4	0.18	732		
8.83	1.88	15.5	3.45	10.1	1.63	12.1	1.7	109	666	48.8	74	18.9	3.99	7.98	13.6	2.37	18.5	0.29	726		
9.24	2.08	18	4.14	12.1	2.02	14.1	2.03	142	662	37.8	79	13.5	4.34	5.46	17.5	2.48	18.2	0.23	723		
9.12	1.95	16.6	3.7	10.6	1.78	12.9	1.89	117	628	41	102	20.2	5.35	7.57	15.3	2.67	19	0.27	748	-11.46	
9.7	2.05	16.3	3.64	10.6	1.76	12.6	1.83	119	623	39.4	104	23.1	4.84	9.48	15.8	2.43	21.4	0.27	732	-10.88	Yang et al.,
8.17	1.66	13.3	2.97	8.51	1.42	9.68	1.39	96	561	48.1	87.3	16.6	4.27	5.65	11.7	2.94	20.4	0.42	734	-11.28	2012
8.81	1.88	15.3	3.41	9.76	1.57	11.6	1.62	111	610	46.6	103	20.4	5.01	6.8	13.1	2.99	20.5	0.40	743	-11.01	
8.03	1.66	12.9	2.97	7.78	1.28	9.27	1.35	83.8	655	34.6	78.1	23.9	4.48	8.73	18.9	2.73	17.4	0.32	728	-10.84	
11.49	2.58	21.7	4.72	13	2.25	15.6	2.18	151	948	10.4	63.2	25.7	5.65	13.8	90.8	1.87	11.2	0.36	708		
8.4	1.92	18	4.35	13.5	2.36	17.6	2.52	150	943	7.94	59.4	40.8	5.36	30.3	119	1.35	11.1	0.37	709	-9.78	

7.37	1.73	15.8	3.64	10.8	1.88	13.5	1.94	141	1001	7.44	58.7	36.6	5.06	29.1	134	1.26	11.6	0.35	705	
7.34	1.72	15.8	3.84	11.9	2.08	15.4	2.29	141	994	7.01	74.7	30.5	6.03	14.1	142	2.17	12.4	0.46	721	-10.39
9.28	2.06	18.2	4.17	12.4	2.1	14.9	2.16	143	949	12.7	75.2	30.1	5.52	13.9	74.7	2.17	13.6	0.44	721	
6.63	1.52	13.7	3.33	10.1	1.82	13.2	1.96	116	1091	7.54	66.3	27	5.85	12.4	145	2.18	11.3	0.38	0	
8.44	1.95	17.2	3.87	12.1	2.08	15.5	2.27	140	1031	8.2	75.9	27.6	6.48	16.8	126	1.64	11.7	0.41	726	-10.73
12.75	2.85	24.5	5.39	15.5	2.58	18.8	2.62	177	1011	7.08	72.2	28.5	6.39	14.1	143	2.03	11.3	0.30	0	-9.77
8.15	1.9	16.9	3.98	11.7	2.01	14.5	2.06	141	991	8	63	28.4	5.39	14.5	124	1.97	11.7	0.64	708	-10.69
9.69	2.28	20.8	4.95	15.1	2.68	19.7	2.88	168	949	8.11	71.6	28.3	6.22	13.6	117	2.09	11.5	0.55	719	
14.37	3.2	27.4	6.18	18	3.04	22.1	3.17	200	951	6.91	59.6	29.1	5.41	12.3	138	2.37	11	0.56	709	
13.65	3.18	28.2	6.53	20	3.65	28.4	4.25	207	983	5.1	55.9	26.2	5.07	11.4	193	2.3	11	0.45	702	-10.39
13.25	2.78	23.1	4.94	13	1.95	12.6	1.7	203	971	8.41	65.9	34.6	5.72	17.4	115	1.99	11.5	0.32	712	-10.12
18.4	3.5	22.8	4.77	13.4	2.09	13.5	1.99	149	602	14.2	64.4	36.5	4.68	9.77		3.7	13.8		713	
9.86	1.78	11.6	2.59	7.34	1.12	7.24	1.05	74.8	1010	7.46	82.7	18.8	4.99	4.01		4.7	16.6		763	He et al., 2010,
13.9	2.71	18.8	4.48	12.8	2.06	14.1	2.1	131	522	23	83	38.7	5.65	9.32		4.2	14.7		740	
8.51	1.89	14.2	3.08	9.87	1.71	12.72	2	109	691	11.2	89	31.6	6.27	11.5	61.7	2.7	14.2	1.31	745	
7.33	1.54	11.1	2.31	6.92	1.13	7.34	1.03	82.8	676	20.3	78.2	27.1	4.96	11.5	33.3	2.4	15.8	1.38	736	Hua et al., 2003
10.76	2.29	16.4	3.33	10	1.71	11.2	1.59	104	559	23.2	85.8	33.3	4.57	8.58	24.1	3.9	18.8	1.42	741	
7.7	1.71	12.8	2.76	8.54	1.45	10.1	1.5	91.1	595	12.9	69.8	36.4	4.73	12.6	46.1	2.9	14.8	1.18	725	
10.4	2.48	18.6	4.14	12.9	2.34	16.6	2.48	132	589	10	64	30	5.04	11.7	58.9	2.6	12.7	1.68	717	
8.01	1.7	13.2	2.78	8.95	1.58	12.15	1.96	80.9	908	17.3	56.6	62.5	4.16	20.5	52.5	3.0	13.6	0.19	740	
8.52	1.67	12.88	2.69	8.32	1.43	10.1	1.59	77.3	916	9.5	62.8	66.1	3.86	26.7	96.4	2.5	16.3	0.02	722	
6.15	1.07	7.9	1.69	5.29	0.87	5.88	0.88	47.5	813	6.2	64.4	58.8	4.44	17.5	131.1	3.4	14.5	0.20	723	
5.37	0.99	7.35	1.51	4.78	0.82	5.57	0.84	42.8	985	11.1	47.3	63.2	3.02	25.6	88.7	2.5	15.7	0.36	707	Li, 2011
3.92	0.6	4.44	0.93	2.87	0.41	2.75	0.4	23.5	643	44.1	100	41.4	3.49	14.1	14.6	2.9	28.7	0.38	758	-11.8
10.1	1.78	12.96	2.75	8.22	1.35	9.01	1.39	79.5	1190	7.8	64.8	61.2	3.56	20.2	152.6	3.0	18.2	0.13	759	-12.2

Yuan, S., Williams-Jones, A.E., Romer, R.L., Zhao, P., Mao, J., 2019.
 Protolith-Related Thermal Controls on the Decoupling of Sn and W in Sn-W Metallogenic Provinces:
 Insights from the Nanling Region, China. *Economic Geology*, 114(5): 1005-1012.

5.73	1.12	8.65	1.8	5.72	1.05	7.52	1.2	50.6	940	11.5	49.1	63.7	3.71	23.6	81.7	2.7	13.2	0.10	709	-15.5	
0.93	0.2	1.42	0.3	1.04	0.19	1.67	0.26	8.5	909	4.4	24.1	103.6	1.82	19.3	206.6	5.4	13.2	0.12	668	-10.7	
4.95	0.95	6.46	1.17	3.77	0.79	6.88	1.1	36.7	943	7.9	37.1	85.6	3.97	42.2	119.4	2.0	9.3	0.17	690	-10.5	
3.61	0.68	4.73	0.84	2.64	0.58	4.99	0.84	29	899	12.5	43.7	61.4	4.87	30.6	71.9	2.0	9.0	0.22	708	-9.9	
8.49	2.02	13.6	3.07	9	1.5	10.9	1.57	95.7	624	6.55	50.5	36.2	4.48	16.4	95.3	2.2	11.3		701	-8.8	
9.47	2.04	11.8	2.44	6.28	0.86	5.5	0.71	70.3	646	12.1	97.2	35.9	5.61	9.64	53.4	3.7	17.3		752	-11.2	
7.02	1.51	9.56	2.17	6.13	1	6.8	1.01	63.4	606	37.6	63.4	30.3	3.72	8.96	16.1	3.4	17.0		716	-9.0	
7.77	1.66	11.5	2.65	7.64	1.2	8.6	1.29	78.2	458	31.6	75.8	25.7	3.79	7.07	14.5	3.6	20.0		729	-10.5	
9.1	1.99	12.9	2.96	7.94	1.15	7.57	1.06	79.5	626	16.6	82.1	34.5	5.1	10.5	37.7	3.3	16.1		736		
9.28	2.18	15.2	3.59	10.7	1.76	12.5	1.86	110	617	7.19	68	32.9	4.97	12.4	85.8	2.7	13.7		721		
8.16	1.83	11.9	2.75	7.79	1.24	8.55	1.2	85.5	639	3.78	48	33.9	3.99	12.6	169.0	2.7	12.0		698		
4.24	0.93	6.49	1.53	4.56	0.74	5.27	0.77	42.3	648	3.69	70.3	33.2	5.56	14.4	175.6	2.3	12.6		724		
5.45	1.28	8.6	2.01	6.11	0.96	7.29	1.03	61.4	539	4.43	70.1	37.8	4.85	11.2	121.7	3.4	14.5		722		
2.99	0.69	4.58	1.09	3.21	0.52	3.49	0.51	27.8	516	5.92	57.1	37.2	4.17	10.7	87.2	3.5	13.7		708		
																					Dong et al., 2014
4	0.92	6.01	1.34	4.02	0.68	4.73	0.66	41.2	576	4.3	53.5	34.1	3.97	13	134.0	2.6	13.5		705		
4.6	1	6.99	1.57	4.54	0.72	4.83	0.69	47.6	596	8.72	70	33.3	4.84	10	68.3	3.3	14.5		723		
4.71	1.06	7.14	1.68	5.05	0.86	6.18	0.88	57.8	597	6.25	61.6	34.1	5.15	11.6	95.5	2.9	12.0		712		
5.4	1.27	9.32	2.3	7.4	1.27	9.65	1.44	69.9	443	7.7	69.2	30.9	4.82	8.6	57.5	3.6	14.4		721	-10.1	
10.65	2.55	17.8	4.01	12	1.96	14.3	2.09	136	679	4.73	58.8	34.7	4.46	12.1	143.6	2.9	13.2		714		
3.47	0.82	5.4	1.2	3.6	0.59	4.35	0.64	34.9	600	6.04	62.3	32.5	4.95	9.46	99.3	3.4	12.6		708		
3.42	0.77	5.1	1.16	3.34	0.55	3.8	0.54	38.4	548	4.98	59.8	33.4	4.57	10.2	110.0	3.3	13.1		710		
7.67	1.72	12	2.7	8.21	1.29	8.6	1.27	80.9	575	4.26	69.9	36.1	5.23	11.3	135.0	3.2	13.4		721	-10.6	
1.84	0.42	2.87	0.64	2.02	0.34	2.7	0.41	18.2	652	1.96	71.9	35.3	5.92	12.9	332.7	2.7	12.1		725		
1.73	0.37	2.32	0.55	1.69	0.3	2.46	0.38	14.4	626	1.34	66.9	34.1	5.34	11.4	467.2	3.0	12.5		722	-8.4	

3.13	0.71	5.03	1.14	3.4	0.59	4.48	0.68	41.6	649	2.1	64.1	28.8	5.36	10	309.0	2.9	12.0	719	-11.2	
4.36	1	6.6	1.39	3.99	0.68	4.65	0.64	56.6	707	3	56	21.4	5.07	13.5	235.7	1.6	11.0	711	-11.3	
2.9	0.6	3.76	0.78	2.45	0.37	2.44	0.38	20.4	351	62.3	110	18.1	5.17	1.92	5.6	9.4	21.3	0.2		
8.37	1.54	9.58	1.96	6.09	0.87	5.72	0.9	54	328	38.9	91.4	34.7	4.48	4.16	8.4	8.3	20.4	0.5		Fang et al.,
6.06	1.17	7.71	1.65	5.24	0.82	5.69	0.89	47.9	247	33.5	63.4	36.1	3.46	8.4	7.4	4.3	18.3	0.4		2016
5.15	1.01	6.76	1.4	4.55	0.68	4.87	0.79	39.6	407	41.7	55.4	29.1	2.96	7.37	9.8	3.9	18.7	0.3		
4.221	0.745	2.283	0.115	0.135	0.013	0.144	0	10.2	927.769	24.047	27.321	48.558	11.778	142.471	38.6	0.3	2.3	2.17	661	
8.829	1.594	4.98	0.221	0.157	0.012	0.125	0.01	20.168	1487.55	29.907	32.683	80.615	9.116	137.005	49.7	0.6	3.6	2.24	666	Hua et al.,
5.094	0.922	2.697	0.107	0.074	0.004	0.091	0.008	9.936	808.23	17.065	28.226	54.555	8.113	150.809	47.4	0.4	3.5	2.53	661	2003
4.635	0.855	2.371	0.135	0.146	0.013	0.174	0	12.504	801.82	36.58	31.111	69.54	9.912	139.415	21.9	0.5	3.1	0.76	674	
1.39	0.3	1.3	0.09	0.08	0.01	0.07	0.01	6.92	510.8	49.7	18.2	22.5	4.38	6.84	10.3	3.3	4.2	2.23	629	
3.29	0.99	3.8	0.21	0.26	0.02	0.17	0.03	19.7	1003	23.6	30.7	56.8	5.72	103.5	42.5	0.5	5.4	0.71	666	Wu, 2017
7.53	2.04	6.26	0.27	0.28	0.02	0.21	0.03	24.3	992.6	26	17.5	41.8	3.01	46.5	35.5	0.9	5.8	0.88	625	
9.06	1.54	4.2	0.18	0.13	0.03	0.15	0.05	17.7	734	17.6	27.3	30.4	7.42	29.7	41.7	1.0	3.7	2.50	660	
7.19	1.69	6.38	0.34	0.29	0.05	0.19	0.05	18.9	647	12.7	21.7	19.8	6.93	17.1	50.9	1.2	3.1	4.00	653	
4.28	0.89	3.79	0.26	0.32	0.05	0.21	0.05	23.1	705	32.8	25.5	15.2	7.41	7.36	21.5	2.1	3.4	1.33	658	
6.15	1.11	4.14	0.34	0.51	0.06	0.45	0.08	15.8	745	24.5	27.1	56.5	6.27	42	30.4	1.3	4.3	1.24	667	
3.39	0.83	3.3	0.19	0.18	0.05	0.27	0.05	21.8	510.81	39.54	18.2	22.46	5.48	6.84	12.9	3.3	3.3	2.23	630	Zuo, 2016
3.29	0.99	3.8	0.21	0.26	0.02	0.17	0.03	13.7	902.3	27.67	30.69	56.79	6.72	53.48	32.6	1.1	4.6	0.71	667	
4.96	0.97	4.32	0.18	0.13	0.02	0.13	0.02	17.2	735.57	25.12	24.89	2.38	7.67	8.55	29.3	0.3	3.2	1.40	650	
6.43	2.04	6.26	0.27	0.28	0.02	0.21	0.04	16.7	992.62	22.57	17.49	21.79	3.01	46.46	44.0	0.5	5.8	1.43	631	
8.27	1.73	5.93	0.31	0.22	0.02	0.16	0.02	22.4	831.79	25.29	26.86	41.9	4.36	31.53	32.9	1.3	6.2	1.23	658	
7.58	1.13	3.83	0.2	0.15	0.02	0.12	0.02	20.4	962.37	32.14	66.09	39.59	7.64	28.75	29.9	1.4	8.7	1.46	720	
7.88	1.57	10.1	2.13	7.23	1.08	7.61	1.13	74.8	664	108	150	63.4	5.77	6.78	6.2	9.4	26.0	0.18	769	-8.0 Guo et al.,
7.87	1.57	9.71	2.11	7.13	1.05	7.75	1.17	69	763	76.4	157	55.3	6.56	7.2	10.0	7.7	23.9	0.59	780	2015

Yuan, S., Williams-Jones, A.E., Romer, R.L., Zhao, P., Mao, J., 2019.
 Protolith-Related Thermal Controls on the Decoupling of Sn and W in Sn-W Metallogenic Provinces:
 Insights from the Nanling Region, China. *Economic Geology*, 114(5): 1005-1012.

7.63	1.58	9.93	2.13	7.25	1.08	7.67	1.15	72.4	682	85.9	146	56.1	5.9	6.74	7.9	8.3	24.7	0.32	771	
7.54	1.54	10.1	2.13	7.5	1.15	8.29	1.24	75.3	661	86.9	153	55.7	6.2	6.95	7.6	8.0	24.7	0.41	778	
8.81	1.78	11.4	2.39	7.84	1.21	8.63	1.32	78.3	659	81	155	58.9	6.81	7.66	8.1	7.7	22.8	0.55	779	
7.74	1.52	9.39	1.94	6.29	0.96	6.84	1.02	62.2	623	97.1	164	46.2	6.41	6.32	6.4	7.3	25.6	0.35	785	-7.9
7.19	1.42	8.34	1.73	5.86	0.85	6.21	0.97	59.6	734	87.6	165	40.6	6.16	6.16	8.4	6.6	26.8	0.03	776	
8.28	1.54	8.98	1.8	6.07	0.9	6.39	0.96	63.4	821	108	172	42.2	6.17	6.08	7.6	6.9	27.9	0.16	779	-9.9
12.1	2.46	15.5	3.33	11.3	1.7	12.4	1.87	107	738	55.8	179	74.4	7.9	10.6	13.2	7.0	22.7	0.37	796	
9.78	1.99	12.2	2.62	8.82	1.32	9.92	1.5	87.4	680	50.5	148	66.4	6.59	14.2	13.5	4.7	22.5	0.15	779	
11	2.2	13.9	2.82	9.45	1.39	10	1.49	92	743	48.7	163	76.6	6.93	11	15.3	7.0	23.5	0.41	788	
19.7	4.23	27.8	5.46	17.8	2.77	20.3	2.95	209	1293	6.79	33.8	38.5	3.7	24.8	190.4	1.6	9.1	0.19	674	-9.0
18.2	4.04	26.7	5.17	17.4	2.76	20.6	3.01	199	1106	6.16	42.2	27.9	5.13	20.7	179.6	1.3	8.2		681	
11.6	2.39	15.4	2.88	9.64	1.57	12	1.74	89.7	1143	8.92	37	24.9	4.42	10.4	128.1	2.4	8.4	0.02	679	-9.7
21.9	4.55	29.6	5.6	18.2	2.71	19.9	2.76	212	1361	8.82	47.2	28.5	4.65	16.6	154.3	1.7	10.2	0.41	697	
21.5	5.03	32.4	6.13	20.7	3.52	27.5	3.96	173	1502	13.6	37.2	27.3	5.06	25.3	110.4	1.1	7.4	0.23	689	
22.7	4.99	32.4	6.23	19.9	3.03	22.9	3.26	229	1155	8.13	66.1	30.7	7.04	12.6	142.1	2.4	9.4	0.13	721	
14.1	2.97	19.1	3.57	11.8	2.03	15.8	2.24	97.7	1511	11.7	34.4	24	4.28	13.9	129.2	1.7	8.0	0.35	683	
17	3.62	23.5	4.84	15.3	2.22	14.9	2.12	163	792	20.9	76.9	43.1	6.22	15.3	37.9	2.8	12.4	0.48	736	-9.8
22.1	4.61	30.5	6	19.5	2.88	20.6	2.93	245	781	9.42	72.4	31.4	7.04	10.5	82.9	3.0	10.3	0.40	726	
11.9	2.45	16	3.2	10.1	1.4	9.85	1.4	103	806	7.51	79.2	43.2	5.44	14.8	107.3	2.9	14.6	0.32	733	
10.7	2.3	15.2	3.13	10.1	1.43	10	1.36	100	717	8	85.3	37.3	5.12	7.58	89.6	4.9	16.7	0.59	741	
21.1	4.64	29.8	5.51	18.2	2.85	21.2	3.05	190	1059	5.48	49.1	26.6	5.53	18.8	193.3	1.4	8.9	0.04	694	-12.9
9.3	1.29	9.9	2.1	6.05	0.87	6.22	0.92	56	458	25	134	23	4.8	3.9	18.3	5.9	27.9	0.44	776	
8	2.66	13.5	2.76	9	1.17	6.43	1.34	74	687	25	153	41	6.7	4.7	27.6	8.7	22.8	0.49	784	Jiang et al.,
14.7	3.07	20.9	4.34	12.69	2.01	12.2	1.68	122	695	10	77	36	4.7	8.9	69.0	4.0	16.4	1.04	727	2006
10.6	4.28	23.5	4.73	14.4	1.85	10	1.91	95	697	14	72	43	4.7	7.9	48.7	5.4	15.3	1.91	726	

Yuan, S., Williams-Jones, A.E., Romer, R.L., Zhao, P., Mao, J., 2019.
 Protolith-Related Thermal Controls on the Decoupling of Sn and W in Sn-W Metallogenic Provinces:
 Insights from the Nanling Region, China. *Economic Geology*, 114(5): 1005-1012.

11.2	5.54	29.3	5.99	19.9	3.03	18.3	3.81	250	962	11	121	82	11.7	9.2	88.1	8.9	10.3	0.60	759		
8.32	1.31	7.81	1.51	4.73	0.67	4.59	0.67	44.8	383	98.9	228	21.2	7.38	2.15	3.9	9.860465	30.9		809		
7.24	1.15	7.16	1.37	4.37	0.6	4.12	0.59	39.8	387	92.4	182	19.4	6.02	2.02	4.2	9.60396	30.2		786		
8.59	1.33	8.22	1.6	4.83	0.67	4.76	0.69	45.1	364	102	213	21.2	7.2	2.19	3.6	9.680365	29.6		801	-8.0	
8.14	1.26	7.61	1.52	4.58	0.67	4.32	0.65	42.3	403	99.5	214	20.3	7.32	2.11	4.1	9.620853	29.2		801	-7.8	
7.9	1.19	7.06	1.38	4.19	0.58	4.04	0.56	39.7	329	88	167	19.6	5.53	2	3.7	9.8	30.2		781	-8.2	
8.79	1.36	8.35	1.64	4.93	0.69	4.72	0.67	46.4	354	111	220	21.4	7.1	2.24	3.2	9.553571	31		806	-8.2	
7.67	1.21	7.23	1.44	4.32	0.63	4.14	0.62	40.9	348	111	192	19.6	6.43	2.05	3.1	9.560976	29.9		794	-8.2	
7.89	1.18	7.03	1.36	4.12	0.61	3.95	0.6	39.2	359	87.5	202	19	6.76	2.01	4.1	9.452736	29.9		797	-8.0	
13.7	2.92	19.9	3.75	12.5	2.2	17.1	2.45	104	789	8.03	30.8	20.9	4.62	19.7	98.3	1.060914	6.7		654	-7.3	
19	3.73	24.5	4.48	14.2	2.26	16.2	2.35	134	922	7.25	43.8	24.5	4.91	11.9	127.2	2.058824	8.9		687	-7.0	
20.4	4.33	29.2	5.61	17.7	2.89	20.6	2.98	162	1036	9.69	31.3	26.7	3.41	14.1	106.9	1.893617	9.2		666	-7.6	
11	2.28	15.2	2.86	9.45	1.63	12.4	1.85	85.3	742	11.1	30.7	24.1	3.92	17.4	66.8	1.385057	7.8		662		
15.9	3.17	21.7	4.15	13.3	2.13	15.7	2.33	142	830	5.33	40.9	23.5	4.68	12.8	155.7	1.835938	8.7		680		
15.6	3.15	21	3.88	12.3	1.95	14.8	2.1	126	935	6.28	27.5	25.1	3.12	14.2	148.9	1.767606	8.8		657	-7.4	
20.2	4.1	26.8	5.06	15.9	2.57	18.4	2.65	160	963	8.56	45.5	27.8	4.97	16	112.5	1.7375	9.2		692	-7.2	
12.5	2.43	16.6	3.33	10.1	1.48	10.1	1.46	101	623	9.71	61.2	33.1	4.01	6.77	64.2	4.889217	15.3		706		
17.2	3.38	22.7	4.54	14.2	2.09	14.3	2.07	135	648	10.8	85.9	33.8	5.55	8.27	60.0	4.087062	15.5		736		
13	2.51	15.7	2.78	8.87	1.47	11.1	1.63	77.2	1002	4.71	28.7	23	4.17	8.23	212.7	2.794654	6.9		664	-6.7	
22.4	4.49	28.8	5.45	16.9	2.71	19.3	2.81	161	815	6.5	32.8	23.1	4.12	10.1	125.4	2.287129	8		665	-6.0	
17.6	3.36	21	3.71	11.6	1.87	13.6	2.02	111	974	6.47	37.8	22.7	4.76	9.94	150.5	2.283702	7.9		678		
20.8	4.27	28.1	5.34	16.9	2.78	21	3.09	158	952	7.26	29.3	23.9	3.72	13.7	131.1	1.744526	7.9		662	-7.1	
19.6	3.8	24.8	4.62	14.6	2.42	18.2	2.64	149	772	7.4	34.4	27	4.24	8.8	104.3	3.068182	8.1		670	-6.8	
14.4	2.93	21.2	4.29	13.7	2.14	15.7	2.23	138	753	13.2	54.7	35.2	4.44	10.9		3.229358	12.3		699		
									774.3	37.5	110.4	66.6	9.6		20.6	0	11.5			785	

Chen B et al.,
2014

Mao et al.,

									696.5	52.4	127.1	59.6	11.7		13.3	0	10.9	786	1995
14.4	2.49	14.7	3.72	11	1.84	13.4	1.81	717.5	39.9	120.2	60.6	10.1		18.0	0	11.9	781	-6.39	
8.66	1.58	10.3	2.56	7.98	1.38	9.87	1.48	625.1	57.3	123.6	65.2	11.5		10.9	0	10.7	776	-6.99	
9.81	1.72	11.9	2.99	9.22	1.62	11.4	1.72	571.4	40.2	113.5	66.3	9.9		14.2	0	11.5	775	-7.33	
11.6	1.88	13.3	3.14	9.83	1.7	11.7	1.76	723.1	50.5	177.9	60.3	9.8		14.3	0	12	805	-7.59	
41.9	7.5	41.7	9.64	27	4.74	35.3	5.07	1149.8	13.4	32.7	19.4	6.1		85.8	0	5.36	686	-7.41	
16.6	2.71	18.9	4.64	13.5	2.34	17.3	2.36	1028.7	7.4	30.4	20.2	9.1		139.0	0	3.34	671	-6.35	
18.6	3.07	20.8	5.27	15.2	2.65	20.1	2.97	779.2	13.3	31.7	24.2	8.3		58.6	0	3.82	674	-7.44	
20.7	3.86	23.4	5.41	16.9	2.88	20.9	2.69	1086.3	8	25.7	21.3	4.5		135.8	0	5.71	656	-7.27	
26.7	4.78	26.6	5.79	17.7	3.06	21.6	3.01	1007.4	8.1	39.9	24.9	7.3		124.4	0	5.47	701	-4.25	
20.5	3.78	21.6	5.03	15.6	2.65	18.9	2.57	904.9	17.3	58.1	37.3	8.9		52.3	0	6.53	715	-7.34	
20.7	3.58	22.3	5.11	15.6	2.68	18.7	2.77	1105.2	20.3	24.6	13.5	6.5		54.4	0	3.78	658	-7.28	
17.6	2.96	18.6	4.31	13.4	2.25	16.1	2.33	685	46.1	36.9	<1.5	5.7		14.9	0	6.47	675	-7.1	
4.13	0.77	4.51	1.14	3.36	0.59	4.27	0.77	682.3	59.7	35.4	<1.5	6.6		11.4	0	5.82	670	-7.53	
								600.9	39.8	42.9	<1.5	7		15.1	0	6.13	689		
7.37	1.21	6.98	1.37	3.87	0.63	3.99	0.59	37.9	375	108	190	17.5	6.5	2.4	3.5	7.3	29.2	794	
8.15	1.31	7.46	1.57	4.22	0.67	4.17	0.66	43.7	378	98	209	19.9	6.4	2.4	3.9	8.3	32.7	803	
7.32	1.19	7.15	1.3	3.89	0.63	3.96	0.59	37.8	390	109	180	17.7	6	2.3	3.6	7.7	30.0	793	
7.73	1.39	7.85	1.54	4.59	0.71	4.49	0.66	43.3	383	88	218	20.8	6.5	2.7	4.4	7.7	33.5	810	
7.49	1.2	7.44	1.49	4.38	0.66	4.02	0.6	40.2	421	90.5	196	19.2	6.9	2.5	4.7	7.7	28.4	797	Chen et al.,
7.74	1.27	7.92	1.56	4.53	0.68	4.46	0.65	42.6	370	75.3	207	19.9	6.9	2.7	4.9	7.4	30.0	806	2016
21.6	5.13	31.4	6.35	19	3.61	28	4.14	159	1175	25.4	40	27.4	4.8	28.4	46.3	1.0	8.3	685	
19.7	4.44	28.1	5.7	17.7	3.38	26	3.91	138.5	857	17.2	35	22.8	4.1	18.7	49.8	1.2	8.5	675	
29.3	6.57	40.8	8.06	24.1	4.48	32.8	4.79	205	1100	4.7	20	15.5	2.4	14.2	234.0	1.1	8.3	640	
20.5	4.26	27.9	5.83	17.15	2.93	21.7	3.16	182.5	773	13.3	54	26.7	4.9	15.9	58.1	1.7	11.0	699	

23	4.9	30.8	6.28	18.1	3.09	23.1	3.41	191.5	995	7.9	56	28.8	5.2	15.2	126.0	1.9	10.8		704		
22.1	4.7	28.9	5.93	17.05	3.12	22.1	3.33	179	945	15.5	44	29.8	4.5	20.5	61.0	1.5	9.8		693		
20.7	4.44	28.4	5.98	17.35	3.07	21.9	3.17	183	848	10.3	40	26	3.9	15.7	82.3	1.7	10.3		678		
22.2	4.78	29.8	6.15	18.55	3.22	22.5	3.31	203	914	13.5	57	29.9	5.8	19.2	67.7	1.6	9.8		711		
38.5	8.78	55	10.8	33.2	6.18	47.8	6.99	238	1190	11	39	25.2	5.8	25.5	108.0	1.0	6.7		690		
23.3	5.11	31.8	6.2	19.5	3.31	21.6	3.16	201	886	25.6	64	41.6	5.3	18.6	34.6	2.2	12.1		724		
19.8	4.25	26.8	5.74	16.65	2.76	18.7	2.74	158	947	6	77	40.7	6	18.4	158.0	2.2	12.8		733		
13.9	2.91	19	3.91	11.4	1.92	13.3	2.01	115.5	940	6.6	61	38.3	4.8	14.55	142.0	2.6	12.7		715		
13.85	2.98	20.46			2.13	14.17	2.09	118.58	653.64	9.26	133.11	37.68	6.94	9.03	70.6	4.2	19.2	0.21	773		
11.11	2.28	14.99			1.42	9.33	1.36	84.38	520.36	13.21	106.74	32.32	5.27	5.8	39.4	5.6	20.3	0.28	756	-7.08	
14.12	2.89	18.97			1.8	11.67	1.69	107.72	631.02	23.06	135.92	32.99	6.54	5.34	27.4	6.2	20.8	0.15	777	-7.32	
5.7	1.19	7.86			0.74	4.71	0.69	41.73	475.51	10.7	106.38	29.8	5.06	3.54	44.4	8.4	21.0	0.27	757		
8.79	1.72	11.24			1.17	7.87	1.17	63.82	581.82	11.04	155.88	31.86	7.16	5.27	52.7	6.0	21.8	0.20	785		
13.63	2.78	18.4			1.79	11.63	1.68	102.24	601.02	18.11	152.25	33.89	6.99	5.3	33.2	6.4	21.8	0.32	785	-7.49	
14.81	2.72	16.61			1.4	8.71	1.23	80.27	525.06	20.14	145.81	39.79	6.62	5.38	26.1	7.4	22.0	0.21	785	-7.53	
10.93	2.17	14.06			1.36	8.91	1.29	71.41	628.3	14.57	133.98	30.11	6.45	5.72	43.1	5.3	20.8	0.06	778		
7.22	1.61	11.13	2.35	7.16	1.14	8.02	1.19	54.6	897.14	3.23	124.27	47.22	7.04	8.62	277.8	5.5	17.7	0.31	776	-7.8	Su, 2017
12.22	2.88	20.5	4.48	13.64	2.12	14.07	2.08	136.81	797.98	2.79	141.75	53.53	8.04	6.61	286.0	8.1	17.6	0.22	777		
11.46	2.58	17.74	3.81	11.75	1.96	13.53	2.03	109.21	891.67	6.28	119.15	50.99	6.98	8.91	142.0	5.7	17.1	0.13	768	-6.16	
13.3	3.09	21.83	4.74	14.29	2.25	14.86	2.18	134.26	805.56	3.37	128.92	48.32	7.52	8.08	239.0	6.0	17.1	0.03	770		
16.69	3.6	23.82	4.95	15.7	2.81	21.61	3.26	141.56	1181.23	4.81	120.63	62.37	8.54	19.17	245.6	3.3	14.1	0.13	780	-5.83	
6.01	1.56	11.65	2.63	8.9	1.67	12.6	1.99	80.66	916.77	1.18	78.72	19.26	7.36	9.82	776.9	2.0	10.7	0.26	733		
9.89	2.58	19.37	4.35	14.57	2.65	19.88	3.12	143.48	1105.82	1.91	69.07	27.01	5.96	12.43	579.0	2.2	11.6	0.06	728		
12.15	3.3	24.94	5.56	18.53	3.35	25	3.84	188.65	1370.46	2.25	73.48	32.79	6.2	14.45	609.1	2.3	11.9	0.16	729		
																					-7.33

																					-8.1		
																						-8.23	
4.7	0.73	3.88	0.78	2.34	0.41	3.04	0.51	22.4	656	175	227	18.8	7.55	2.64	3.7	7.1	30.1	0.79	819				
8.13	1.42	8.39	1.59	4.62	0.74	4.98	0.73	47.4	400	71	160	24.6	5.35	4.82	5.6	5.1	29.9	0.40	791				
15.77	3.59	24.3	4.83	14.9	2.89	21.1	3.19	148	770	8	75.6	26.2	2.52	12.1	96.3	2.2	30.0	0.43	726				
3.46	0.53	2.94	0.58	1.79	0.35	2.57	0.44	18.9	470	129	127	19.2	4.23	4.28	3.6	4.5	30.0	0.99	786				
5.46	1.06	6.9	1.42	4.42	0.79	5.38	0.81	45.1	471	35.8	71.8	17.2	2.39	3.39	13.2	5.1	30.0	0.02	734	Chen G et al.,			
4.24	0.91	6.67	1.49	4.59	0.84	5.81	0.88	48.3	359	36.4	60.1	11.8	2	2.08	9.9	5.7	30.1	0.66	716	2013, 2014			
6.48	1.55	11.2	2.33	8.12	1.66	12.7	1.94	69.4	918	7.21	64.9	25.6	2.16	15.9	127.3	1.6	30.0	0.42	717				
9.2	1.5	8.69	1.57	4.67	0.74	4.81	0.67	44.7	444	48.6	173	15.5	5.77	2.02	9.1	7.7	30.0	0.45	798				
4.7	0.73	3.88	0.78	2.34	0.41	3.04	0.51	22.4	656	175	226	18.8	7.55	2.64	3.7	7.1	29.9	0.79	820				
8.13	1.42	8.39	1.59	4.62	0.74	4.98	0.73	47.4	400	71	160	24.6	5.35	4.82	5.6	5.1	29.9	0.40	792				
12.02	2.38	14.61	3.04	9.66	1.52	10.03	1.47	95.35	664.19	32.34	132.21	28.16	5.1	6.2	20.5	4.5	25.9	0.09	792				
6.74	1.17	7.51	1.53	4.5	0.78	5.75	0.85	42.41	518.9	43.51	141.1	26.15	4.64	6.82	11.9	3.8	30.4		782				
13.54	2.96	20.97	4.53	14.46	2.61	18.92	3.17	128	819.2	10	96	33.1	3.3	9.6	81.9	3.4	29.1	0.08	748	Yao et al.,			
9.34	2.04	13.55	2.82	8.83	1.5	11.48	1.81	77.83	803.7	10	96	38.9	3.7	14.3	80.4	2.7	25.9	0.24	750	2013			
5.54	0.98	6.13	1.3	3.87	0.66	4.4	0.69	36.21	381.5	40	7	19.3	3.6	2.7	9.5	7.1	1.9	0.33	734				
11.67	2.67	18.47	3.75	12.99	2.53	19.68	3.02	70.61	76.3	1.95	88.77	27.58	1.12	17.69	39.1	1.6	79.3		752				
4.969	0.786	4.446	0.897	2.734	0.393	2.852	0.426	23.74	283.7	182.8	150.9	15.76	4.56	2.308	1.6	6.8	4.6		778				
6.741	1.165	7.506	1.525	4.651	0.775	5.754	0.85	42.41	518.9	43.51	141.1	26.15	4.64	6.82	11.9	3.8	4.6		784				
7.33	1.24	6.76	1.3	3.32	0.48	2.6	0.32	31.62	375	49	127	20.8	5.1	1.9	7.7	10.9	5.1	0.28	761				
5.54	0.98	6.13	1.3	3.87	0.66	4.43	0.69	36.21	384.5	40	76	19.3	3.6	2.7	9.6	7.1	3.6	0.17	730	Liu et al.,			
																					2008		
9.34	2.04	13.55	2.82	0.3	1.58	11.48	1.81	77.3	803.7	10	96	38.9	3.7	14.3	80.4	2.7	3.7	0.18	751				

Yuan, S., Williams-Jones, A.E., Romer, R.L., Zhao, P., Mao, J., 2019.
 Protolith-Related Thermal Controls on the Decoupling of Sn and W in Sn-W Metallogenic Provinces:
 Insights from the Nanling Region, China. *Economic Geology*, 114(5): 1005-1012.

14.4	3.55	25	5.37	16.4	2.78	19.76	2.95	121	572	26.9	88.7	24.4	8.31	16.61	21.3	1.5	10.7	767	-8.87	
11.4	2.29	15	3.24	9.61	1.49	10.04	1.5	97.4	852	11.2	132	29.5	6.03	7.84	76.1	3.8	21.9	782	-8.78	
12	2.38	15.7	3.4	10.05	1.56	10.64	1.59	106	814	11.2	159	34.7	6.99	9.23	72.7	3.8	22.7	800		
11.3	2.18	14	3	8.89	1.38	9.35	1.41	98.1	801	15.1	158	28.5	6.84	7.58	53.0	3.8	23.1	800	-8.67	
13.8	3.38	24.8	5.68	17.75	2.88	20.06	3.09	193	825	7	116	45.8	7.78	16.36	117.9	2.8	14.9	778	-8.6	
13	2.97	20.5	4.6	13.7	2.16	14.77	2.24	147	1119	20.7	132	38	7.93	12.64	54.1	3.0	16.6	772	-8.76	
11.2	2.02	12.4	2.61	7.56	1.16	7.6	1.13	74.8	833	12	211	28.5	7.46	6.71	69.4	4.2	28.3	860		
10.4	1.94	12.6	2.72	8.32	1.32	9	1.36	78.9	662	14.7	219	30.1	7.68	7.13	45.0	4.2	28.5	894	-8.76	
10.5	2.02	13	2.8	8.35	1.3	8.85	1.32	77.7	904	14.6	136	28.4	5.98	8.12	61.9	3.5	22.7	789	-7.79	
10.1	2.05	13.4	2.91	8.69	1.4	9.61	1.46	94.8	1083	23.5	145	26.5	6.88	9.29	46.1	2.9	21.1	800		Zhou et al.,
10.7	2.08	13.4	2.88	8.59	1.35	9.16	1.39	81.9	793	13	176	29	7.31	8.44	61.0	3.4	24.1	792		2013
14.3	3.19	21	4.31	11.79	1.75	11.35	1.65	140	1070	10.9	86.2	46.2	6.03	11.58	98.2	4.0	14.3	777		
9	1.78	11.5	2.48	7.39	1.17	8.12	1.22	70.5	940	10.8	120	29.43	5.52	12.2	87.0	2.4	21.7	800	-7.3	
11	2.61	18.8	4.25	13.04	2.11	14.72	2.26	139	946	6.7	105	30.3	6.77	13.12	141.2	2.3	15.5	765	-8.93	
10.8	2.33	149	3.24	9.69	1.49	9.2	1.36	102	995	4.34	97.2	36.4	5.97	10.8	229.3	3.4	16.3	0.25	753	
17.3	3.7	23.9	4.88	14.6	2.14	14.8	2.06	161	675	10.6	85	34.5	5.98	8.79	63.7	3.9	14.2		737	Zheng and
18.4	3.86	24.7	5.12	15.1	2.27	15.4	2.23	189	916	5.99	98.2	43.9	6.84	12.5	152.9	3.5	14.4	0.32	753	Guo, 2012
15.3	3.12	19.9	4.16	12	1.83	11.5	1.63	154	632	7.25	86.4	33.6	5.7	8.93	87.2	3.8	15.2	0.87	745	
10.8	1.86	10.3	1.94	5.7	0.88	5.03	0.73	54.3	323	49.6	127	22.3	5.31	3.21	6.5	6.9	23.9	0.51	781	Zhang, 2014
10.8	1.91	10.7	2.01	5.8	0.96	5.46	0.77	56.1	346	42.4	141	22	5.47	3.16	8.2	7.0	25.8	0.44	788	

9.2	1.53	8.4	1.6	4.76	0.79	4.59	0.68	47.6	342	69.3	130	15.4	5.01	2.42	4.9	6.4	25.9	0.45	780	-7
14.8	2.53	13.5	2.49	7.11	1.1	6.08	0.85	60.4	272	83.4	211	28.3	7.47	3.69	3.3	7.7	28.2	0.37	816	-6.1
9.3	1.43	7.6	1.42	4.25	0.63	3.69	0.59	39.6	275	88.6	199	18.1	6.99	2.41	3.1	7.5	28.5	0.83	819	-6.5
11.4	1.86	10.3	1.98	5.75	0.97	5.41	0.77	55	293	66.7	184	24	6.5	3.25	4.4	7.4	28.3	0.32	802	
11.2	1.92	11.3	2.15	6.37	1.05	6.12	0.89	61	317	68.2	176	23.2	6.15	3.18	4.6	7.3	28.6	0.29	799	
7.2	1.3	8.1	1.59	4.49	0.69	3.73	0.53	41.7	412	16.6	102	32	5.29	5.59	24.8	5.7	19.3	0.69	756	
22.5	4.04	27.6	6.26	19.82	2.68	18.81	2.69	129.3	684.3	31.6	157.2	35.8	9.59	6.52	21.7	5.5	16.4	0.37	790	-7.1
19	3.39	24.6	5.58	16.8	2.47	16.99	2.46	111.8	586.4	35.3	198.5	34.6	10.7	10.68	16.6	3.2	18.6	0.17	810	-7.1
																				-7.3
																				-6.8
																				-6.8
																				-7.3
																				-7.2
																				-6.2
																				-6.6
																				-5.7
																				-6.4
																				-6.4
																				-5.1
9.37	1.19	7.96	1.66	4.54	0.65	3.99	0.64	41.65	264.08	204.21	298.74	31.54	7.45	2.99	1.3	10.5	40.1	0.46	817	-6.9
8.21	1.06	6.90	1.47	4.13	0.62	3.91	0.63	37.37	330.69	209.92	254.14	27.83	5.95	3.00	1.6	9.3	42.7	0.42	800	-6.6
9.06	1.13	7.25	1.55	4.40	0.65	4.03	0.66	39.40	366.26	236.76	269.70	26.92	6.12	3.17	1.5	8.5	44.0	0.45	813	
13.07	1.91	13.86	3.01	8.64	1.30	8.22	1.32	78.29	517.14	117.86	85.99	35.30	3.19	3.90	4.4	9.1	27.0	0.43	715	
7.31	0.96	6.26	1.37	3.99	0.59	3.78	0.62	36.05	367.72	161.68	273.08	27.28	6.31	2.77	2.3	9.8	43.3	2.96	826	
7.47	0.97	6.49	1.35	3.85	0.57	3.53	0.59	34.88	325.33	199.56	230.18	23.45	5.60	3.01	1.6	7.8	41.1	0.37	803	-7.3

Zhao, et al.,
2012

8.21	1.01	6.55	1.36	3.69	0.52	3.34	0.51	34.07	367.07	204.16	237.20	24.05	5.41	2.77	1.8	8.7	43.9	0.40	819	-7.6
10.48	1.56	8.83	1.64	4.67	0.69	4.38	0.66	43.84	220.89	194.76	275.09	29.04	9.03	2.65	1.1	11.0	30.5	0.66	810	-6.8
8.99	1.35	7.47	1.41	4.07	0.59	3.69	0.56	36.78	230.62	177.21	224.66	24.40	7.65	2.45	1.3	10.0	29.4	0.59	774	-6.2
13.06	1.80	11.77	2.42	7.52	1.01	6.63	0.94	68.32	427.20	91.76	462.70	50.85	9.56	6.70	4.7	7.6	48.4	0.42	861	
11.19	1.59	10.13	2.16	6.65	0.95	6.04	0.86	63.25	421.00	152.70	372.20	47.65	8.00	5.19	2.8	9.2	46.5	0.41	837	-5.5
10.39	1.47	8.41	1.71	4.29	0.66	4.33	0.65											0.43		
11.49	1.47	9.18	1.90	5.69	0.76	4.84	0.73	50.34	250.70	223.30	316.30	33.00	6.86	3.20	1.1	10.3	46.1	0.40	822	-5.8
8.47	1.33	7.59	1.49	4.27	0.66	4.19	0.62	41.4	422.22	223.28	233.49	22.95	7.59	2.64		8.7	30.8		812	
8.51	1.34	7.57	1.48	4.29	0.67	4.19	0.63	41.99	387.2	230.33	289.21	23.43	8.88	2.49		9.4	32.6		827	
6.7	1.04	5.73	1.11	3.25	0.52	3.18	0.48	31.62	420.64	176.97	208.26	19.31	6.93	2.27		8.5	30.1		801	
9.55	1.51	8.48	1.66	4.83	0.75	4.72	0.75	47.23	293.34	176.4	307.07	30.56	10.03	3.42		8.9	30.6		829	
9.11	1.42	7.89	1.56	4.55	0.7	4.47	0.67	44.57	433.42	183.29	237.69	26.94	7.7	3.3		8.2	30.9		804	
14.9	2.41	13.97	2.73	7.88	1.17	7.23	1.05	76.98	328.54	168.84	311.32	45.22	10.06	4.55		9.9	30.9		818	
3.52	0.6	3.32	0.66	1.95	0.35	2.19	0.35	19.76	322.82	111.83	85.17	12.13	2.91	2.13		5.7	29.3		728	
7.85	1.24	6.97	1.36	3.91	0.62	3.8	0.57	38.67	468.29	159.16	227.94	21.05	7.38	2.25		9.4	30.9		797	
8.08	1.22	6.7	1.31	3.73	0.57	3.52	0.52	37.07	312.54	176.32	181.82	22.9	5.72	2.3		10.0	31.8		779	Deng et al.,
7.76	1.22	6.86	1.34	3.92	0.61	3.76	0.56	38.45	260.33	162.35	203.93	23.89	6.68	2.65		9.0	30.5		787	2005
9.51	1.42	7.89	1.5	4.12	0.61	3.62	0.53	42.21	262.3	220.84	266.07	15.66	8.28	1.68		9.3	32.1		812	
6.67	1.07	5.99	1.16	3.45	0.56	3.51	0.52	34.23	383.87	144.6	173.15	21.01	5.78	2.7		7.8	30.0		785	
6.64	1.19	7.41	1.55	4.97	0.87	6	0.92	49.2	654.46	21.96	166.76	27.71	7.79	5.25		5.3	21.4		789	
3.17	0.53	2.8	0.57	1.71	0.31	1.97	0.31	18.39	493.07	58.73	126.05	12.08	4.26	1.42		8.5	29.6		767	
4.94	0.87	5.02	1.02	3.17	0.56	3.64	0.57	31.48	400.71	85.03	150.15	17.95	5.46	3.02		5.9	27.5		781	
7.39	1.2	6.84	1.36	3.99	0.64	4.04	0.6	40.14	399.96	11.46	164.43	25.34	5.48	2.8		9.1	30.0		781	
8.6	1.34	7.57	1.46	4.09	0.63	3.79	0.56	41.42	274.77	227.55	215.48	23.13	6.57	2.34		9.9	32.8		794	
9.76	1.55	8.85	1.72	4.92	0.74	4.45	0.67	48.34	260.25	213.96	316.36	30.32	9.48	2.81		10.8	33.4		825	

Yuan, S., Williams-Jones, A.E., Romer, R.L., Zhao, P., Mao, J., 2019.
 Protolith-Related Thermal Controls on the Decoupling of Sn and W in Sn-W Metallogenic Provinces:
 Insights from the Nanling Region, China. *Economic Geology*, 114(5): 1005-1012.

8.76	1.38	7.91	1.55	4.45	0.67	4.19	0.62	44.49	238.53	222.58	299.13	29.36	8.76	2.79		10.5	34.1		832	
8.92	1.37	7.59	1.46	4.23	0.64	4.2	0.61	42.1	364.78	160.17	230.38	27.46	7.1	2.59	3.8	10.6	32.4	0.06	803	-7.6
7.99	1.18	6.72	1.26	3.58	0.52	3.49	0.49	36.93	354.19	151	242.63	25.01	6.99	2.84	4.1	8.8	34.7	0.06	804	-8.3
7.13	1.25	7.46	1.47	4.35	0.66	4.57	0.65	45.5	411.28	116.97	187.25	26.23	6.43	3.57	2.6	7.3	29.1	0.02	791	-7.7
9.03	1.42	8.59	1.65	4.88	0.75	4.89	0.72	50	313.45	169.28	222.78	28.89	7.09	2.92	3.4	9.9	31.4	0.04	798	-7.5
5.36	0.81	4.65	0.95	2.89	0.46	3.34	0.52	29.63	408.08	111.2	159.47	15.84	6	2.03	3.8	7.8	26.6	0.02	781	
7.71	1.23	6.88	1.33	3.94	0.61	3.97	0.57	39.46	290.17	148.76	249.39	23.65	8.19	2.26	2.0	10.5	30.5	0.06	811	
6.98	1.06	5.86	1.13	3.27	0.49	3.28	0.5	33.79	212.86	122.23	197.72	21.15	6.34	2.13	1.7	9.9	31.2	0.04	797	-7.7
5.96	0.88	5.42	1.09	3.27	0.51	3.3	0.49	33.21	371.73	120.29	138.13	19.53	4.84	2.34	3.1	8.3	28.5	0.07	766	
7.45	1.09	5.78	1.1	3.14	0.45	3.11	0.42	31.53	245.8	201.98	204.04	21.53	5.98	1.75	1.2	12.3	34.1	0.14	788	
13.06	1.8	11.77	2.42	7.52	1.01	6.63	0.94	68.32	427.2	91.76	462.7	50.85	9.56	6.7	4.7	7.6	48.4	0.42	861	-8.6
11.49	1.47	9.18	1.9	5.69	0.76	4.84	0.73	50.34	250.7	223.3	316.3	33	6.86	3.2	1.1	10.3	46.1	0.40	822	
5.91	0.89	5.12	0.96	2.71	0.4	2.65	0.35	28.48	278.7	112.89	148.55	22.49	4.65	3.2	2.5	7.0	31.9	0.13	769	-5.6
6.22	1.09	6.69	1.39	4.42	0.72	5.34	0.79	45.81	549.01	19.18	147.54	27.88	6.12	3.39	28.6	8.2	24.1	0.05	781	
6.8	1.18	7.53	1.57	5.11	0.85	5.92	0.91	51.03	551.84	21.48	153.02	30.06	6.52	4.09	25.7	7.3	23.5	0.00	788	
5.28	0.76	4.85	0.99	3.21	0.46	3.41	0.5	29.05	493.96	72.85	168.8	20.6	5.92	2.4	6.8	8.6	28.5	0.07	786	
4.96	0.88	5.9	1.15	3.71	0.58	4.37	0.57	35.16	427.49	57.79	179.81	23.28	7.68	3.44	7.4	6.8	23.4	0.13	799	
5.49	0.8	4.53	0.93	2.69	0.44	2.91	0.46	24.6	416	61	151	23.7	6.6	2.7	6.8	8.8	22.9	0.22	785	
7.17	1.24	7.37	1.57	4.88	0.87	6.15	0.95	47.48	506.6	19	221	30.2	8.8	0.9	26.7	33.6	25.1	0.21	818	
7.14	1.22	7.31	1.5	4.43	0.8	5.4	0.8	39.11	504.8	33	155	30.2	5.7	6	15.3	5.0	27.2	0.13	789	
6.8	1.16	7.2	1.47	4.42	0.77	5.3	0.81	42.76	515.3	54	150	28.1	6.9	5.2	9.5	5.4	21.7	0.11	776	
8.57	1.42	7.95	1.69	4.91	0.88	6	0.86	45.34	383.1	113	194	28.4	7.8	4.6	3.4	6.2	24.9	0.22	792	
6.75	1.06	5.68	1.14	3.04	0.47	2.82	0.41	29.6	359.6	124	187	22.2	6.3	2.5	2.9	8.9	29.7	0.19	821	
8.98	1.49	8.52	1.68	4.68	0.79	5.3	0.83	46.35	424.4	96	172	24.7	6.5	3.2	4.4	7.7	26.5	0.32	790	
9.35	1.46	8.22	1.66	4.48	0.69	4.42	0.65	42.28	273.9	200	262	28.7	9.8	3.5	1.4	8.2	26.7	0.41	808	-6.98

Fu et al.,
2006

Bai et al.,
2005

7.36	1.16	6.5	1.29	3.46	0.55	3.34	0.48	33.91	307.6	161	216	24.9	7.1	2.3	1.9	10.8	30.4	0.20	795	
9.01	1.44	8.02	1.54	4.18	0.65	3.84	0.55	39.24	278.7	168	237	24.9	8.1	2.1	1.7	11.9	29.3	0.32	802	-7.57
7.56	1.24	6.85	1.36	3.79	0.59	3.79	0.54	36.29	317.1	145	180	23	7.1	2.8	2.2	8.2	25.4	0.20	787	
11.16	1.8	10.89	2.03	5.5	0.81	4.83	0.73	51	255.5	146	243	27.7	8.6	2.9	1.8	9.6	28.3	0.17	803	-7.41
8.6	1.36	7.77	1.5	4.07	0.65	4.06	0.59	39.14	252	211	288	29.9	9.4	2.7	1.2	11.1	30.6	0.24	813	-6.93
8.7	1.33	7.62	1.48	4.02	0.63	3.94	0.57	37.02	239.6	232	228	24.1	8.3	1.7	1.0	14.2	27.5	0.31	792	
7.38	1.13	6.45	1.42	3.75	0.61	3.96	0.6	39.43	319.33	196.91	240.9	26.51	7.29	2.75		9.6	33.0		812	
8.68	1.37	8.59	1.9	5.19	0.78	5.06	0.71	55.85	130.1	273.46	265.03	24.49	7.73	2.37		10.3	34.3		804	
9.69	1.32	6.93	1.46	3.85	0.58	3.77	0.55	41.75	283.99	225.82	269.52	25.93	7.95	2.58		10.1	33.9		812	
6.8	0.94	4.96	1.12	3.14	0.47	3.15	0.48	32.45	317.04	146.88	256.99	18.55	7.86	2.02		9.2	32.7		823	
6.67	0.97	5.65	1.25	3.33	0.53	3.41	0.5	36.36	372.26	159.59	294.11	21.19	8.25	2.29		9.3	35.6		836	
8.02	1.14	6.72	1.4	3.9	0.56	3.84	0.53	40.06	341.5	230.7	279.75	28.85	8.03	2.84		10.2	34.8		814	
7.74	1.06	5.53	1.18	3.58	0.57	3.65	0.56	34.6	405.64	144.45	199.53	23.96	6.95	3.32		7.2	28.7		799	
10.36	1.53	8.26	1.69	4.54	0.67	4.27	0.62	48.38	318.73	271.01	265.41	34.85	7.21	3.02		11.5	36.8		807	
7.58	1.17	6.56	1.36	3.74	0.58	3.81	0.54	40.19	301.01	157.89	328.3	26.22	9.42	2.49		10.5	34.9		839	Li et al.,
7.16	1.09	6.16	1.22	3.27	0.53	3.35	0.49	35.77	279.41	181.2	284.61	24.03	8.09	2.34		10.3	35.2		823	2010
7.17	1.04	5.89	1.18	3.41	0.51	3.33	0.5	35.3	340.63	165.81	216.41	22.79	6.29	2.49		9.2	34.4		802	
7.56	1.27	8.24	1.82	5.37	0.86	6.09	0.91	53.34	461.12	42.35	126.6	24.91	5.69	4.24		5.9	22.2		768	
7.48	1.25	7.95	1.75	5.14	0.88	5.93	0.82	48.84	478.19	51.79	117.52	23.8	5.42	4.22		5.6	21.7		782	
4.47	0.76	4.86	1.07	3.32	0.51	3.49	0.52	34.34	474.96	49.87	95.06	18.01	4.32	2.41		7.5	22.0		745	
7.34	1.21	7.41	1.54	4.48	0.7	4.61	0.68	46.84	470.01	103.44	125.21	27.94	4.4	3.46		8.1	28.5		766	
7.02	1.19	6.83	1.53	4.42	0.67	4.5	0.61	44.21	372.19	117.56	160.83	24.95	5.68	3.35		7.4	28.3		785	
4.7	0.7	4.07	0.95	2.97	0.49	3.75	0.61	31.04	446.58	78.1	203.8	21.64	8.23	2.77		7.8	24.8		812	
8.19	1.72	12.03	2.59	8.18	1.65	12.42	1.8	40.54	1078.07	38.79	92.27	34.11	7.08	14.03		2.4	13.0			

Zircon saturation temperature (T_{zr}) were calculated using the method of Watson and Harrison, 1983.

$$T_{Zr} = 12,900/[2.95 + 0.85M + \ln(496,000/Zr)]; M = (Na + K + 2Ca)/(Al \cdot Si).$$

Table DR2 Zircon Lu-Hf isotopic data of the representative Late Jurassic (160-150 Ma)
 W-Sn-related granite in the Nanling region, South China

	Spot	$^{176}\text{Yb}/^{177}\text{Hf}$	$^{176}\text{Lu}/^{177}\text{Hf}$	$^{176}\text{Hf}/^{177}\text{Hf}$	$\varepsilon_{\text{Hf}}(t)$	T_{DM2} (Ma)	Reference
	XHS-4@1		0.001074	0.282345	-11.7	1950	
	XHS-4@2		0.000914	0.282405	-9.6	1817	
	XHS-4@3		0.002677	0.282399	-10.0	1842	
	XHS-4@4		0.001147	0.282374	-10.7	1888	
	XHS-4@5		0.001436	0.282373	-10.8	1938	
	XHS-4@6		0.001161	0.282362	-11.2	1850	
	XHS-4@7		0.000974	0.282400	-9.8	1915	
	XHS-4@8		0.000982	0.282395	-10.0	1828	
	XHS-4@9		0.001834	0.282429	-8.7	1841	
	XHS-4@10		0.001038	0.282405	-9.6	1767	
	XHS-4@11		0.001145	0.282387	-10.3	1818	
	XHS-4@12		0.002485	0.282393	-10.2	1860	
	XHS-4@13		0.002686	0.282349	-11.7	1854	
	XHS-4@14		0.003719	0.282470	-7.6	1952	
	XHS-4@15		0.002645	0.282342	-12.0	1689	
	XHS-4@16		0.001200	0.282360	-11.2	1964	
	XHS-4@17		0.001082	0.282423	-9.0	1920	
	XHS-4@18		0.003316	0.282458	-8.1	1774	
	XHS-4@19		0.002722	0.282547	-4.8	1717	
Xihuashan W deposit	XHS-4@20		0.001254	0.282340	-11.9	1510	Guo et al., 2012
	XHS-4@21		0.001360	0.282407	-9.6	1965	
	XHS-4@22		0.001083	0.282284	-14.0	1817	
	XHS-4@23		0.001388	0.282362	-11.2	2091	
	XHS-4@24		0.003337	0.282393	-10.4	1919	
	XHS-4@25		0.001208	0.282438	-8.5	1993	
	XHS-4@26		0.001353	0.282363	-11.1	2006	
	XHS-4@27		0.001840	0.282413	-9.4	1913	
	XHS-4@28		0.001581	0.282413	-9.4	1804	
	XHS-4@29		0.000887	0.282365	-11.0	1804	
	XHS-4@30		0.000911	0.282348	-11.7	1908	
	XHS-4@31		0.002117	0.282362	-11.3	1946	
	XHS-4@32		0.002377	0.282419	-9.3	1921	
	XHS-4@33		0.001603	0.282357	-11.4	1796	
	XHS-22@1		0.002630	0.282410	-9.5	1813	
	XHS-22@2		0.001673	0.282329	-12.2	1988	
	XHS-22@3		0.001783	0.282310	-13.1	2037	
	XHS-22@4		0.002153	0.282384	-10.5	1871	
	XHS-22@5		0.003066	0.282397	-10.0	1846	
	XHS-22@6		0.003878	0.282514	-6.0	1589	
	XHS-22@7		0.002671	0.282407	-9.5	1819	

XHS-22@9	0.003142	0.282326	-12.2	1997
XHS-22@11	0.002496	0.282383	-10.2	1869
XHS-22@12	0.001948	0.282391	-9.8	1845
XHS-22@13	0.003121	0.282391	-9.9	1852
XHS-22@14	0.003895	0.282459	-7.8	1709
XHS-22@16	0.003512	0.282411	-9.4	1814
XHS-22@17	0.002346	0.282386	-9.8	1854
XHS-22@18	0.002360	0.282363	-10.9	1912
XHS-22@19	0.002351	0.282429	-8.8	1769
XHS-22@20	0.002257	0.282360	-11.2	1922
XHS-15@1	0.002716	0.282339	-12.0	1974
XHS-15@2	0.002026	0.282345	-11.7	1954
XHS-15@3	0.001479	0.282425	-8.9	1775
XHS-15@4	0.000952	0.282398	-9.9	1834
XHS-15@5	0.001481	0.282364	-11.0	1909
XHS-15@6	0.001900	0.282388	-10.3	1862
XHS-15@7	0.001135	0.282404	-9.7	1821
XHS-15@8	0.002149	0.282405	-9.7	1824
XHS-15@9	0.001800	0.282382	-10.5	1873
XHS-15@10	0.003114	0.282443	-8.4	1744
XHS-15@11	0.001429	0.282439	-8.4	1742
XHS-15@12	0.000808	0.282369	-11.0	1900
XHS-15@13	0.001449	0.282429	-8.8	1768
XHS-15@14	0.002067	0.282431	-8.9	1769
XHS-15@15	0.001103	0.282408	-9.5	1811
XHS-15@16	0.003159	0.282396	-10.2	1852
XHS-15@17	0.002431	0.282363	-11.2	1918
XHS-15@18	0.001964	0.282397	-9.9	1839
XHS-15@19	0.001120	0.282365	-10.9	1906
XHS-15@20	0.002603	0.282460	-7.7	1700
XHS-15@21	0.000946	0.282362	-11.1	1915
XHS-15@22	0.002382	0.282324	-12.8	2012
XHS-15@23	0.001724	0.282397	-10.0	1841
XHS-15@24	0.003243	0.282417	-9.4	1806
XHS-15@25	0.001578	0.282395	-9.9	1840
XHS-15@26	0.002969	0.282455	-8.1	1720
XHS-15@27	0.002964	0.282300	-13.5	2063
XHS-15@28	0.001868	0.282286	-13.9	2089
XHS-15@29	0.001536	0.282320	-12.5	2008
XHS-37@1	0.001242	0.282334	-12.1	1975
XHS-37@2	0.001945	0.282365	-11.1	1913
XHS-37@3	0.002244	0.282295	-13.6	2070
XHS-37@4	0.001009	0.282422	-9.0	1781
XHS-37@5	0.001677	0.282380	-10.5	1877

XHS-37@6		0.001255	0.282400	-9.7	1827
XHS-37@7		0.001126	0.282371	-11.0	1901
XHS-37@8		0.002117	0.282408	-9.8	1822
XHS-37@9		0.001654	0.282354	-11.5	1935
XHS-37@10		0.001021	0.282361	-11.2	1917
XHS-37@11		0.001333	0.282352	-11.6	1940
XHS-37@12		0.001205	0.282402	-9.8	1829
XHS-37@13		0.000939	0.282372	-10.8	1893
XHS-37@14		0.001895	0.282390	-10.3	1859
XHS-37@15		0.001081	0.282379	-10.5	1875
XHS-37@16		0.002001	0.282470	-7.4	1678
XHS-37@17		0.001443	0.282425	-9.0	1776
XHS-37@18		0.001925	0.282391	-10.2	1855
XHS-37@19		0.002531	0.282445	-8.4	1737
XHS-37@20		0.001328	0.282384	-10.4	1867
XHS-37@21		0.001281	0.282346	-11.7	1951
XHS-37@22		0.000939	0.282391	-10.1	1849
XHS-37@23		0.001850	0.282386	-10.4	1865
XHS-37@24		0.002540	0.282442	-8.5	1746
XHS-37@25		0.001294	0.282349	-11.6	1945
XHS-37@26		0.001151	0.282289	-13.7	2078
XHS-37@27		0.001141	0.282400	-9.8	1831
XHS-37@28		0.001948	0.282411	-9.5	1810
XHS-37@29		0.002124	0.282476	-7.2	1667
XHS-37@30		0.000947	0.282365	-11.0	1907
XHS-37@31		0.001428	0.282341	-11.9	1964
XHS-37@32		0.001266	0.282410	-9.5	1809
XHS-37@33		0.001318	0.282360	-11.2	1920
XHS-37@34		0.001453	0.282442	-8.4	1738
XHS-37@35		0.002797	0.282361	-11.3	1927
<hr/>					
XHS-19@1	0.029240	0.001020	0.282296	-13.5	
XHS-19@2	0.012240	0.000450	0.282298	-13.4	
XHS-19@3	0.064760	0.002090	0.282310	-13.1	
XHS-19@4	0.031470	0.001080	0.282346	-11.7	
XHS-19@5	0.032420	0.001210	0.282274	-14.3	
XHS-19@6	0.024090	0.000850	0.282323	-12.5	
XHS-19@7	0.023770	0.000840	0.282271	-14.3	
XHS-19@9	0.024630	0.000870	0.282345	-11.7	Yang et al., 2018
XHS-19@10	0.054150	0.001870	0.282352	-11.6	
XHS-19@11	0.030110	0.001000	0.282257	-14.9	
XHS-19@13	0.030340	0.001060	0.282333	-12.2	
XHS-19@14	0.036880	0.001370	0.282340	-12.0	
XHS-19@16	0.040930	0.001550	0.282306	-13.2	
XHS-19@17	0.034980	0.001180	0.282287	-13.8	

XHS-19@18	0.030310	0.001060	0.282306	-13.1	
XHS-19@19	0.024420	0.000900	0.282344	-11.8	
XHS-19@20	0.028680	0.001070	0.282349	-11.6	
XHS-9@8	0.134650	0.004380	0.282339	-12.3	
XHS-9@10	0.056690	0.001970	0.282323	-12.6	
XHS-9@15	0.133490	0.004450	0.282320	-13.0	
XHS-9@17	0.071940	0.002740	0.282331	-12.4	
XHS-9@18	0.078130	0.002860	0.282343	-12.0	
XHS-9@19	0.041430	0.001510	0.282356	-11.4	
XHS-9@20	0.217450	0.007760	0.282351	-12.2	
XHS-10@4	0.029760	0.001030	0.282353	-11.5	
XHS-10@5	0.127690	0.004430	0.282347	-12.0	
XHS-10@6	0.027770	0.001050	0.282335	-12.1	
XHS-10@10	0.101210	0.003690	0.282358	-11.6	
XHS-10@18	0.075790	0.002830	0.282341	-12.1	
XHS-10@19	0.131340	0.004740	0.282355	-11.8	
SZY-23-01	0.020000	0.000500	0.282429	-9.0	1768
SZY-23-02	0.020000	0.000800	0.282471	-7.3	1671
SZY-23-03	0.020000	0.000700	0.282415	-9.3	1797
SZY-23-04	0.020000	0.000700	0.282437	-8.6	1748
SZY-23-05	0.020000	0.000800	0.282366	-11.1	1908
SZY-23-06	0.020000	0.000600	0.282447	-8.1	1722
SZY-23-07	0.030000	0.001200	0.282410	-9.6	1812
SZY-23-08	0.020000	0.000800	0.282469	-7.5	1677
SZY-23-09	0.020000	0.000500	0.282423	-9.1	1779
SZY-23-10	0.040000	0.001000	0.282473	-7.3	1668
SZY-23-11	0.040000	0.001000	0.282497	-6.6	1618
SZY-23-12	0.030000	0.000700	0.282401	-9.8	1828
SZY-23-14	0.050000	0.001200	0.282421	-9.1	1784
SZY-23-15	0.050000	0.001500	0.282434	-8.7	1758
SZY-28-01	0.020000	0.000500	0.282454	-7.8	1705
SZY-28-02	0.030000	0.001000	0.282405	-9.8	1823
SZY-28-03	0.020000	0.000500	0.282434	-8.6	1753
SZY-28-04	0.030000	0.000800	0.282411	-9.5	1808
SZY-28-05	0.020000	0.000700	0.282406	-9.6	1816
SZY-28-06	0.020000	0.000600	0.282405	-9.7	1820
SZY-28-08	0.030000	0.001000	0.282395	-10.1	1844
SZY-28-09	0.030000	0.000800	0.282448	-8.1	1721
SZY-28-10	0.030000	0.000900	0.282455	-7.9	1707
SZY-28-11	0.020000	0.000700	0.282459	-7.7	1694
SZY-28-12	0.030000	0.000900	0.282395	-10.0	1839
SZY-28-15	0.030000	0.000800	0.282419	-9.2	1787
SZY-28-16	0.020000	0.000700	0.282480	-6.9	1648

Qianlishan Sn-W
deposit

Guo et al., 2015

SZY-14-01	0.030000	0.001000	0.282404	-9.8	1824
SZY-14-02	0.030000	0.001000	0.282412	-9.5	1804
SZY-14-04	0.020000	0.000700	0.282409	-9.5	1808
SZY-14-05	0.020000	0.000700	0.282430	-8.7	1761
SZY-14-06	0.020000	0.000800	0.282452	-8.1	1718
SZY-14-07	0.020000	0.000700	0.282417	-9.2	1791
SZY-14-08	0.020000	0.000700	0.282470	-9.4	1673
SZY-14-09	0.030000	0.000900	0.282412	-9.4	1804
SZY-14-10	0.020000	0.000700	0.282412	-9.5	1803
SZY-14-11	0.020000	0.000700	0.282459	-7.9	1701
SZY-14-12	0.030000	0.000900	0.282464	-7.6	1689
SZY-14-13	0.020000	0.000700	0.282440	-8.5	1741
SZY-14-14	0.020000	0.000700	0.282433	-8.8	1759
SZY-14-15	0.030000	0.001000	0.282441	-8.5	1741
SZY-30-01	0.030000	0.000800	0.282480	-7.2	1655
SZY-30-02	0.030000	0.001000	0.282426	-8.9	1770
SZY-30-03	0.030000	0.000800	0.282420	-9.1	1785
SZY-30-04	0.020000	0.000600	0.282511	-5.8	1578
SZY-30-05	0.020000	0.000700	0.282440	-8.4	1739
SZY-30-06	0.020000	0.000800	0.282490	-6.7	1630
SZY-30-07	0.030000	0.001200	0.282487	-6.8	1638
SZY-30-08	0.020000	0.000900	0.282460	-7.8	1697
SZY-30-09	0.030000	0.001000	0.282435	-8.7	1755
SZY-30-10	0.020000	0.000500	0.282441	-8.4	1738
SZY-30-11	0.020000	0.000700	0.282455	-8.0	1708
SZY-30-12	0.030000	0.000800	0.282382	-10.5	1871
SZY-30-13	0.030000	0.000800	0.282394	-10.3	1849
SZY-30-14	0.020000	0.000800	0.282412	-9.3	1799
SZY-30-15	0.030000	0.000800	0.282476	-7.2	1660
SZY-21-01	0.020000	0.000600	0.282487	-6.8	1636
SZY-21-02	0.040000	0.001200	0.282462	-7.8	1697
SZY-21-03	0.030000	0.001000	0.282480	-7.1	1653
SZY-21-04	0.020000	0.000600	0.282500	-6.4	1608
SZY-21-05	0.030000	0.000900	0.282492	-6.6	1626
SZY-21-06	0.020000	0.000700	0.282496	-6.5	1617
SZY-21-07	0.020000	0.000800	0.282509	-6.0	1586
SZY-21-08	0.020000	0.000700	0.282483	-7.0	1646
SZY-21-09	0.030000	0.000900	0.282479	-7.1	1654
SZY-21-10	0.020000	0.000700	0.282495	-6.5	1617
SZY-21-11	0.030000	0.000900	0.282521	-5.7	1562
SZY-21-12	0.030000	0.000900	0.282528	-5.4	1545
SZY-21-13	0.020000	0.000700	0.282449	-8.2	1722
SZY-21-14	0.030000	0.000800	0.282514	-5.7	1572

SZY-21-15	0.020000	0.000800	0.282521	-5.6	1560
SZY-22-01	0.040000	0.001200	0.282397	-10.1	1843
SZY-22-02	0.040000	0.001200	0.282465	-7.7	1690
SZY-22-03	0.120000	0.003600	0.282433	-8.9	1771
SZY-22-04	0.020000	0.000800	0.282452	-8.1	1715
SZY-22-05	0.030000	0.000900	0.282428	-8.9	1769
SZY-22-06	0.030000	0.001000	0.282523	-5.5	1556
SZY-22-07	0.050000	0.001500	0.282511	-6.0	1586
SZY-22-08	0.090000	0.002600	0.282496	-6.7	1627
SZY-22-09	0.030000	0.000900	0.282535	-5.1	1530
SZY-22-10	0.040000	0.001300	0.282442	-8.5	1741
SZY-22-11	0.030000	0.000900	0.282492	-6.7	1629
SZY-22-12	0.040000	0.001200	0.282510	-6.1	1588
SZY-22-13	0.040000	0.001200	0.282473	-7.4	1670
SZY-22-14	0.040000	0.001400	0.282462	-7.9	1698
SZY-22-15	0.020000	0.000700	0.282479	-7.0	1650
SZY-22-16	0.020000	0.000800	0.282494	-6.7	1624
SZY-22-17	0.030000	0.000900	0.282376	-10.7	1886
SZY-22-18	0.030000	0.001100	0.282480	-7.1	1653
SZY35-2	0.038120	0.000700	0.282480	-7.2	1663
SZY35-3	0.033880	0.000730	0.282520	-5.7	1569
SZY35-4	0.045060	0.000960	0.282390	-10.2	1856
SZY35-5	0.031720	0.000680	0.282520	-5.7	1569
SZY35-6	0.036990	0.000770	0.282360	-11.1	1913
SZY35-7	0.043540	0.000940	0.282480	-6.9	1645
SZY35-8	0.057020	0.001230	0.282390	-10.3	1860
SZY35-8-2	0.036510	0.000780	0.282450	-8.1	1720
SZY35-9	0.046920	0.001000	0.282370	-11.0	1907
SZY35-10	0.057890	0.001230	0.282310	-13.0	2032
SZY35-11	0.078520	0.001630	0.282400	-10.0	1843
SZY35-12	0.036330	0.000780	0.282500	-6.2	1600
SZY35-13	0.037810	0.000800	0.282550	-4.4	1487
SZY35-14	0.041620	0.000890	0.282420	-9.4	1800
SZY35-15	0.033290	0.000720	0.282520	-5.6	1563
SZY35-16	0.032060	0.000700	0.282530	-5.2	1538
SZY35-17	0.032550	0.000700	0.282520	-5.8	1573
SZY35-18	0.038370	0.000820	0.282460	-7.8	1703
SZY35-19	0.028900	0.000620	0.282530	-5.1	1530
SZY35-20	0.038690	0.000830	0.282390	-10.4	1865
SZY35-21	0.040550	0.000880	0.282320	-12.7	2014
SZY35-22	0.030670	0.000670	0.282390	-10.2	1855
SZY35-23	0.049180	0.001120	0.282380	-10.6	1877
SZY35-24	0.031360	0.000680	0.282460	-7.6	1692

Chen et al., 2016

SZY35-25	0.041700	0.000890	0.282490	-6.7	1631	
SZY35-26	0.042750	0.000920	0.282350	-11.5	1935	
HN013-001	0.018368	0.000644	0.282473	-7.3	1670	
HN013-002	0.020115	0.000700	0.282607	-2.4	1360	
HN013-003	0.020384	0.000708	0.282545	-4.8	1510	
HN013-004	0.022336	0.000780	0.282513	-5.9	1580	
HN013-007	0.042322	0.001450	0.282550	-4.8	1500	
HN013-009	0.014609	0.000511	0.282552	-4.4	1490	
HN013-010	0.014888	0.000512	0.282490	-6.7	1630	
HN013-011	0.017140	0.000604	0.282523	-5.5	1550	
HN013-012	0.015413	0.000537	0.282597	-3.0	1390	
HN013-014	0.028944	0.000975	0.282464	-7.7	1690	
HN013-014	0.019317	0.000688	0.282560	-4.3	1470	
HN013-015	0.017218	0.000620	0.282436	-8.7	1750	
HN013-016	0.010919	0.000395	0.282420	-9.1	1780	
HN013-017	0.010919	0.002258	0.282606	-3.0	1380	Liu, 2011
HN013-018	0.016808	0.000572	0.282614	-2.3	1350	
HN013-020	0.017387	0.000610	0.282512	-5.9	1580	
HN013-021	0.017322	0.000586	0.282573	-3.9	1450	
HN013-022	0.018468	0.000645	0.282380	-10.4	1870	
HN013-024	0.018564	0.000628	0.282514	-5.9	1580	
HN013-25	0.013669	0.000479	0.282435	-8.6	1750	
HN013-27	0.017548	0.000616	0.282403	-9.6	1820	
HN013-27	0.014685	0.000511	0.282394	-10.2	1840	
HN013-28	0.028234	0.001006	0.282519	-5.7	1570	
HN013-29	0.019170	0.000683	0.282430	-8.7	1760	
HN013-30	0.060576	0.002031	0.282707	0.6	1160	
HN013-31	0.021138	0.000719	0.282613	-2.4	1360	
QLS-76.1	0.029067	0.001064	0.282523	-5.4	1553	
QLS-76.3	0.021437	0.000818	0.282478	-7.0	1652	
QLS-76.5	0.033760	0.001301	0.282412	-9.4	1803	
QLS-76.6	0.020239	0.000782	0.282351	-11.5	1937	
QLS-76.7	0.031034	0.001142	0.282510	-5.9	1582	
QLS-76.8	0.015941	0.000627	0.282398	-9.8	1830	
QLS-76.9	0.014308	0.000554	0.282383	-10.3	1864	
QLS-76.10	0.009115	0.000359	0.282516	-5.6	1564	Chen B et al., 2014
QLS-76.11	0.029620	0.001090	0.282352	-11.5	1935	
QLS-76.12	0.016495	0.000629	0.282509	-5.9	1582	
QLS-76.14	0.020786	0.000791	0.282377	-10.5	1877	
QLS-76.15	0.034032	0.001284	0.282251	-15.1	2163	
QLS-76.16	0.025095	0.000899	0.282442	-8.3	1734	
QLS-76.17	0.027012	0.001007	0.282280	-14.0	2097	
QLS-76.20	0.024330	0.000904	0.282452	-7.9	1710	

	QLS-76.21	0.020635	0.000783	0.282531	-5.1	1532	
	QLS-29.1	0.099826	0.003492	0.282543	-5.1	1523	
	QLS-29.2	0.031502	0.001153	0.282450	-8.1	1720	
	QLS-29.3	0.128115	0.004401	0.282565	-4.4	1483	
	QLS-29.5	0.063225	0.002206	0.282520	-5.8	1570	
	QLS-29.6	0.155639	0.005156	0.282513	-6.3	1604	
	QLS-29.7	0.055027	0.001772	0.282516	-5.9	1576	
	QLS-29.8	0.092594	0.003026	0.282502	-6.5	1615	
	QLS-29.9	0.029013	0.001067	0.282490	-6.7	1629	
	QLS-29.10	0.085015	0.002804	0.282499	-6.6	1621	
	QLS-29.11	0.284608	0.008845	0.282616	-3.0	1396	
	QLS-29.12	0.111278	0.003678	0.282549	-4.9	1513	
	QLS-29.13	0.162841	0.006120	0.282512	-6.4	1613	
	QLS-29.14	0.474624	0.014592	0.282722	0.1	1195	
	QLS-29.15	0.299959	0.009029	0.282641	-2.2	1341	
	QLS-29.16	0.139684	0.004646	0.282428	-9.3	1791	
	QLS-29.17	0.163528	0.005150	0.282494	-7.0	1645	
	QLS-29.18	0.072337	0.002755	0.282442	-8.6	1747	
	QLS-29.19	0.097144	0.003319	0.282515	-6.0	1588	
	QLS-29.20	0.084606	0.002961	0.282542	-5.0	1525	
	ZK14B04-02-1	0.025492	0.000657	0.282452	-8.1	1371	
	ZK14B04-02-5	0.047723	0.001229	0.282436	-8.6	1401	
	ZK14B04-02-6	0.031403	0.000874	0.282462	-7.7	1354	
	ZK14B04-02-7	0.027740	0.000752	0.282461	-7.7	1354	
	ZK14B04-02-8	0.029599	0.000830	0.282444	-8.3	1385	
	ZK14B04-02-9	0.048912	0.001259	0.282438	-8.5	1397	
	ZK14B04-02-10	0.030425	0.000846	0.282370	-10.9	1514	Zhou et al., 2015
	ZK14B04-02-11	0.032385	0.000864	0.282471	-7.4	1338	
	ZK14B04-02-12	0.054171	0.001463	0.282448	-8.3	1382	
	ZK14B04-02-13	0.035361	0.000895	0.282444	-8.4	1385	
	ZK14B04-02-14	0.052787	0.001385	0.282400	-10.0	1464	
Xitian Sn deposit	ZK14B04-02-15	0.027140	0.000791	0.282368	-11.0	1516	
	ZK14B04-02-17	0.022403	0.000604	0.282460	-7.8	1357	
	XT60-02	0.282495	0.002112	0.060348	-6.6	1620	
	XT60-18	0.282501	0.001203	0.033668	-6.3	1600	
	XT60-22	0.282543	0.003616	0.103302	-5.1	1520	
	XT60-24	0.282454	0.000830	0.023782	-8.0	1700	
	XT60-25	0.282474	0.001262	0.036938	-7.3	1660	
	XT60-26	0.282506	0.001071	0.032947	-6.2	1590	Yao et al., 2013
	XT60-27	0.282485	0.001188	0.034087	-6.9	1640	
	XT60-28	0.282478	0.001283	0.037870	-7.2	1650	
	XT60-34	0.282517	0.001700	0.046509	-5.8	1570	
	XT60-36	0.282443	0.001108	0.031579	-8.4	1730	

XT60-37	0.282514	0.002855	0.081250	-6.0	1580
XT60-38	0.282517	0.005776	0.163173	-6.2	1590
XT60-39	0.282557	0.006665	0.192480	-4.9	1510
XT60-40	0.282491	0.004421	0.127374	-7.0	1640
XT60-41	0.282489	0.003780	0.102548	-7.0	1650
XT60-42	0.282483	0.004566	0.131216	-7.3	1660
XT60-43	0.282514	0.001581	0.045160	-5.9	1570
XT32-02	0.038427	0.000896	0.282421	-9.0	1780
XT32-03	0.035846	0.000850	0.282427	-7.0	1654
XT32-06	0.027815	0.000674	0.282464	-7.4	1681
XT32-07	0.031956	0.000764	0.282462	-7.5	1687
XT32-08	0.039126	0.000900	0.282426	-8.8	1769
XT32-09	0.032823	0.000787	0.282465	-7.4	1681
XT32-10	0.034470	0.000815	0.282459	-7.6	1695
XT32-11	0.026931	0.000646	0.282512	-5.8	1575
XT32-12	0.033279	0.000811	0.282500	-6.1	1601
XT32-13	0.036039	0.000851	0.282443	-8.2	1731
XT32-15	0.028992	0.000716	0.282350	-11.5	1938
XT32-17	0.029300	0.000719	0.282364	-11.0	1906
XT32-20	0.027212	0.000674	0.282461	-7.6	1691
XT33-01	0.027964	0.000688	0.282461	-7.6	1691
XT33-03	0.030158	0.000737	0.282433	-8.6	1755
XT33-04	0.026585	0.000656	0.282455	-7.8	1704
XT33-05	0.029558	0.000732	0.282395	-10.0	1838
XT33-06	0.029229	0.000719	0.282369	-10.8	1896
XT33-08	0.029952	0.000738	0.282398	-9.8	1831
XT33-09	0.025779	0.000643	0.282428	-8.7	1763
XT33-10	0.035472	0.000856	0.282404	-9.6	1819
XT33-11	0.056731	0.001371	0.282446	-8.2	1729
XT33-12	0.039074	0.000947	0.282328	-12.3	1990
XT33-13	0.035025	0.000863	0.282393	-10.0	1844
XT33-14	0.027932	0.000683	0.282454	-7.8	1704
XT33-15	0.035865	0.000843	0.282457	-7.8	1703
XT33-16	0.026741	0.000667	0.282473	-7.2	1665
XT33-17	0.036707	0.000884	0.282401	-9.7	1826
XT33-18	0.028791	0.000721	0.282422	-9.0	1780
XT33-19	0.036133	0.000884	0.282464	-7.5	1684
XT33-20	0.028723	0.000711	0.282442	-8.3	1733
XT35-02	0.044438	0.001100	0.282412	-9.3	1803
XT35-04	0.039967	0.001057	0.282388	-10.2	1855
XT35-05	0.044349	0.000961	0.282411	-9.3	1803
XT35-10	0.060071	0.001392	0.282414	-12.8	2022
XT35-11	0.031774	0.000779	0.282442	-8.2	1733

Su et al., 2015

	XT35-12	0.032884	0.000810	0.282402	-9.6	1822	
	XT35-13	0.024966	0.000624	0.282438	-8.4	1740	
	XT35-14	0.072006	0.001793	0.282385	-10.4	1867	
	XT35-15	0.030543	0.000753	0.282447	-8.1	1722	
	XT35-16	0.034625	0.000853	0.282393	-10.0	1842	
	XT35-18	0.027519	0.000693	0.282496	-6.3	1611	
	XT35-19	0.020081	0.000515	0.282457	-7.7	1697	
	XT35-20	0.028099	0.000706	0.282421	-9.0	1779	
	HN016-1-01	0.010561	0.000400	0.282611	-2.2	1351	
	HN016-1-03	0.027834	0.000991	0.282620	-1.9	1332	
	HN016-1-04	0.016332	0.000603	0.282462	-7.4	1682	
	HN016-1-05	0.019285	0.000686	0.282384	-10.4	1861	
	HN016-1-06	0.016853	0.000631	0.282503	-5.9	1558	
	HN016-1-07	0.026116	0.009240	0.282423	-8.8	1769	
	HN016-1-08	0.016883	0.000623	0.282447	-7.5	1705	
	HN016-1-11	0.030475	0.001123	0.282426	-8.8	1768	
	HN016-1-12	0.021670	0.000804	0.282601	-2.5	1373	
	HN016-1-13	0.015957	0.000587	0.282579	-3.1	1417	
	HN016-1-14	0.022143	0.000824	0.282419	-8.9	1777	
	HN016-1-15	0.022554	0.000846	0.282391	-10.2	1848	
	HN016-1-16	0.152600	0.000561	0.282387	-9.8	1842	
	HN016-1-17	0.016401	0.000601	0.282490	-6.4	1618	
	HN016-1-18	0.014634	0.000542	0.282480	-6.9	1646	
	HN016-1-19	0.014824	0.000566	0.282484	-6.3	1625	Liu, 2011
Furong Sn deposit	HN016-1-20	0.014597	0.000528	0.282299	-13.2	2042	
	HN016-1-21	0.016564	0.000603	0.282449	-7.8	1710	
	HN016-1-22	0.018789	0.000658	0.282440	-8.0	1725	
	HN016-1-23	0.020916	0.000742	0.282491	-6.3	1617	
	HN016-1-24	0.015622	0.000579	0.282507	-5.8	1580	
	HN016-1-25	0.047311	0.001662	0.282542	-4.8	1513	
	HN016-1-26	0.014572	0.000542	0.282454	-7.8	1701	
	HN016-1-27	0.042435	0.001494	0.252483	-7.1	1651	
	HN016-1-28	0.016301	0.000598	0.282554	-4.1	1475	
	HN016-1-29	0.014983	0.000553	0.282534	-4.8	1519	
	HN016-1-30	0.015933	0.000586	0.282494	-6.3	1611	
	HN016-1-31	0.038232	0.001374	0.282519	-5.4	1559	
	HN016-1-32	0.071075	0.002707	0.282425	-9.2	1786	
	HN016-1-32	0.056636	0.002093	0.282544	-4.9	1516	
					-4.7	1330	
					-3.4	1270	
					-4.8	1340	Shan et al., 2014
					-6.7	1450	
Hehuaping Sn deposit	WXL-16-2	0.056376	0.002033	0.282378	-10.7	1875	Zheng and Guo,
	WXL-16-4	0.032758	0.001244	0.282439	-8.5	1736	2012

WXL-16-7	0.140164	0.005044	0.282433	-9.1	1774	
WXL-16-8	0.084101	0.002961	0.282488	-6.9	1638	
WXL-16-9	0.025353	0.001013	0.282418	-9.2	1783	
WXL-16-10	0.066319	0.002233	0.282480	-7.1	1651	
WXL-16-11	0.038059	0.001248	0.282411	-9.5	1799	
WXL-16-15	0.087039	0.002768	0.282533	-5.4	1538	
WXL-16-18	0.014363	0.000591	0.282433	-8.7	1746	
WXL-16-19	0.052882	0.001833	0.282458	-7.9	1697	
HHPD42	0.021733	0.000538	0.282554	-4.3	1480	
HHPD42	0.053642	0.001387	0.282573	-3.7	1440	
HHPD42	0.036157	0.000977	0.282438	-8.5	1740	
HHPD42	0.054865	0.001650	0.282556	-4.4	1480	
HHPD42	0.023077	0.000479	0.282460	-7.6	1690	
HHPD42	0.039746	0.000874	0.282530	-5.2	1530	
HHPD42	0.052750	0.001402	0.282476	-7.2	1660	
HHPD42	0.046966	0.001249	0.282546	-4.7	1500	
HHPD42	0.060853	0.001431	0.282590	-3.1	1400	
HHPD42	0.041848	0.001063	0.282577	-3.6	1430	
HHPD42	0.035583	0.000823	0.282528	-5.3	1540	
HHPD42	0.139680	0.003765	0.282520	-5.8	1570	
HHPD42	0.076295	0.002172	0.282510	-6.0	1590	
HHPD42	0.026679	0.000734	0.282494	-6.5	1610	
HHPD42	0.053343	0.001187	0.282703	-0.9	1150	
HHPD42	0.079947	0.002407	0.282495	-6.6	1620	
HHPD42	0.122678	0.002798	0.282601	-2.9	1390	
HHPD42	0.112687	0.003176	0.282550	-4.8	1500	Zhang, 2014
HHPD42	0.114617	0.002597	0.282586	-3.4	1420	
HHPD42	0.176605	0.004796	0.282553	-4.8	1510	
HHPD42	0.095725	0.002313	0.282530	-5.3	1540	
HHPD42	0.136189	0.003941	0.282553	-4.7	1500	
HHPD42	0.070564	0.002242	0.282509	-6.1	1590	
6302-38	0.024857	0.000889	0.282407	-9.6	1810	
6302-38	0.096506	0.003295	0.282539	-5.2	1530	
6302-38	0.075415	0.002435	0.282422	-9.2	1780	
6302-38	0.098066	0.003377	0.282483	-7.2	1660	
6302-38 06	0.047048	0.001631	0.282508	-6.1	1590	
6302-38 08	0.075875	0.002575	0.282448	-8.3	1730	
6302-38 09	0.024065	0.000836	0.282505	-6.1	1590	
6302-38 13	0.088940	0.002968	0.282532	-5.4	1540	
6302-38 14	0.041995	0.001602	0.282881	-7.1	750	
6302-38 15	0.018257	0.000661	0.282506	-6.1	1580	
6302-38 18	0.040874	0.001425	0.282451	-8.1	1710	
6302-38 20	0.087443	0.002988	0.282539	-5.2	1530	

6302-38 21	0.051792	0.001813	0.282513	-5.9	1580
6302-38 23	0.225678	0.007387	0.282508	-6.7	1620
6302-38 25	0.093270	0.003147	0.282512	-6.1	1590
6302-38 28	0.070967	0.002545	0.282496	-6.6	1620
6302-38 29	0.156718	0.005330	0.282521	-6.0	1580
6302-38 30	0.107783	0.003734	0.282567	-4.2	1470

Reference

- Bai, D.Y., Chen, J.C., Ma, T.Q., Wang, and X.H., 2005, Geochemical Characteristics and Tectonic Setting of Qitianling A-type Granitic Pluton in Southeast Hunan: *Acta Petrologica et Mineralogica*, v. 24, p.255-272 (in Chinese with English abstract)
- Chen, B., Ma, X.H., and Wang, Z.Q., 2014, Origin of the fluorine-rich highly differentiated granites from the Qianlishan composite plutons (South China) and implications for polymetallic mineralization: *Journal of Asian Earth Sciences*, v. 93, p. 301-314.
- Chen, D., Shao, Y.J., Liu, W., Ma A.J., and Liu YR.. 2013, Petrological and geochemical characteristics of Xitian pluton in Hunan province: *Geology and Mineral Resources of South China*, v. 31, p.11-25 (in Chinese with English abstract)
- Chen, D., Chen, Y.M., Ma, A.J., Liu, W., Liu, Y.R., and Ni, Y.J., 2014, Magma mixing in the Xitian pluton of Hunan Province: Evidence from petrography, geochemistry and zircon U-Pb age: *Geology in China*, v. 41, p. 61-78 (in Chinese with English abstract).
- Chen, Y.X., Li, H., Sun, W.D., Ireland, T., Tian, X.F., Hu, Y.B., Yang, W.B., Chen, C., and Xu, D.R., 2016, Generation of Late Mesozoic Qianlishan A2-type granite in Nanling Range, South China: Implications for Shizhuyuan W-Sn mineralization and tectonic evolution: *Lithos*, v. 266-267, p. 435-452.
- Deng, X.G., Li, X.H., Liu, Y.M., Huang, G.F., and Hou, M.S., 2005, Geochemical characteristics of Qitianling granites and their implications for mineralization: *Acta Petrologica et Mineralogica*, v. 24, p. 93-102 (in Chinese with English abstract)
- Dong, S.H., Bi, X.W., Hu, R.H., and Chen, Y.W., 2014, Petrogenesis of the Yaogangxian granites and implications for W mineralization, Hunan Province. *Acta Petrologica Sinica*: v. 30, p. 2749-2764 (in Chinese with English abstract)
- Fang, G.C., Cheng, Y.C., Chen, Z.H., Zeng, Z.L., Liu, C.H., Tong, Q.Q., Sun, J., and Zhu, G.H., 2016, Petrology and geochemistry of granite in the Pangushan tungsten deposit, south Jiangxi Province: *Geology in China*, v. 43, p. 1558-1568 (in Chinese with English abstract).
- Fu, J.M., Xie, C.F., Peng, S.B., Yang, X.J., and Mei, Y.P., 2006, Geochemistry and Crust-Mantle Magmatic Mixing of the Qitianling Granites and Their Dark Microgranular Enclaves in Hunan Province: *Acta Geoscientica Sinica*, v. 27, p. 557-569 (in Chinese with English abstract).
- Guo, C.L., Chen, Y.C., Zeng, Z.L., and Lou, F.S., 2012, Petrogenesis of the Xihuashan granites in southeastern China: Constraints from geochemistry and in-situ analyses of zircon U-Pb-Hf-O isotopes: *Lithos*, v. 148, p. 209-227.
- Guo, C.L., Wang, R.C., Yuan, S.D., Wu, S.H., and Yin, B., 2015, Geochronological and geochemical constraints on the petrogenesis and geodynamic setting of the Qianlishan granitic pluton, Southeast China: *Mineralogy and Petrology*, v. 109, p. 253-282.
- He, Z.Y., Xu, X.S., Zou, H.B., Wang, X.D., and Yu, Y., 2010, Geochronology, petrogenesis and metallogeny of Piaotang granitoids in the tungsten deposit region of South China: *Geochemical Journal*, v. 44, p. 299-313.

- Hua, R.M., Zhang, W.L., Chen, P.R., and Wang, R.C., 2003, Comparison in the characteristics, origin and related metallogeny granites in Dajishan and Piaotang, southern Jiangxi, China: *Geological Journal of China Universities*, v.9, p. 609-619 (in Chinese with English abstract)
- Ishihara, S., 1981, The granitoid series and mineralization: *Economic Geology*, 75th Anniversary Volume, p. 458-484.
- Jiang, Y.H., Jiang, S.Y., Zhao, K.D., and Ling, H.F., 2006, Petrogenesis of Late Jurassic Qianlishan granites and mafic dykes, Southeast China: implications for a back-arc extension setting: *Geological Magazine*, v. 143, p.457-474.
- Li, G.L., 2011, The evolution of Yanshanian granite and tungsten mineralization in southern Jiangxi Province and adjacent region: A Dissertation submitted to China University of Geosciences for doctor degree (in Chinese with English abstract).
- Li, X.M., Hu, R.Z., Bi, X.W., and Peng, J.T., 2010, Geochemistry and tin metallogenic potential for Qitianling granite mass in southern Hunan: *Journal of jilin University*, v. 40, p. 81-108 (in Chinese with English abstract).
- Liu, G.Q., Wu, S.H., Du, A.D., Fu, J.M., Yang, X.J., Tang, Z.H., and Wei, J.Q., 2008, Metallogenic ages of the Xitian tungsten-tin deposit, eastern Hunan province: *Geotectonica et Metallogenia*, v. 32, p. 63-71 (in Chinese with English abstract).
- Liu, Y., 2011, Crust-mantle interaction of Yanshanian granitic magma in Qitianling and Daoxian area southern Hunan: Dissertation submitted to Chinese Academy of Geological Sciences for Doctoral Degree (in Chinese with English abstract).
- Mao, J.W., and Li, H.Y., 1995, Evolution of the Qianlishan granite stock and its relation to the Shizhuyuan polymetallic tungsten deposit: *International Geology Review*, v. 37, p. 63-80.
- Mole, D.R., Fiorentini, M.L., Thebaud, N., Cassidy, K.F., McCuaig, T.C., Kirkland, C.L., Romano, N., Belousova, E.A., Barnes, S.J., and Mill, J., 2014, Archean komatiite volcanism controlled by the evolution of early continents: *PNAS* v. 111, p. 10083-10088.
- Shan, Q., Zeng, Q.S., Li, J.K., Lu, H.Z., Hou, M.Z., Yu, X.Y., and Wu, C.J., 2014, Diagenetic and metallogenic sources of Furong tin deposit, Qitianling: Constraints from Lu-Hf and He-Ar isotope for fluid inclusions: *Acta Geologica Sinica*, v. 88, p. 704-715(in Chinese with English abstract).
- Su, H.Z., Guo, C.L., Wu, S.C., Hou, K.J., and Zhang, Y., 2015, Magma-hydrothermal fluid activity duration and material sources in the Xitian Indosian-Yanshanian complex: *Acta Geologica Sinica*, v. 89, p. 1853-1872 (in Chinese with English abstract).
- Su, H.Z., 2017, The petrogenesis studies of the Mesozoic Xiangyuan tungsten-tin deposit and related granites in Hunan Province: A Dissertation submitted to China University of Geosciences for master degree (in Chinese with English abstract).
- Watson, E.B., and Harrison, T. M., 1983, Zircon saturation revisited: temperature and composition effects in a variety of crustal magma types: *Earth and Planetary Science Letters*, v.64, p. 295-304.
- Wu, M.Q., 2017, Mineralogy, geochemistry, and metallogeny of the Yichun and the Dajishan deposits: A Dissertation submitted to China University of Geosciences for doctor degree (in Chinese with English abstract).
- Yao, Y., Chen, J., Lu, J.J., and Zhang, R.Q., 2013, Geochronology, Hf isotopic compositions and geochemical characteristics of Xitian A-type granite and its geological significance: *Mineral Deposits*, v. 32, p. 467-488 (in Chinese with English abstract).
- Yang, J.H., Peng, J.T., Zhao, J.M., Fu, Y.Z., Cheng, Y., and Hong, Y.L., 2012, Petrogenesis of the Xihuashan Granite in Southern Jiangxi Province, South China: Constraints from Zircon U-Pb

- Geochronology, Geochemistry and Nd Isotopes: *Acta Geologica Sinica (English Edition)*, v. 86, p. 131-152
- Yang, J.H., Kang, L.F., Peng, J.T., Zhong, H., Gao, J.F., and Liu, L., 2018, In-situ elemental and isotopic compositions of apatite and zircon from the Shuikoushan and Xihuashan granitic plutons: Implication for Jurassic granitoid-related Cu-Pb-Zn and W mineralization in the Nanling Range, South China, *Ore Geology Reviews*, v. 93, p.382-403.
- Zhang, R.Q., 2014, Petrogenesis and metallogeny of the W- and Sn-bearing granites in southern Hunan province: Case study from Wangxianling and Xintianling: A Dissertation submitted to Nanjing University for doctor degree (in Chinese with English abstract).
- Zhao, K.D., Jiang, S.Y., Yang, S.Y., Dai, B.Z., and Lu, J.J., 2012, Mineral chemistry, trace elements and Sr-Nd-Hf isotope geochemistry and petrogenesis of Cailing and Furong granites and mafic enclaves from the Qitianling batholith in the Shi-Hang zone, South China: *Gondwana Research*, v. 22, p. 310-324.
- Zheng, J.H., and Guo, C.L., 2012, Geochronology, geochemistry and zircon Hf isotopes of the Wangxianling granitic intrusion in South Hunan Province and its geological significance: *Acta Petrologica Sinica*, v. 28, p. 75-90 (in Chinese with English abstract)
- Zhou, Y., Liang, X.Q., Liang, X.R., Wu, S.C., Jiang, Y., Wen, S.N., and Cai, Y.F., 2013, Geochronology and Geochemical Characteristics of the Xitian Tungsten-Tin-Bearing A-type Granites, Hunan Province, China: *Geotectonica et Metallogenia*, v. 37, p. 511-529 (in Chinese with English abstract).
- Zhou, Y., Liang, X.Q., Wu, S.C., Cai, Y.F., Liang, X.R., Shao, T.B., Wang, C., Fu, J.G., and Jiang, Y., 2015, Isotopic geochemistry, zircon U - Pb ages and Hf isotopes of A-type granites from the Xitian W - Sn deposit, SE China: Constraints on petrogenesis and tectonic significance: *Journal of Asian Earth Sciences*, v. 105, p. 122-139.
- Zuo, M.L., 2016, The research of differences of the rare-metal granites mineralization between Yichun Yashan and Quannan Dajishan in Jiangxi Province: A Dissertation submitted to China University of Geosciences for doctoral degree (in Chinese with English abstract).

